Politecnico di Milano

SCHOOL OF INDUSTRIAL AND INFORMATION ENGINEERING

Master of Science – Energy Engineering

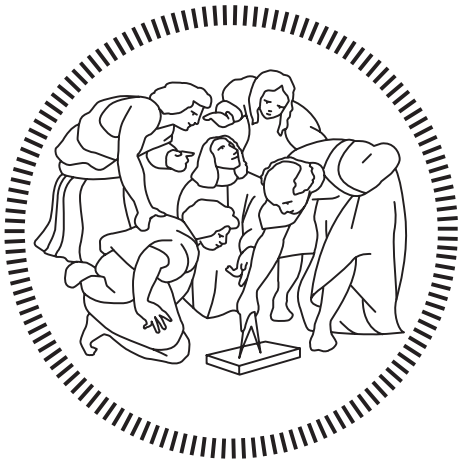

Literature Review on Supercritical CO_2 Power Cycles: Optimization Methodology, Cycle Layouts and Possible Applications

Supervisor

Prof. Marco Astolfi

Co-Supervisor

Ing. Dario Alfani

Master Thesis Candidate

Altea Camparsi – 899262

Academic Year 2019 – 2020

Sommario

La storia dei cicli supercritici a CO_2 inizia nel 1948, dove i vantaggi della CO_2 furono subito identificati e per questo vennero effettuate ricerche in molti paesi. Il ciclo a CO_2 supercritica sfrutta gli alti valori di compressibilità e densità nelle vicinanze del punto critico, che permettono di minimizzare il lavoro di compressione con la conseguente possibilità di raggiungiere grandi efficienze termiche. Questi cicli hanno anche altri vantaggi importanti rispetto al ciclo Rankine a vapore come ad esempio una maggiore compattezza delle turbomacchine, la capacità di operare efficientemente anche con raffreddamento ad aria ed espansione senza cambio di fase eliminando in questo modo il rischio di erosione per le pale della turbina. A differenza dei fluidi organici è chimicamente inerte, non tossica, non corrosiva, non infiammabile, facilmente accessibile, economica e caratterizzata da una facile gestione con minori costi di manutenzione annessi. Le applicazioni più interessanti associate ai cicli a CO_2 supercritica sono: nucleare, carbone, impianti a concentrazione solare e il recupero di calore. In letteratura sono presenti diversi tipi di ottimizzazione: termodinamiche, termoeconomiche, a singolo obiettivo o multi-obiettivo. Ogni studio ha le sue particolarità, le sue assunzioni e vincoli, che possono essere simili o diversi per ogni tipo di studio, inoltre questi cicli devono rispettare i possibili vincoli dettati dalla integrazione con la fonte di calore. Lo scopo di questa tesi è non solo quello di riportare e riassumere i principali risultati significativi trovati in letteratura, ma anche quello di confrontare gli studi ed elaborare delle considerazioni preliminari importanti sul ciclo/i che sembrano essere i migliori candidati per ogni particolare applicazione. Tutte le assunzioni tipiche sono riassunte e spiegate e il lavoro viene concluso riportanto le correlazioni di costo maggiormente utilizzate nelle analisi termoeconomiche. Le relazioni sono rappresentate graficamente, confrontate e analizzate. Grazie agli importanti progressi degli ultimi anni nella ricerca scientifica e dei progetti realizzati e ancora in corso, la commercializzazione di questa tecnologia sembra sempre più vicina.

Parole Chiave: CO_2 supercritica, ottimizzazione, layout, applicazione, termodinamica, termoeconomica

Abstract

The history of supercritical CO_2 Brayton cycle begins in 1948, where the advantages of CO_2 fluid were quickly realized and investigation on supercritical CO_2 cycles was carried out in many countries. Supercritical CO_2 power cycles take advantage of high compressibility factor and density near the critical point to minimize the compression work with the associated higher thermal efficiencies. Supercritical CO_2 cycle has also other important advantages over steam Rankine cycle such as more compact turbomachinery, ability to operate efficiently with dry cooling and no phase change during expansion eliminating erosion risk for the turbine. Differently from organic fluids it is chemically inert, non-toxic, non-corrosive, non-flammable, accessible, affordable and it is characterized by easy handling with associated lesser maintentance costs. The most interesting applications applied to supercritical CO_2 cycles are nuclear, coal, concentrated solar power and waste heat recovery. There are diffent type of optimizations in the literature for every application: thermodynamic, thermo-economic, single objective, multi-objectives. Every study has its peculiarities, its assumptions and constraints that could be similar or different from the other studies in the literature, moreover the supercritical CO_2 cycle has to be tailored to deal with the heat source system integration constraints. The aim of this work is not only to summarize the main findings and significant results in the literature, but to compare the studies, to give some important preliminary considerations and conclusions on the layout that seems to be the best suited for every particular application. All the typical assumptions are summarized and explained. The work is concluded reporting the cost correlations assumed for the main components of the supercritical CO_2 cycles in the thermo-economic ivestigations, the correlations are represented graphically, compared and analyzed. Thanks to the recent huge steps forward in research and development projects and acitivities the commercialization of this technology seems more and more closer.

Key Words: supercritical CO_2, optimization, layout, application, thermodynamics, thermo-economic

Table of Contents

List of Figures

List of Tables

1. Introduction

1.1 History of Supercritical CO_2 Cycles

The history of supercritical CO_2 Brayton cycle begins in 1948, when Sulzer Bros patented a partial condensation CO_2 Brayton cycle [1]. The advantage of CO_2 fluid was quickly realized and investigation of supercritical CO_2 cycles was carried on in many countries: Gokhstein and Verhivker in the Soviet Union [2][3], Angelino in Italy [4][5], Feher in the United States [6], Sulzer Brown – Boveri in Switzerland [7] are the most important among many others, but the first landmark in the development of the supercritical CO_2 (s-CO_2) power cycles was set by the original works of Angelino [4][5] and Feher [6][8]. These authors, working in Italy (Politecnico di Milano) and United States (Douglas Aircraft Co.) respectively, presented the theoretical fundamentals of this innovative technology and proposed a series of possible configurations of the working cycle, drawing attention to the great potential of carbon dioxide used as working fluid in supercritical and transcritical power cycles, thanks to its advantageous thermodynamic properties.

Feher's Cycle

The original Feher cycle [6] operates between 700°C and 20°C with a pump inlet pressure of 13.8 MPa. The cycle works entirely above the critical pressure of CO_2, is regenerative and the compression is performed entirely in the liquid phase. His results show the small dependence of cycle efficiency on the pressure ratio once the pressure ratio of 2 is exceeded. It is important to point out that he kept the pump inlet pressure constant, therefore, he failed to determine whether an optimum pump inlet pressure exists. The investigation of recuperation at different pinch-point temperatures revealed that the higher the pinch-point temperature the more pronounced is the effect of the pressure ratio. Due to the low pumping power the pump efficiency does not have a significant effect on cycle efficiency. The effects of turbomachinery efficiency and pressure drops on the cycle efficiency were investigated as well. Feher defined the total system fractional pressure drop as:

$$\frac{\Delta p_{\mathrm{cyc}}}{\Delta p_{\mathrm{t}}} = \frac{\Delta p_{\mathrm{p}}}{\Delta p_{\mathrm{t}}} - 1$$

where Δp_{cyc} is the sum of the pressure drops from the compressor outlet to turbine inlet and from turbine outlet to the compressor inlet, Δp_p is the pressure rise across the pump and Δp_t is the pressure rise across the turbine. A fractional pressure drop of 0.075 reduces the cycle efficiency by about 5%. The Figure 1.1 clearly identifies the importance of pressure drops for efficiency calculations.

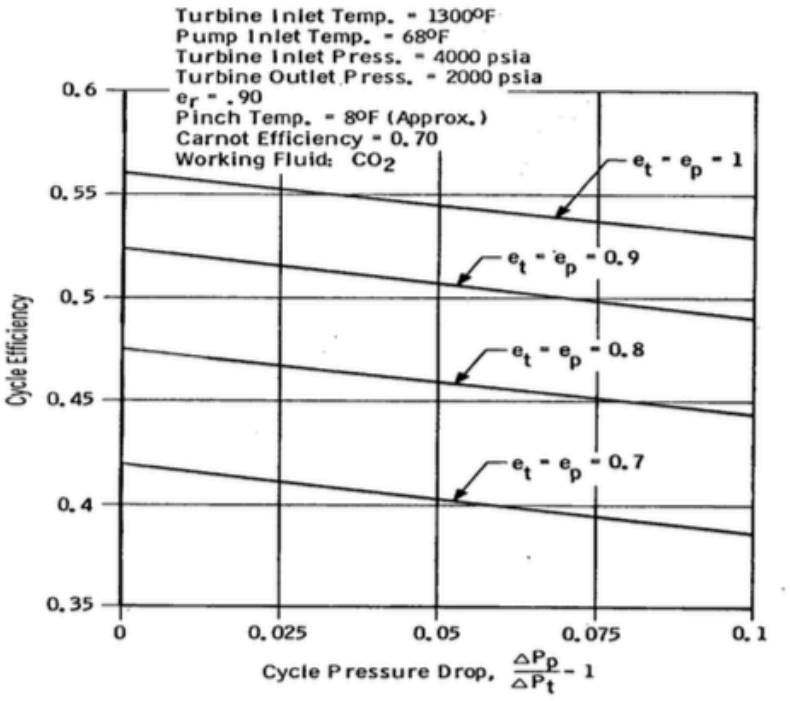

Figure 1.1 – Effect of pressure drops on cycle efficiency [6]

The advantages of this cycle, as claimed by the author, were twofold. On one hand, the capability to overcome some of the limitations inherent to Rankine cycles such as temperature restrictions, turbine exhaust in saturated steam/vapour conditions and a large number of turbine stages (due to the large expansion ratios). On the other, the possibility to solve restrictions of Brayton cycles such as large compression work (fluid in gaseous state), high sensitivity of cycle performance to pressure drops and compressor efficiency and large heat transfer areas due to the low density at the usual operating pressures.

Condensation Cycles by Angelino

His original work focused on condensation cycles [4][5][9] but some layouts such as the recompression cycle, partial cooling cycle, and precompression cycle (introduced in order to make the turbine exhaust pressure independent of the condensing pressure) that were suggested in his work and reported in the Figure 1.2 are still being investigated in the s-CO_2 cycle research field. He showed that the efficiency of the recompression cycle with 650°C turbine inlet

temperature is competitive to the reheat steam Rankine cycle. He summarized his work [4][9] on the CO_2 condensation cycle for two temperature range applications; one is for the mild temperature range (450-550°C) even though the cycle's efficiency is inferior to that of the steam cycle its simplicity and compactness could prove more economic, the other is for the high temperature range (650-800°C) with high efficiency as well as simplicity and compactness.

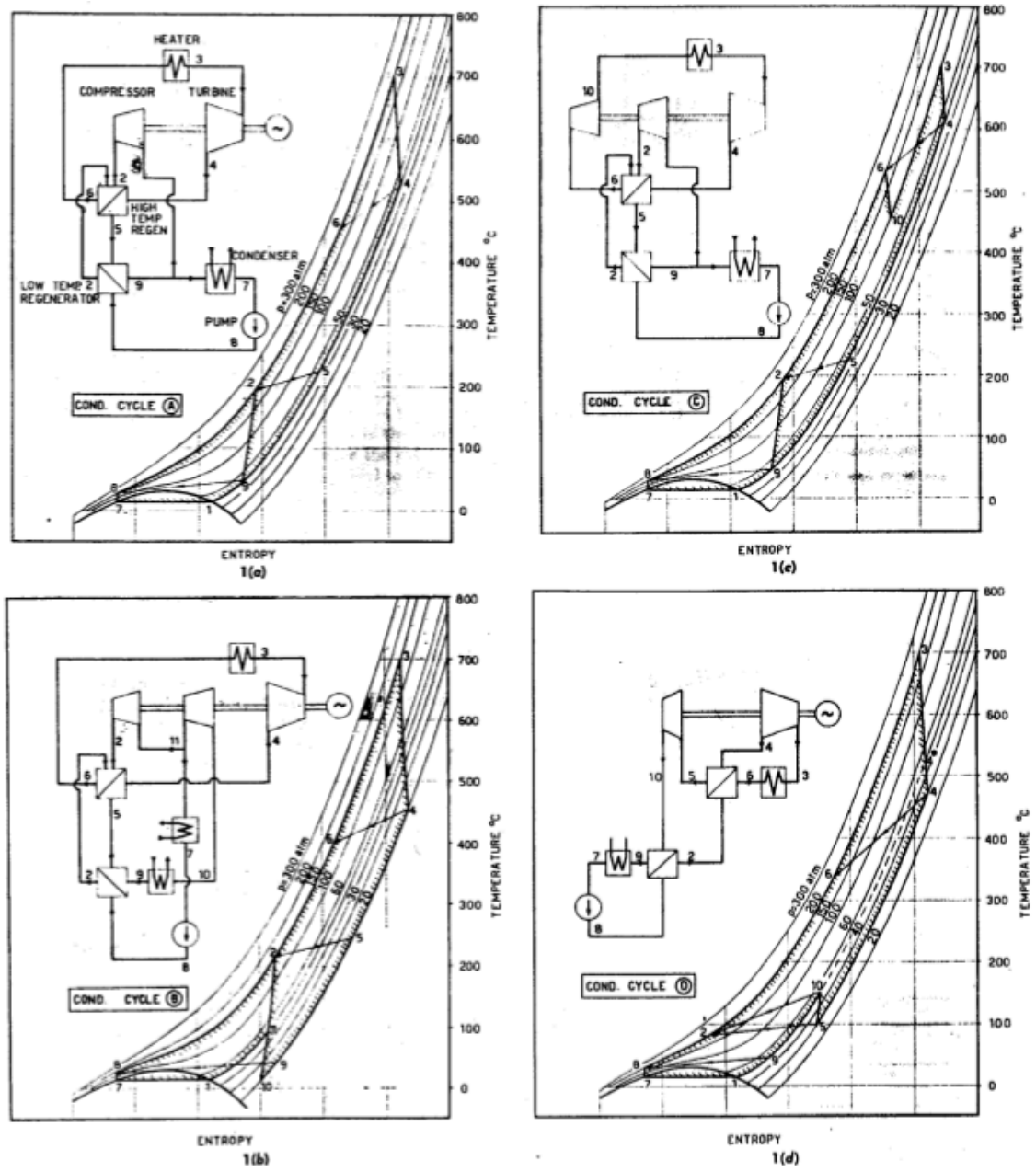

Figure 1.2 – Condensing cycles proposed by Angelino [4], a) Recompression cycle, b)Recompression with pre-compression, c)Recompression cycle with partial expansion before heat addiction (so that the heat source can operate at lower pressure), d)pure pre-compression cycle

In 1969 Angelino [5] summarized his previous findings and extended the analysis to higher pump inlet temperatures and a wider range of operating pressures. Some of these cycle layouts were investigated in his preceding studies, however this one looked at a wider range of operating conditions. In addition to availability and low cost of CO_2, this fluid has very good thermal stability up to 1,500°C for the investigated pressures (2-40 MPa).

The final conclusions drawn by Feher and Angelino were similar. Both authors agreed that the supercritical CO_2 cycle enabled higher efficiencies (close to 50%) than conventional Brayton cycles with moderate turbine inlet temperatures. Also, with respect to Rankine cycles, s-CO_2 cycles offered potentially higher efficiencies at temperatures higher than 600°C but, more interestingly, much smaller footprint. The main flaw of both analyses was nevertheless the oversimplification of the thermodynamic calculations as some of the assumptions were far from reality and yielded misleading results. For instance, it was not realistic to neglect pressure drops in a system operating at 20 MPa, or to consider ideal compression and expansion processes (both in Feher). The concern about the results obtained by Angelino is shared by Dostal [10], he stated that the assumptions made regarding turbomachinery efficiency must be updated (mainly for the compressor and pump) and the same applies to the pinch point differences in the high and low temperature recuperators. Dostal indicates also that the pressure losses considered by Angelino are too optimistic and thus the efficiency of the more complex cycles would have to be corrected to a lower value. In any case, these observations are valid for thermal efficiency only as nothing is said about auxiliary power or mechanical losses. With all this in mind, it is concluded that the figures obtained by Angelino and Feher in their fundamental contribution, provide a very good initial approach to the topic.

Dostal PhD thesis

Dostal in his Doctor of Science Thesis [10] performed a systematic, detailed major component and system design evaluation and multiple parameter optimization under practical constraints of the family of s-CO_2 Brayton power cycles for application to advanced nuclear reactors with core outlet temperature above 500°C in either direct or indirect versions. To perform the cycle calculations a code called CYCLES was developed in Fortran 90. Intercooling, reheating, recompressing and precompressing were considered. The recompression cycle was found to yield the highest efficiency, while still retaining simplicity. Main results were that intercooling is not attractive for this type of cycle as it offers a very modest efficiency improvement while reheating has a better potential, but it is applicable only to indirect cycles (anyway more than one reheating is economically unattractive). For the basic design, turbine inlet temperature was conservatively selected to be 550°C the compressor outlet pressure set at 20 MPa and the compressor inlet temperature set at 32°C while the optimization parameters were considered the pressure ratio, the ratio of precooler (PC), High Temperature Recuperator (HTR) and Low Temperature Recuperator (LTR) volume to the total volume, HTR length and LTR length with the constraint of a fixed total volume of heat exchangers equal to 120 m^3. For these operating conditions the direct cycle achieves a thermal efficiency of 45.27% and reduces the cost of the power plant about 18% compared to conventional Rankine steam cycle. The current reactor

operating experience with CO_2 is up to 650°C, which is used as the turbine inlet temperature of an advanced design. The thermal efficiency of the advanced design is close to 50% and the reactor system with the direct s-CO_2 cycle is about 24% less expensive than the steam indirect cycle. It is expected in the future that high temperature materials will become available and a higher performance design with turbine inlet temperatures of 700°C will be possible. This higher performance design achieves a thermal efficiency approaching 53%, which yields additional cost savings.

1.2 Theoretical Bases and Thermodynamics

In the temperature and pressure range of interest for power production, CO_2 does not behave as an ideal gas. This is caused by the fact that the critical temperature and pressure of CO_2 are 7.38 MPa and 30.98°C. The behavior of a gas near its critical point is very sensitive to pressure and temperature. Fluid properties are affected showing significantly nonlinear variations as we can see for specific heat capacity (c_p), density (ρ), dynamic viscosity (μ) and compressibility factor (Z) in Figure 1.3. Therefore, unlike for an ideal gas, cycle operating conditions have a strong effect on cycle performance. The main mechanism of improving cycle efficiency in s-CO_2 power cycles is represented by the reduction of compressor work performing the compression process close to the critical point. The reduction of the compressor work comes from the low compressibility of CO_2 near the critical point. This is the main reason why s-CO_2 cycles achieve an advantage over the ideal gas Brayton cycle, where the gas exhibits the same trends in both turbine and compressor. Unfortunately, the reduction of the compressor work is only one of the effects caused by the non-ideal properties. The specific heat, which affects recuperator design in particular, also varies widely. It is known [6], that for certain cycle operating conditions a pinch-point exists inside the recuperator. The pinch-point is the location in the recuperator with the lowest temperature difference. Due to the radical temperature and pressure dependence of specific heat, the temperature difference between the hot and the cold fluid varies widely within the recuperator. The pinch-point problem denotes the inefficiency of a heat exchanging process due to the pinch point occurring inside the heat exchanger instead of locating at the terminal point of heat exchanger. This pinch-point problem may occur to the recuperator and cooler in the cold-end of the s- CO_2 cycle due to the mismatch of thermal capacity in the two sides caused by the dramatic change of specific heat capacity (c_p) near the CO_2 critical point. The pinch-point problem can significantly limit the effectiveness of cycle regeneration if not well addressed.

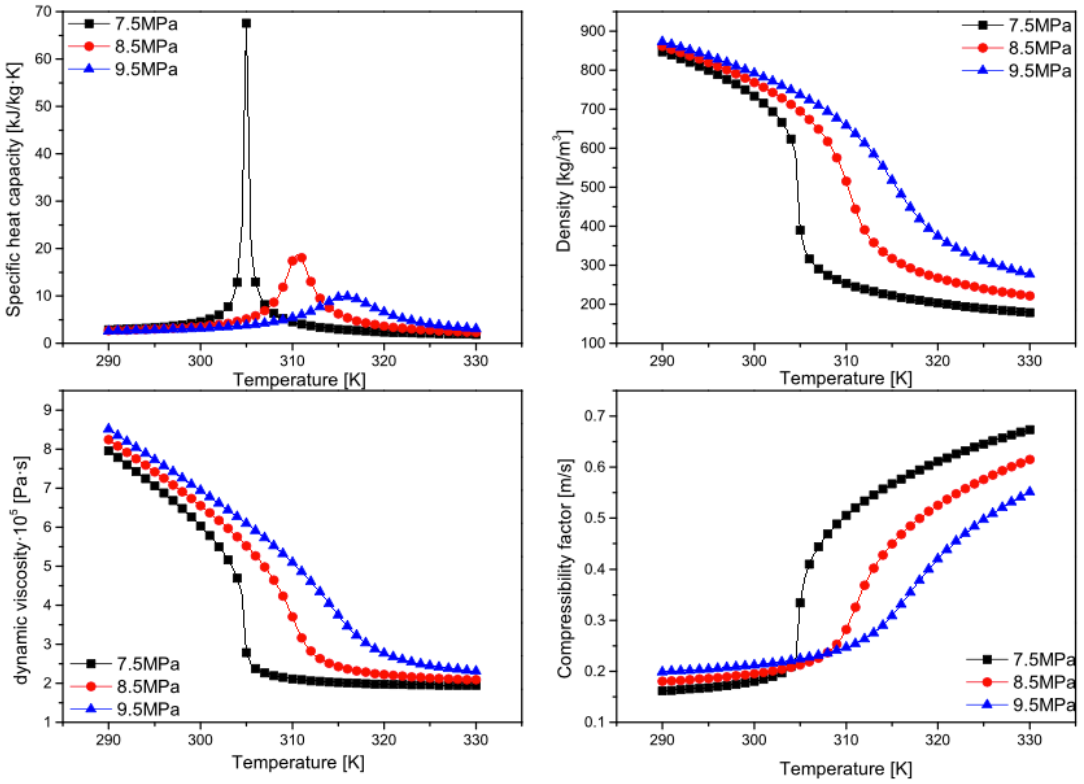

Figure 1.3 – Variation of CO_2 thermodynamic properties near the critical point [11]

As already said in the working conditions of interest for s-CO_2 as an interesting working fluid for power generation, it doesn't behave as an ideal fluid so we need to refer to a database to account for its real fluid behavior and properties. All the physical property data mainly used in the literature are computed through the REFFPROP software by NIST.

NIST-REFPROP DATABASE

REFPROP is an acronym for REference Fluid PROPerties. This program, developed by the National Institute of Standards and Technology (NIST) provides tables and plots of the thermodynamic and transport properties of industrially important fluids and their mixtures. REFPROP is based on the most accurate pure fluid and mixture models currently available. It implements three models for the thermodynamic properties of pure fluids: equations of state explicit in Helmholtz energy, the modified Benedict-Webb-Rubin equation of state, and an extended corresponding states (ECS) model. Mixture calculations employ a model which applies mixing rules applied to the Helmholtz energy of the mixture components; it uses a departure function to account for the departure from ideal mixing. Viscosity and thermal conductivity are modeled with either fluid specific correlations or an ECS method. These models are implemented in a suite of Fortran subroutines. They are written in a structured format, are internally documented with extensive comments, and have been tested on a variety of compilers. Routines are provided to calculate thermodynamic and transport properties at a

given (T,x) state. Iterative routines provide saturation properties, including surface tension, for a specified (T,x) or (P,x) state. Flash calculations describe single or two-phase states given a wide variety of input combinations [(P,h,x), (P,T,x), etc]. A separate graphical user interface, designed for the Windows operating system, provides a convenient means of accessing the models. It generates tables and plots for a user-specified mixture or a number of predefined mixtures. An on-line help system provides information on how to use the program. Information screens that display fluid constants and documentation for the property models can be called up at any time. Numerous options to customize the output are available as well as capabilities to copy and paste to and from other applications. The property models can also be accessed by other applications (such as spreadsheets) through use of a provided dynamic link library (DLL).

The objective in selecting property models for use in REFPROP was to implement the most accurate models currently available. The user should be aware that the uncertainties in these models vary considerably depending on the fluid, property, and thermodynamic state. It is thus impossible to give a simple, global statement of uncertainties. Even for the most-studied fluids with equations of state based on accurate, wide-ranging data, uncertainties are complicated functions of the temperature and pressure. The user is further cautioned that, by the very nature of a calculations database, property data are often displayed with more digits than can be justified based on the accuracy of the property models or the uncertainties in the experimental data to which the models were fitted [12].

Mathematical modeling

Various s-CO_2 power cycle layouts have been proposed to fulfill different requirements, such as high efficiency, high power output, compactness and low cost. Based on the first and second laws of thermodynamics, researchers theoretically investigated the cycle optimization and performance analysis of s-CO_2 power cycle to obtain the optimum layouts and performance.

In order to simplify the mathematical model of the s-CO_2 power cycle, some assumptions were adopted, which depended on the purposes of the researches. To date, the vast majority of studies on the s-CO_2 power cycles were assumed that the cycles operated at steady-state condition. Other essential assumptions are employed as follows:

1. The variations of kinetic and potential energies are negligible
2. Pressure losses in pipes (and in many studies even in heat exchangers) are neglected
3. The turbine, the pump and the compressor are modelled through isentropic efficiencies
4. A pinch point temperature difference is adopted in heat exchangers

The critical components in s-CO_2 power cycles include compressor, turbine and heat exchangers. According to different locations in the system, heat exchangers could be categorized as primary heat exchanger (heat source), high-temperature recuperator, low-temperature recuperator, cooler (or condenser in transcritical cycles). The general equations, namely mass conservation (1.1), energy conservation (1.2) and exergy balance (1.3), are applied to the thermodynamic models of the critical components as follows [13]:

$$\sum \dot{m}_{in} = \sum \dot{m}_{out} \tag{1.1}$$

$$\sum \dot{Q} + \sum \dot{m}_{in} h_{in} = \sum \dot{W} + \sum \dot{m}_{out} h_{out} \tag{1.2}$$

$$\sum \dot{m}_{in} e_{in} + \sum \dot{E}_Q = \sum \dot{m}_{out} e_{out} + \sum \dot{W} + \dot{E}_D + \dot{E}_{Loss} \tag{1.3}$$

where subscripts *in* and *out* represent the inlet and outlet of control volume; $\dot{Q}$ and $\dot{W}$ denote the heat transfer rate and work transfer rate between the control volume and environment; h means the specific enthalpy of the working fluid; $\dot{E}_Q$, $\dot{E}_D$ and $\dot{E}_{Loss}$ signify the exergy rate related to heat transfer, destruction and losses, respectively.

According to the assumptions of pure fluid (chemical exergy results zero) and negligible variations of kinetic and potential energies, the specific exergy of a stream (1.4) coincides with its physical exergy (1.5):

$$e = e_{ph} + e_{ch} \tag{1.4}$$

$$e_{ph} = (h - h_0) - T_0(s - s_0) \tag{1.5}$$

where subscript 0 refers to the reference state.

Heat exchanger

The heat transfer model introduced below is valid for the Primary Heat Exchanger (PHX), High Temperature Recuperator (HTR) and Low Temperature Recuperator (LTR) in the cycle. These heat exchangers are generally assumed to be of counter-flow type. The energy conservation for these heat transfers is defined as (1.6):

$$\dot{Q}_{HX} = \dot{m}_{HT}\left(h_{HT_{in}} - h_{HT_{out}}\right) = \dot{m}_{LT}\left(h_{LT_{out}} - h_{LT_{in}}\right) \tag{1.6}$$

where $\dot{Q}_{HX}$ denotes the heat transfer rate through heat exchangers, while HT and LT denote the the high temperature side and low temperature side of heat exchangers, respectively.

The exergetic destruction ($\dot{E}_{d,HX}$) during a heat transfer process is evaluated as in the equation (1.7):

$$\dot{E}_{d,HX} = \dot{m}_{HT}\left(e_{HT_{in}} - e_{HT_{out}}\right) - \dot{m}_{LT}\left(e_{LT_{out}} - e_{LT_{in}}\right) \tag{1.7}$$

For the PHX, the temperature approach is specified to determine the heat exchanger performance and to calculate the unknown thermal states for the model. For the recuperators, the effectiveness (eff_{HX}) is defined (1.8) for the evaluation of recuperation process:

$$eff_{HX} = \begin{cases} \dfrac{h_{HT_{in}} - h_{HT_{out}}}{h_{HT_{in}} - h(T_{LT_{in}}, P_{HT_{in}})} & if\ (\dot{m}\,\bar{c}_p)_{HT} \le (\dot{m}\,\bar{c}_p)_{LT} \\ \dfrac{h_{HT_{in}} - h_{HT_{out}}}{h\left(T_{LT_{out}}, P_{HT_{in}}\right) - h_{LT_{in}}} & if\ (\dot{m}\,\bar{c}_p)_{HT} > (\dot{m}\,\bar{c}_p)_{LT} \end{cases} \tag{1.8}$$

Heat sink

The coolers in the cycle include the PC and intercooling cold-end configuration (IC). They serve as heat sinks in the cold end of the cycle. The amount of heat removal in a cooler ($\dot{Q}_C$) is calculated as (1.9):

$$\dot{Q}_C = \dot{m}_{HT}\left(h_{HT_{in}} - h_{HT_{out}}\right) \tag{1.9}$$

The exergetic destruction associated with the heat removal in a cooler ($\dot{E}_{d,C}$) is calculated as (1.10):

$$\dot{E}_{d,C} = \dot{m}_{HT}\left(e_{HT_{in}} - e_{HT_{out}}\right) \tag{1.10}$$

Turbine

The CO_2 working fluid expands in the turbine to output work. The output work of turbine ($\dot{W}_T$) is calculated as (1.11):

$$\dot{W}_T = \dot{m}_{CO_2}\sum_{i=1}^{n}\left(h_{in,i} - h_{out,i}\right) = \dot{m}_{CO_2}\sum_{i=1}^{n}\left(h_{in,i} - h_{out_{is,i}}\right)\eta_{T_{is}} \tag{1.11}$$

where $h_{out_{is}}$ is the ideal outlet enthalpy after an isentropic expansion, $\eta_{T_{is}}$ denotes the isentropic efficiency of the turbine and i denotes the i-th stage of the turbine. The exergetic destruction through the expansion process ($\dot{E}_{d,T}$) is computed as (1.12):

$$\dot{E}_{d,T} = \dot{m}_{CO_2}(e_{in} - e_{out}) - \dot{W}_T \tag{1.12}$$

Compressor

The CO_2 working fluid is compressed in the compressors to be pressurized. The power consumed by the compressor ($\dot{W}_C$) is calculated as (1.13):

$$\dot{W}_C = \dot{m}_{CO_2} \sum_{i=1}^{n} \left(h_{in,i} - h_{out,i}\right) = \dot{m}_{CO_2} \sum_{i=1}^{n} \left(h_{in,i} - h_{out_{is,i}}\right) / \eta_{C_{is}} \tag{1.13}$$

where i denotes the i-th stage of the compressor and $\eta_{C_{is}}$ denotes the isentropic efficiency of the compressor.

The exergetic destruction through the compression process ($\dot{E}_{d,C}$) is defined as (1.14):

$$\dot{E}_{d,C} = \dot{W}_C - \dot{m}_{CO_2} \sum_{i=1}^{n} \left(e_{in,i} - e_{out,i}\right) \tag{1.14}$$

The pressure ratio of each stage (π_i) is defined as the ratio of outlet and inlet pressures (1.15). Besides, the ratio of pressure ratio of each stage (RPR_i) is defined (1.16) to denote the ratio of the pressure ratio distributed to a certain stage.

$$\pi_i = \frac{p_{out,i}}{p_{in,i}} \tag{1.15}$$

$$RPR_i = \frac{\ln(\pi_i)}{\ln(\pi)} \tag{1.16}$$

where $p_{out,i}$ and $p_{in,i}$ denote the inlet and outlet pressure of the i-th stage of the compressor.

Splitter/Mixer

At the splitter point of the system, one stream is split into two without changes in thermodynamic states. The split ratio (*SR*) is defined as (1.17):

$$SR = \frac{\dot{m}_1}{\dot{m}} = \frac{\dot{m}_1}{\dot{m}_1 + \dot{m}_2} \tag{1.17}$$

$$SRh_{in,1} + (1 - SR)h_{in,2} = h_{out} \tag{1.18}$$

At the mixer point, the two streams merge into one. The energy conservation for this process and the exergy destruction ($\dot{E}_{d,Mixer}$) are expressed in Eq. (1.19) and Eq. (1.20), respectively [11].

$$\dot{m}_{in,1}h_{in,1} + \dot{m}_{in,2}h_{in,2} = \dot{m}_{out}h_{out} \tag{1.19}$$

$$\dot{E}_{d,Mixer} = \dot{m}[(SR)e_{in,1} + (1 - SR)e_{in,2}] - e_{out} \tag{1.20}$$

Based on the thermodynamic theories, thermal efficiency (η_{th}) and exergy efficiency (η_{ex}) are applied to evaluate the performance of the s-CO_2 power cycle. They could be defined as in the Equations (1.21) and (1.22):

$$\eta_{th} = \frac{\dot{W}_{net}}{\dot{Q}_{core}} \tag{1.21}$$

$$\eta_{ex} = \frac{\dot{W}_{net}}{\dot{E}_{in}} \tag{1.22}$$

Where $\dot{W}_{net}$ represents the net power output of the power cycle and $\dot{Q}_{core}$ refers to the heat absorbed by the cycle from the heat source.

1.3 Advantages of Supercritical CO_2 Cycles over Steam Rankine Cycles

The principal benefit of s-CO_2 power cycle is the high thermal efficiency at moderate temperature due to the small compression work and large amount of heat in the turbine exhaust that is recuperated and turned into power. The high-power density of s-CO_2 means all system component are much smaller, leading to a reduced footprint and potentially lower capital costs. The low-pressure ratio of the turbine reduces the number of stages required. Compression, expansion and heat rejection are carried out in a single phase, reducing the complexity of the system [14] and eliminating the blade erosion risk for the turbine. Lower operation and maintenance costs for s-CO_2 power cycles are possible because plant personnel will not be needed for water treatment and quality control that are typically found in steam-based plants. Another potential benefit is the compatibility of the s-CO_2 cycle with dry cooling due to the relatively high heat rejection temperature. This could make the s-CO_2 cycle more practical than the steam cycle in locations where water is scarce [13][15][16].

On the other hand, while pure and dry CO_2 is virtually inert at temperatures lower than 500°C, corrosion of steels and nickel alloys can occur when exposed to s-CO_2 at temperatures higher than 600°C, particularly in the presence of even small quantities of water and other contaminants. Materials for advanced ultrasupercritical steam cycles are designed to withstand high temperatures, however for s-CO_2 applications, the oxidation reaction kinetics and the rate of internal carburization of alloy canditates over 1000-5000 hours in s-CO_2 at high pressures (20-35 MPa) and high temperatures (650-750°C) needs to be established. Futhermore s-CO_2 is more dense than supercritical steam under the same temperature and pressure conditions, so the required mass flow rate will be much greater than it is in steam system. As a result, s-CO_2 cycles will experience high density fluid flow rates at high velocities, therefore, even a tiny amount of particles present in the s-CO_2 stream could cause substantial erosion to turbine components. Creep and fatigue of materials are potentially the major limitations to the lifetime of s-CO_2 turbomachinery and heat exchangers [14].

1.4 Advantages of Supercritical CO_2 Cycles over ORC

Organic Rankine Cycles (ORC) systems offer the possibility to select the best suited working fluid for the temperature level of the heat recovery application. A potential disadvantage of ORC media is the necessity of a further heat transfer medium between heat source and ORC due to its inflammability. Nevertheless even thermo oil, which is used for heat transfer in many cases, is combustible and so the problem is rather reduced than solved. An interesting alternative are s-CO_2 cycles for power generation, CO_2 as a working medium is harmless and no additional heat transfer cycle is necessary. Additionally, critical conditions of CO_2 (p_c=7.375 MPa, T_c=30.98°C) are advantageous for heat transfer to ambient and fluid properties of CO_2 lead to small heat recovery system dimensions. Low compressibility values for the real gas in the vicinity of the critical point create conditions for the development of closed gas turbine cycles for heat recovery, by using CO_2 as working medium.

The main advantages of CO_2 can be summed up as [17]:

- It is chemically inert, non-toxic, non-corrosive, non-stimulating and non-flammable with associated lesser maintenance costs
- It is accessible and affordable, the cost of CO_2 is only 1/10 of helium and 1/70 of organic working fluid
- The high operating pressure enables smaller size components
- S-CO_2 cycles achieve high efficiencies at low temperatures
- It is compatible with standard materials and lubricants and is not harmful to the environment
- It has potentially favorable thermodynamics and transports properties
- It is not hazardous to waters
- It has high power density
- It has low surface tension (reduced effects of cavitation in the machinery)
- It has low molecular leak due to higher molecular mass
- It is characterized by easy handling

1.5 Experimental Activities

Sandia National Laboratory

The Sandia National Laboratory (SNL) primarily explored the performance test of compressor near the CO_2 critical point. They further designed an integrated system with Barber Nichols Company and evaluated the impact of working fluid leakage. The results indicated that the prototype compressor presents a stable and controllable operation near the critical point, but windage losses in the rotor cavity and thermal losses in the vicinity of the turbine and from piping were issues of particular note [18]. The cycle layout under research is the recompressing cycle with two alternator turbo-compressors (2-TAC) and the heat introduced in the cycle reaches 780 kW_{th}. The cycle efficiency that SNL should be able to achieve with target conditions should be 31.5% and an electricity generation of 250 kW_e. The operating paramets of the system are summarized in the table 1.1, but it is aimed to reach higher turbine inlet temperatures, pressure ratio and rotating speed to reach the taget values [16][13][15].

Turbine inlet temperature [°C]	537 (target)/ 342 (achieved)
Pressure ratio [-]	1.8 (target)/ 1.65 (achieved)
Rotating speed [rpm]	75,000 (target)/ 52,000 (achieved)
Turbine efficiency	86%(turbine-1)/ 87%(turbine-2)
Compressor efficiency	67% (MC)/ 70% (RC)
Compressor inlet pressure [MPa]	7.68
Compressor inlet temperature [°C]	32

Table 1.1 – Operating parameters of Sandia National Laboratory experimental loop [16]

Betchel Marine Propulsion Company

Bechtel Marine Propulsion Corporation (BMPC) is testing a supercritical carbon dioxide (s-CO_2) Brayton system at the Bettis Atomic Power Laboratory. The 100 kW_e Integrated System Test (IST) is a two-shaft recuperated closed Brayton cycle with a variable speed turbine driven compressor and a constant speed turbine driven generator using s-CO_2 as the working fluid. The IST was designed to demonstrate operational, control and performance characteristics of a s-CO_2 Brayton power cycle over a wide range of conditions. The IST design includes a comprehensive instrumentation and control system to facilitate precise control of loop operations and to allow detailed evaluation of component and system performance. A detailed dynamic performance model is being used to predict IST performance, support test procedure development and evaluate test results.

Testing in the IST was initiated in 2012. Test operations to date included successful system startup, initial transition to electrical power generation, increased power operations and transition to load control testing using independent speed control of the turbomachinery.

IST operation has been limited in power level due to issues with the permanent magnet rotor and motor-generator controller for the turbine-generator. Remagnetization of the rotor along with motor-generator controller improvements have increased the power output capability of the generator to at least 40 kW_e.

Due to the small scale of the IST equipment, overall loop efficiency is much lower than is predicted for larger s-CO_2 Brayton cycles.

The IST component layout is shown in Figure 1.4, Figure 1.5 shows the physical arrangement of the test loop while the main operating parameters and performance are reported in table 1.2. The heat source for the IST is a 1 MW_{th} electrically heated organic heat transfer fluid system which transfers heat to the CO_2 through a standard shell-and-tube heat exchanger. The heat sink is a chilled water system which rejects heat from the PC and other heat loads to a refrigerated chiller. This chilled water system is broken into two loops so that cooling flow can always be provided to auxiliary heat loads throughout the system while the precooler can either be cooled from this chilled loop or heated during startup through a separate water loop to achieve supercritical conditions in the CO_2 .

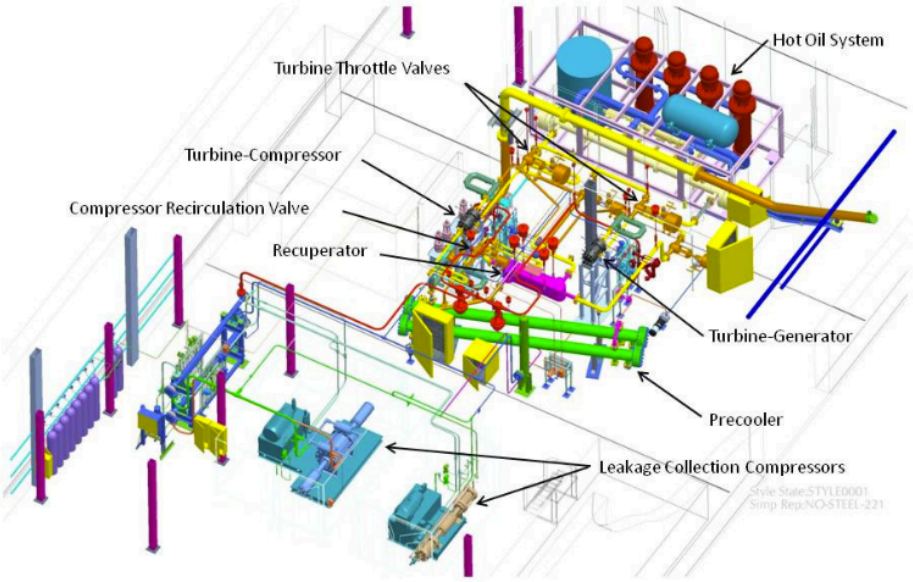

Figure 1.4 – IST component arrangement [19]

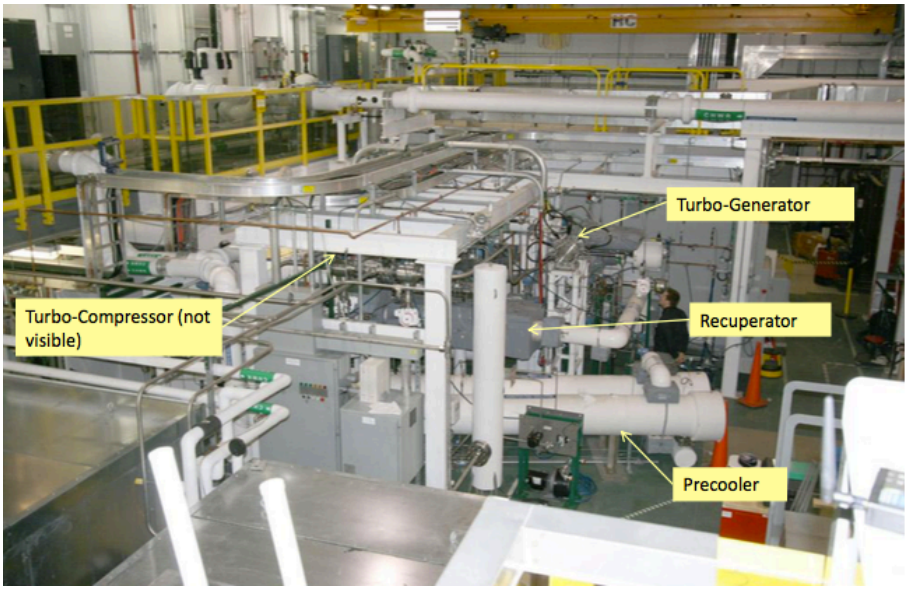

Figure 1.5 – Physical layout of the IST system [20]

Operating pressures [MPa]	9.03-13.5
Operating temperatures [°C]	36-299
Turbine efficiency	79.7% (turbine-1)/ 79.8% (turbine-2)
Rotating speed [rpm]	60,000
Electricity generation [kW_e]	40
Cycle efficiency	14.7%

Table 1.2 – Operating parameters and performances of Betchel Marine Propulsion Corporation experimental loop [13]

The IST continues to make progress in meeting its intended purpose of demonstrating controllability of the s-CO_2 Brayton cycle. The system has been operated to a maximum turbine-generator output power of 40 kW_e with the expectation that approximately 50 kW_e is achievable by operating at a higher speed and with less restrictive operating limits. The operating conditions for the loop have been modified based on this new maximum system power limit to maintain the objective of having the compressor recirculation valve at the minimum flow position at maximum system power. Testing through the full range of system power levels with the turbine-compressor operating in the thermal hydraulically balanced condition is planned to further demonstrate the controllability of the system.

The overall Brayton cycle has performed very closely to expectations for the operations performed to date. No inherent issues with the s-CO_2 Brayton cycle have been identified.

Electrical issues with the motor-generator controllers and mechanical issues with gas foil thrust bearings have limited system operating power and the amount of testing that has been able to be accomplished. These issues are a result of using equipment that is not typical of what would be used in a larger system due to the small scale and high turbomachinery speed of the IST [18][19].

Tokyo Institute of Technology & Institute of Applied Energy

Tokyo Institute of Technology is a national research university located in Greater Tokyo Area, Japan. Tokyo Institute is the largest institution for higher education in Japan dedicated to science and technology, and it is generally considered to be one of the most prestigious universities in Japan.

The development of a closed cycle gas turbine with supercritical carbon dioxide as a working fluid is under way in order to generate power from waste heat source of a low or intermediate temperature range from industry. Its demonstration test plan using a reduced scale turbomachine is described. Principal specifications are net power output of around 10 kW_e and recirculation CO_2 flow rate of 1.2 kg/s. Optimized range of compressor inlet temperatures as well as pressure are investigated under the given turbine inlet conditions of 277°C and 12 MPa respectively, moreover detailed aerodynamic design of the centrifugal compressor as well as radial turbine was executed, which resulted in that optimum rotational speed was 100,000 rpm.

The final design was the simple recuperated cycle with two recuperators connected in series. The operating parameters and performances of this test loop are summarized in table 1.3. Unfortunately cycle efficiency of could be only 7% due to the windage losses in the rotor [21].

Operating pressures [MPa]	8-12
Operating temperatures [°C]	37-277
Pressure ratio [-]	1.4
Rotating speed [rpm]	69,000
Turbine efficiency	65%
Compressor efficiency	48%
Heat [kW]	160
Net power output [kW]	10
Cycle efficiency	7%

Table 1.3 – Operating parameters and performances of Tokyo Institute of Technology & Institute of Applied Energy experimental loop [13]

Kaeri-Kaist-Postech

Korea Atomic Energy Research Institute (KAERI) has been installing a Supercritical CO_2 Brayton Cycle Integral Experiment Loop (SCIEL) to develop the element technologies for the s-CO_2 turbomachinery and compact heat exchanger with Korea Advanced Institute of Science & Technology (KAIST) and Pohang University of Science and Technology (POSTECH) joint research team.

As the s-CO_2 cycle is considered as the promising candidate for the Sodium-Cooled Fast Reactor (SFR) power conversion system, KAERI designed SCIEL with KAIST and POSTECH. The generated data from SCIEL will be utilized to simulate the steady and transient state of s-CO_2 cycle and establish the control logics for the operation scenarios such as part load operation and loss of power operation. For SCIEL design process, KAERI, KAIST and POSTECH are responsible for the overall system, turbomachinery and heat exchanger, respectively [22].

As the design pressure ratio is high, the two-stage of compression and expansion process is considered. As CO_2 behaves more like an incompressible fluid, the compressor work is reduced and therefore splitting compressor and turbine by having two separate shafts layout was considered for the SCIEL design. By utilizing the low pressure turbine (LPT) and low pressure compressor (LPC), the simple Brayton cycle can be demonstrated. For the high pressure ratio operation, the high pressure turbine (HPT) and the high pressure compressor (HPC) will have TAC configuration. The SCIEL can be constructed step by step as the compressor and turbine are not mechanically connected. Thus, the two turbomachinery operate at different rotating speed. For the heat exchanger such as recuperator and precooler, the promising candidate is the Printed Circuit Heat Exchanger (PCHE) which has been widely used for the s-CO_2 cycle research. The operational temperature and pressure of PCHE are wide and the compactness is high [23]. For the SCIEL design, a series of PCHEs will be utilized to recuperate heat. Figure 1.6 shows the 3D view of current SCIEL facility [24] and table 1.4 summerize the target operating conditions and performances.

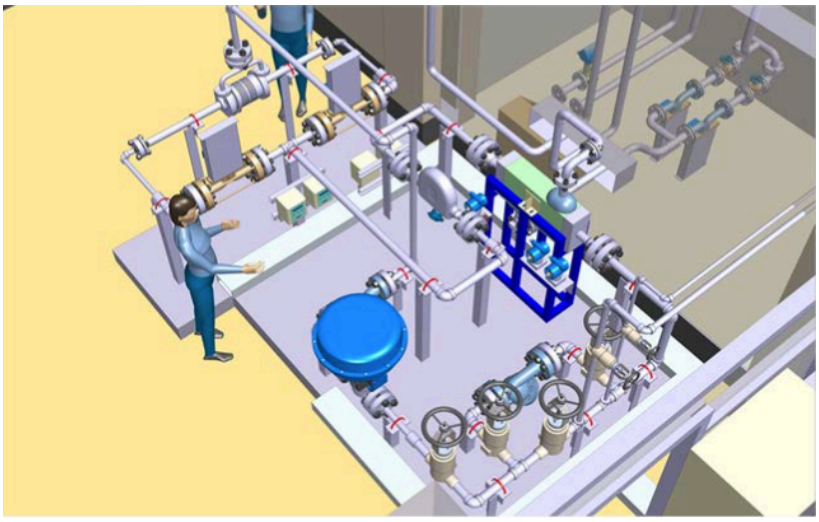

Figure 1.6 – 3D view of current SCIEL facility [24]

Operating pressures [MPa]	7.78-20 (target)
Operating temperatures [°C]	33.2-500 (target)
Heat [kW]	1,320
Pressure ratio [-]	2.67 (target)
Rotating speed [rpm]	75,000 LPT/ 70,000 LPC/ 68,000 HPT&HPC
Turbine efficiency	85%
Compressor efficiency	65%
Mass flow rate [kg/s]	6.4
HRT/LTR effectiveness	57/ 74%
Cycle efficiency	22.5% (target)

Table 1.4 – Target operating parameters and performances of SCIEL facility [13]

The objectives of SCIEL development are:

1. To accumulate the operating experience of the s-CO_2 cycle including steady state and transient operations
2. To establish the control logic for the s-CO_2 cycle power system by comparing transient simulation results to the experiment data
3. To establish a system operational strategy for startup, normal operation, normal and emergency shutdown processes for future application
4. To understand the underlying physical phenomena in component level and suggest an advanced concept for each component to improve the overall system performance in the future

Sunshot project

Southwest Research Institute (SwRI) along with its partners developed a novel, high-efficiency s-CO_2 hot-gas turbo-expander optimized for the highly transient solar power plant duty cycle profile. The team consists of SwRI; General Electric (GE); Thar Energy LLC (Thar); Bechtel Marine Propulsion Corporation, operator of Knolls Atomic Power Lab (KAPL); Aramco Services Co., and Electric Power Research Institute (EPRI). This MW-scale s-CO_2 turbo-expander design advances the state-of-art of s-CO_2 turbo-expanders from a current technology readiness level (TRL) 3 (initial small-scale laboratory-size testing) to a full TRL 6 (MW_e-scale prototype demonstration, the first MW_e-scale s-CO_2 power cycle demonstration at 700°C temperatures). A secondary objective of this project is to optimize novel PCHE for s-CO_2 applications to reduce drastically their manufacturing costs.

The s-CO_2 turbo-expander and novel s-CO_2 heat exchanger will be tested in a 1-MW_e s-CO_2 test loop, fabricated to demonstrate component performance and the performance of the optimized s-CO_2 Brayton cycle over a wide range of part-load conditions and during transient operations representative of a typical Concentrated Solar Power (CSP) duty cycle [25].

The scalable s-CO_2 expander design and improved heat exchanger address and close two critical technology gaps required for an optimized CSP s-CO_2 power plant and provide a major stepping stone on the pathway to achieving CSP at 0.06 $/kWh Levelized Cost of Electricity (LCOE), increasing energy conversion efficiency to greater than 50%, and reducing the total power block cost to below 1,200 $/$kW_e$ installed. Since the Solar Energy Technologies Office (SETO) launched the SunShot Initiative in 2011, solar has made great strides in the United States. In early 2011, solar power comprised less than 0.1% of the U.S. electricity supply with an installed capacity of just 3 gigawatts. As of 2017, solar supplies more than 1% of U.S. electricity demand with an installed capacity of more than 47 gigawatts.

The project started in 2016 (this is a five-year project) and solar office has continuously worked toward its goal of enabling solar electricity costs to be competitive with conventionally generated electricity by 2020, without subsidies. During this time, the solar industry has seen tremendous progress in cost reduction. In 2017, the solar industry achieved SunShot's original 2020 cost target of 0.06 $/kWh for utility-scale photovoltaic (PV) solar power three years ahead of schedule, dropping from about 0.28 $/kWh to 0.06 $/kWh. Building off and updating the original SunShot vision, the SETO set goals for 2030. The goals cut the LCOE of PV solar by an additional 50% to 0.03 $/kWh for utility-scale and cut the LCOE of concentrating solar power to 0.05 $/kWh for baseload power plants, while also addressing grid integration challenges and addressing key market barriers in order to enable greater solar adoption. Achieving these goals would make solar one of the least expensive sources of new electricity generation and spur growth across the country. In addition to the 50% reduction in LCOE, the solar office will work to advance grid integration solutions, including integration of solar with energy storage, enhanced grid flexibility, communications, and controls. Combining very low-cost storage (capital costs at 100 $/kWh for an 8-hour battery by 2040) with low-cost PV could enable solar energy to supply a large share of U.S. electricity by 2050 [26].

STEP project

A team led by Gas Technology Institute (GTI), Southwest Research Institute (SwRI) and General Electric Global Research (GE) has initiated a project to design, construct, commission, and operate a versatile and reconfigurable 10 MW_e Supercritical Carbon Dioxide Pilot Plant Test Facility located at SwRI's San Antonio, Texas campus. The project called STEP Demo (Supercritical Transformational Electric Power) is one of the largest scale and most comprehensive in the world. A key project goal is to advance the state-of-art for high temperature s-CO_2 power cycle performance from Proof of Concept (TRL 3) to System Prototype validated in an operational system (TRL 7). The United States Department of Energy (U.S. DOE) has awarded $84 million for this $119 million project, while cost share is provided by the team, component suppliers and other stakeholders interested in s-CO_2 technology[27].

Several technical risks and challenges will be mitigated in this project: the aerodynamics, seals and durability of turbomachinery; the design, size, fabrication and durability of recuperators; the corrosion, creep and fatigue of materials and the start up, transients and load following for system integration and operability [28].

The project has several key objectives:

1. Demonstrate the operability of the indirect s-CO_2 power cycle
2. Verify the performance of components (turbomachinery, recuperators, etc.)
3. Show the potential for producing a lower cost of electricity and the potential for a thermodynamic cycle efficiency greater than 50% at commercial scales
4. Demonstrate at least a 700°C turbine inlet temperature and a Recompression Closed Brayton Cycle (RCBC) configuration that demonstrates system and component design and performance, including generating at least 10 MW_e
5. Reconfigurable facility to accommodate future testing: system and cycle upgrades, new cycle configurations (cascade cycles, direct fired cycles, etc.) and upgrade of components

The testing will occur in two distinct phases. The initial system configuration will be the s-CO_2 Simple Cycle which comprises a single compressor, turbine, recuperator, and cooler. Heat will be supplied by a natural-gas fired heater that closely resembles a duct-fired Heat Recovery Steam Generator. In Simple Cycle testing, s-CO_2 will be delivered to the turbine at approximately 500°C and 25 MPa. This test configuration offers the shortest time to steady-state and transient data, while demonstrating controls and operability of the system, and performance validation of key components. In the second phase of testing, the system will be reconfigured to the RCBC. This is a high-efficiency cycle capable of achieving efficiencies higher than 50%, the goal of the program. In this phase, a second (lower-temperature) recuperator and a bypass compressor will be installed. The turbine inlet temperature will be increased to the target level of 715°C. This phased testing approach will address specific technical risks while minimizing added complexity at each phase [23][24].

The STEP project was launched in October 2016, it is a six-year effort with three distinct budget periods, summarized in table 1.5.

BUDGET PERIOD 1	BUDGET PERIOD 2	BUDGET PERIOD 3
Detailed Facility and Equipment Design (28 months)	Fabrication and Construction (24 months)	Facility Operation and Testing (20 months)
-System analysis, Piping and Instrumentation Diagrams (P&IDs), Component Specs -Design major equipment -Procure heat source, cooling tower and long-lead items -Materials and seal tests -Start site construction	-Complete site construction and civil works -Fabrication and installation of major equipment -Commissioning and simple-cycle test	-Facility reconfiguration -Test recompression cycle

Table 1.5 – Budget period description of STEP project [29]

NET

NET Power's investors funded the development of the plant, and they include: 8 Rivers Capital, the technology developer; Exelon Generation; McDermott and Oxy Low Carbon Ventures, a subsidiary of Occidental Petroleum. Design works for the project commenced in 2010, project agreements between the partners were finalised in October 2014, construction works started in March 2016, and commissioning phase is anticipated to start in late-2016 and scheduled to be completed in 2017. NET Power has successfully achieved first fire of its supercritical CO_2 demonstration power plant and test facility in La Porte, Texas, USA in 2018. The 50 MW_{th}, 25 MW_e plant was constructed over a two-year period, and it is said to be the world's only industrial scale supercritical CO_2-based power plant and CO_2 cycle test facility. The plant is designed to demonstrate NET Power's Allam Cycle technology, which uses a new turbine and combustor developed specifically for the process by Toshiba. The development includes combining gas turbine and steam turbine technologies in the production of the CO_2 turbine NET Power, said that it is targeting global deployment of 300 MW_e commercial scale plants beginning in 2022.

Toshiba's technology has the following potential capabilities:

- Efficiency of about 55-59% when running on natural gas
- Efficiency of about 51-52% when running on gasified coal
- 100% carbon capture with no efficiency penalty

The combustor process in the cycle is critically important, because the working fluid and pressure are different from typical heavy-duty gas turbines. The major characteristics of this combustor are:

- Zero nitrogen oxides (NO_x) emissions because of the use of oxygen as opposed to air
- The temperature is not as high as existing combustors for heavy-duty gas turbines
- The pressure is much higher than is the case in existing combustors

According to a spokesperson for NET Power, the potential market for carbon capture is enormous. "Fossil fuels provide a low-cost, reliable dispatchable fuel source. In the developing world in particular, countries are focused on using these resources. If we can affordably eliminate air emissions from the processes that use these fuels through carbon capture technologies, it will play a major role in the global energy mix going forward."

Fossil fuels are still by far the most dominant energy source worldwide, and they will remain so for decades to come, according to most projections.

With an efficiency of 55.1-58.9%, NET Power concludes that the system is comparable in efficiency with combined cycle gas turbine power plants, and expects it will be cost-competitive with combined cycle plants very quickly because of the additional revenues from CO_2 and Argon [31].

Summary of main characteristics [32]:

- Zero emissions: no air pollutants
- No water needed
- Complements renewables: NET Power is the perfect zero emissions match for intermittent renewable energy thanks to its inherent energy storage capabilities and output flexibility
- Multiple revenue streams: rather than emitting greenhouse gases, industrially useful and valuable CO_2 is captured and salable, along with other industrial gas byproducts such as Argon and Nitrogen
- Made for anywhere: the NET Power technology solution is tailored to market needs, it complements current infrastructure, available in multiple size variations, compatible with low-grade fuels, capable of water-free production, a significantly smaller land footprint and universally permittable

Allam Cycle for Natural Gas Fuel

Fuel is burned with pure oxygen. This creates CO_2 that is sent through the rest of the cycle. New CO_2 is captured and the remaining is recycled, nothing is released into the atmosphere. The cycle reuses CO_2 over and over again, which helps efficiency and makes the cost of electricity lower. Excess CO_2 that's created through the cycle is pipeline & commercially-ready to be sold to crucial industries (e.g. oil recovery, industrial and agricultural feedstock), this enhances the value of the power plant.

The Allam-Fetvedt Cycle is pretty simple and is schematically represented in Figure 1.7. It burns natural gas with pure oxygen, and the resulting CO_2 is sent through the combustor, turbine, heat exchanger, and compressor, altogether creating low-cost energy. Extra CO_2 that's produced is pipeline ready and sold to industries who need it, such as the medical, agricultural, and industrial sectors. It can also be cheaply sequestered.

Step 1: The Burn

Oxy combustion is the process of burning natural gas with pure oxygen (instead of air). When air is used as the primary oxidant, nitrogen oxides (NO_X) are released into the atmosphere. This isn't only bad for the environment, it's also less efficient. When pure oxygen is the primary oxidant, fuel consumption is reduced, and flame temperatures are increased, adding efficiency.

Step 2: The Expansion & Cooldown

The high-pressure CO_2 moves along into the turbine, where it expands and goes into the heat exchanger. Any water is removed, and the remaining CO_2 is compressed and pumped back into high-pressure.

Step 3: Reuse & Recycle

Most of the high-pressure CO_2 is reheated in the heat exchanger and returned to the combustor, where the whole cycle begins again.

Step 4: Piping

The excess CO_2 that comes from step 2 is pipeline ready. It's inherently captured, not released into the atmosphere, and can be sold to industries who need it or simply sequestered.

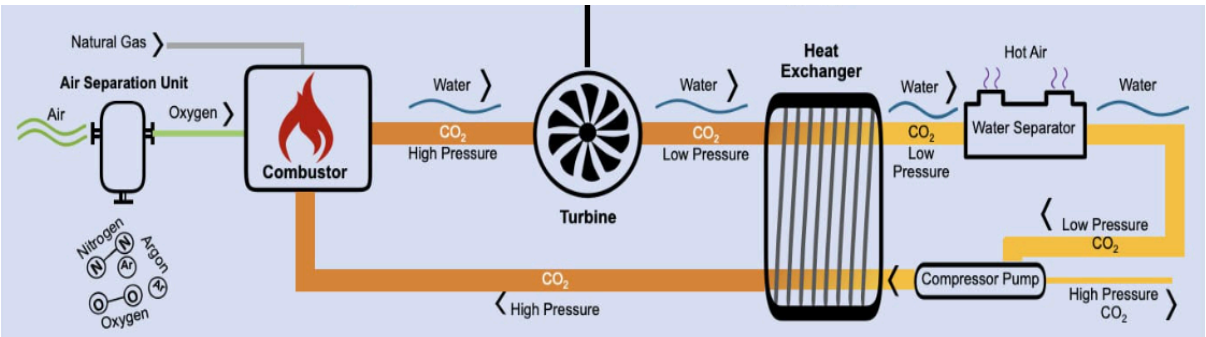

Figure 1.7 – Representation of the Allam-Fetvedt Cycle [32]

1.6 Commercial Products

Echogen Power Systems, a private company headquartered in Akron, Ohio, founded in 2007, is commercializing the harnessing of waste heat for power and cooling applications. Echogen has developed a breakthrough power generation cycle called the Thermaefficient Waste Heat Recovery Engine. It uses supercritical carbon dioxide as the working fluid. S-CO_2 is environmentally benign, non-toxic, and has favorable heat and mass transport properties which allow for an energy dense, compact thermodynamic system. Echogen's target customer groups include power generation and large energy consumers in the industrial sectors of oil & gas production and transmission, petroleum refining, chemical processing, iron, steel, glass, or any other sectors typically operating with large sources of energy loss from hot exhaust gases and residual heat in liquid product streams.

The s-CO_2 heat engine consists of five main components: exhaust and recuperator heat exchangers, condenser, system pump, and power turbine. Ancillary components (valves and sensors) provide system monitoring and control. Heat energy is introduced to the s-CO_2 power cycle through an exhaust heat exchanger installed into the exhaust stack from a gas turbine or reciprocating engine or into a flue gas stream from a fuel-fired industrial process. Echogen's technology recycles the wasted thermal energy and provides integrated power and heating or cooling with flexible system architectures, configurable for power, co-generation or tri-generation [33].

Echogen heat engine

The frst commercial 7.5 MW_e closed s-CO_2 Brayton cycle heat engine EPS100 (Fig. 1.8), developed by Echogen Energy Systems, was brought to the market in 2019. It turns waste heat from various industrial processes to electricity and operates at relatively low temperatures. A recuperated closed condensing Brayton cycle with multiple stages of recuperation and heat extraction from the primary heat source is employed by EPS100. It is designed to operate both in condensing and non-condensing modes, as the supply and temperature of the coolant permits. Under high cooling temperature and/or cooling flow conditions, the conditions at the pump are in fact supercritical. The EPS100 uses two separate turbines. One, the 'drive turbine' is connected directly to the compressor, while the other 'power turbine' is coupled to a generator for power generation. The power turbine operates at a constant speed. The turbo-compressor speed can be varied independently over a wide range to maintain the optimal flow rate for the fluid loop for the given heat source and coolant conditions. Figure 1.9 shows a simplified cycle layout of the EPS100. The heat energy of the exhaust stream from industrial processes or gas turbines is recovered through a waste heat exchanger (s-CO_2 heater) by heating a flow of compressed s-CO_2. Downstream of the s-CO_2 heater, the heated s-CO_2 flow is split into two main streams. Approximately two-thirds of the flow is directed to the power turbine, while the remainder is directed to the drive turbine that provides the shaft power for the main s-CO_2 compressor. The s-CO_2 streams exiting from the power turbine and drive turbine pass through

recuperators to preheat the CO_2 stream from the main compressor before being cooled, compressed and then sent to the s-CO_2 heater to complete the cycle. The power turbine has a single-stage radial design. The recuperators and CO_2 coolers are all of the PCHE type, while the s-CO_2 heater has a shell and finned tube design. Echogen can now provide standard heat engines scalable from 1 to 9 MW_e (net power)[34]. The commercial operation of Echogen's heat engines proves the technical and economic viability of s-CO_2 cycles for power generation.

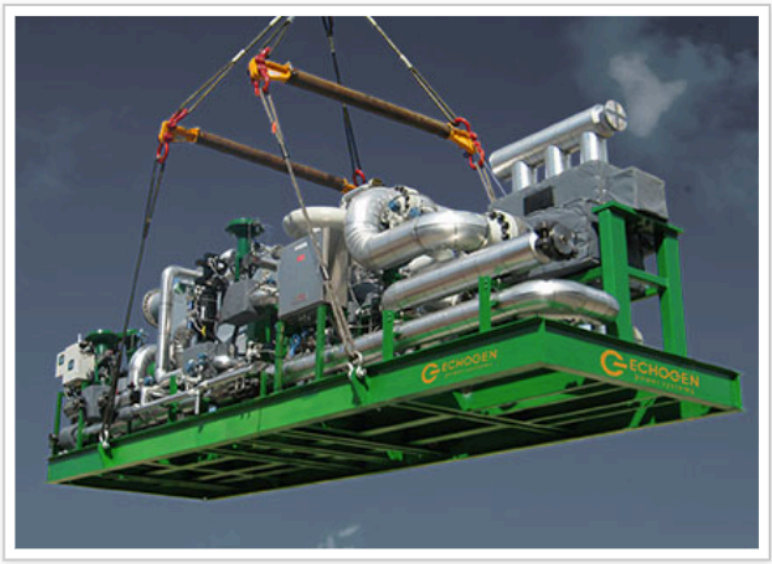

Figure 1.8 – Picture of EPS100 [33]

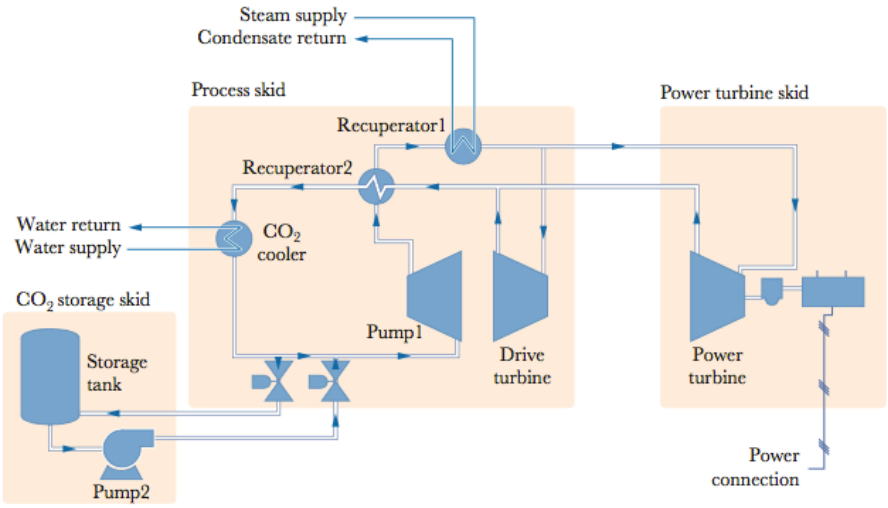

Figure 1.9 – Simplified cycle layout of EPS100 [34]

2. Supercritical CO_2 Cycles Applications

2.1 Nuclear

2.1.1 Introduction to the Energy Source

The s-CO_2 power cycle can potentially be utilized for Small and Medium sized Reactors (SMR), the International Atomic Energy Agency (IAEA) defines 'small' as under 300 MW_e, and up to about 700 MW_e as 'medium', large size conventional water-cooled reactors and Fourth Generation Nuclear Reactors. Fourth generation nuclear power, or Generation IV, implies a system of reactors and nuclear fuel cycle facilities that together may manage the weaknesses often associated with nuclear power of today.

Quick facts about Generation IV nuclear power [35]:

1) It is significantly more fuel-efficient than current nuclear power
2) Does not leave long lived radioactive wastes
3) Designed never to cause accidents with severe consequences: no scenarios are allowed where a malfunction within the facility or an external event leads to release of radioactive material to the surroundings
4) Shall be economically competitive as compared to current nuclear power and to other means of power production
5) The fuel cycle is designed so that diversion of fissile material for weapons production is unattractive, this is achieved by assuring that uranium and plutonium are never separated but only ever present mixed together and with other elements, thus the quality of the nuclear material becomes too poor to serve as weapons material, but good enough for fuelling a reactor

If all criteria are fulfilled, the nuclear system can be called fourth generation. Note that it may take various forms as there are several different reactor types that may fulfil the criteria, and there is also a range of fuels and different options for the chemical reprocessing of spent fuel. In practice, it is sufficient that the system has the ability to meet all criteria for us to refer to it as a Generation IV system. For example, it would be hard to show that a system would be cheaper than the current power production before it has been industrialised.

Since the early 2000s, numerous countries have cooperated to develop Generation IV (Gen IV) nuclear reactors. Sodium-cooled Fast Reactor (SFR), Lead-cooled Fast Reactor (LFR), Gas-cooled Fast Reactor (GFR), Super-Critical Water-cooled Reactor (SCWR), Very High Temperature gas-cooled Reactor (VHTR), and Molten Salt Reactor (MSR) were selected as Gen IV reactor candidates. Characteristics of Gen IV reactors vary in neutron energy spectrum and the fluid type used for coolant. The operating temperatures of Gen IV reactors are

commonly higher, compared with conventional water-cooled reactors, which operates around 300 °C [36].

The Generation-IV consortium seeks to develop a new generation of nuclear energy systems for commercial deployment by 2030–2040. The science base for the VHTR and SFR systems is reasonably established, although there are gaps. For the VHTR, these include the performance of graphite at high neutron doses, and the performance of the fuel. For the SFR, the behaviour of fuels containing minor actinides, and processes for their recycling and refabrication into new fuel, must be established. The GFR presents many technical challenges, because it would need fuel and structural materials capable of withstanding extremes of fast neutron flux and high temperatures. Adequate heat removal from the core under fault conditions is likely to determine its feasibility [37].

The main reason why Gen IV reactors have high operating temperatures is to increase the nuclear power plant efficiency which is currently lower than fossil fuel power plants. Therefore, the Gen IV reactor thermal efficiency can be improved with an increase of reactor outlet temperature. Furthermore, several related issues of current nuclear power plants can be solved as well. For example, the cooling water requirement for existing nuclear power plants is distinctively higher compared with those of other power plants and it is usually criticized not only from the economic but also from the environmental protection point of view. Therefore, Gen IV reactors should not only enhance thermal efficiency but also minimize the influence on the environment [38].

The denotation Generation IV is derived from the early commercial reactors constituting the first generation, the larger models being the second generation, and the modern reactors being built around the world today belonging to the third generation. The continued development thus becomes the fourth generation. (Today, water cooled reactors are the most common).

There are no systems of reactors and fuel cycle facilities in operation today that could be called Generation IV systems, but the programmes for developing breeder reactors continue and new full-scale prototypes are on their way.

In the literature the studies focus particularly on Pressurized Water Ractor (PWR), SFR; LFR and High Temperature Gas Reactor (HTGR), that are able to provide heat power in the range 100-750 MW_{th}. Operating TITs depend on the nuclear reactor and vary in the range 275-850°C.

2.1.2 Cycle layouts studied and analyzed

Simple supercritical CO_2 Brayton cycle

The Simple supercritical CO_2 Brayton cycle (Fig. 2.1) is a simple recuperated Brayton cycle adapted to the supercritical region. It is aimed at overcoming the inherent limitations presented by a standard/classic Brayton cycle, such as the very high compression work and large heat transfer areas due to a high specific volume. Taking advantage of the thermo-physical properties of carbon dioxide in the supercritical region, not only is compression work drastically reduced, but the resulting system is also much more compact and less sensitive to pressure drops [6]. The reduction of compressor work brings about a lower compressor delivery temperature

which, in combination with the low pressure ratio and recuperative nature of the cycle, enables substantially higher thermal efficiencies [4]. This process is nonetheless more complex than in a standard Brayton cycle, due to the large variations of CO_2 properties near the critical point, and it also has technological implications on the design of turbomachinery and heat exchangers [5]. Indeed, the aerodynamic design of the compressor is halfway from hydraulic to thermal machinery theory and the occurrence of an internal pinch point in the low temperature recuperator or in the cooler is also likely [39], limiting heat exchanger effectiveness and the attainable efficiency of the cycle [10]. The Simple cycle is the most essential layout composed only by five components: compressor, turbine and three heat exchangers. The CO_2 is compressed near the critical point and then heated through a regenerative heat exchanger (recuperator). The actual heat recovery from the heat source takes place in a second heat exchanger (heater). Afterwards, the high enthalpy CO_2 is expanded in the turbine and later cooled in the low-pressure side of the recuperator. Before being compressed once again in the next cycle, the working fluid at the recuperator outlet is further cooled in a third heat exchanger (cooler), in which the actual heat rejection to the heat sink takes place. This layout is often used as a reference to compare the performances of more complex configurations.

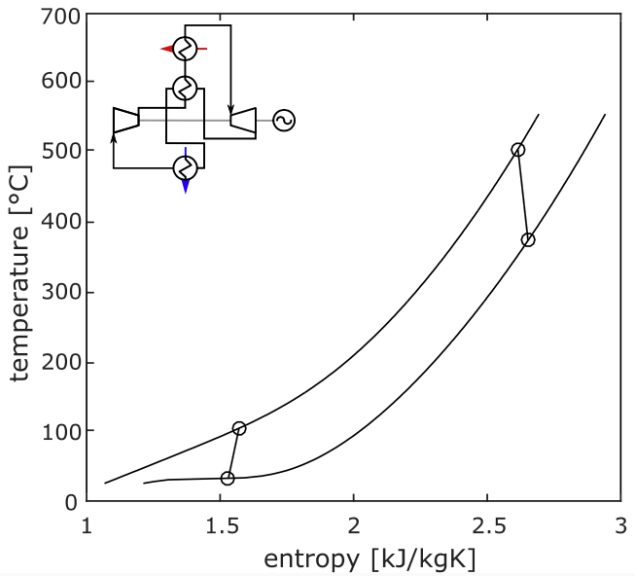

Figure 2.1 – Schematic layout and T-s diagram of a Simple supercritical CO_2 Brayton cycle for nuclear application [40]

Recompression supercritical CO_2 Brayton cycle

The Recompression supercritical CO_2 Brayton cycle (Fig. 2.2) is the evolution of the previous configuration proposed by Angelino [4][9]. In the recompression cycle, the s-CO_2 stream is split downstream the low-pressure side of the low-temperature recuperator. The recompressor is located in parallel to the main compressor, which means that there are two different flows for the compression process. The first steam flows into the cooler where its temperature is reduced to a value close to the critical temperature. The second stream is not cooled but compressed

directly in the re-compressor. The benefits of this layout are twofold. First, the pinch point problem in the low temperature recuperator is attenuated due to the change in heat capacity brought about by the dissimilar mass flow rates on the high (reduced flow) and low pressure (full flow) sides of the equipment. Second, the thermal duty of the cooler is also reduced, hence reducing the size of this equipment. This configuration is composed of a main compressor, a recompression compressor, a turbine, LTR, HTR, intermediate heat exchanger and PC. This is the most promising layout for nuclear applications as demonstrated by Dostal [10]. The recompression cycle with reheating (Fig 2.3) aimed at increasing the net power produced or intercooling (Fig. 2.4) aimed at decreasing the compression work are also investigated in the literature. Both these processes lead to higher performances of the cycle but they increase the number of components and plant complexity.

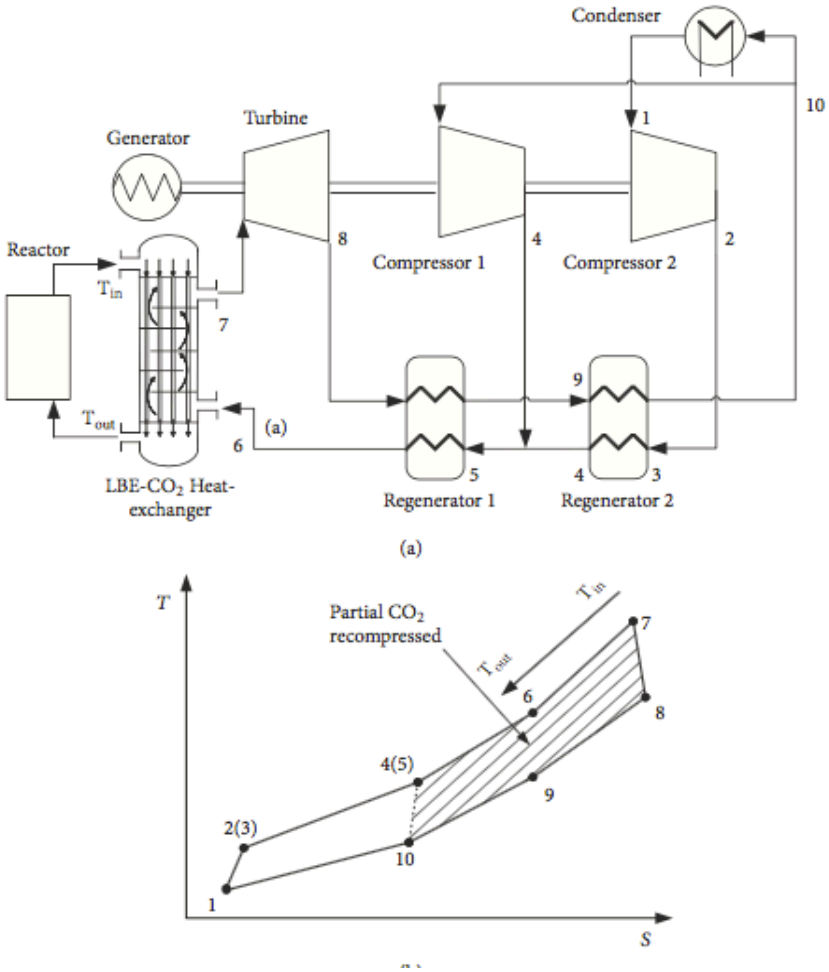

Figure 2.2 – Schematic layout and T-s diagram of a Recompression supercritical CO_2 Brayton cycle for nuclear application [41]

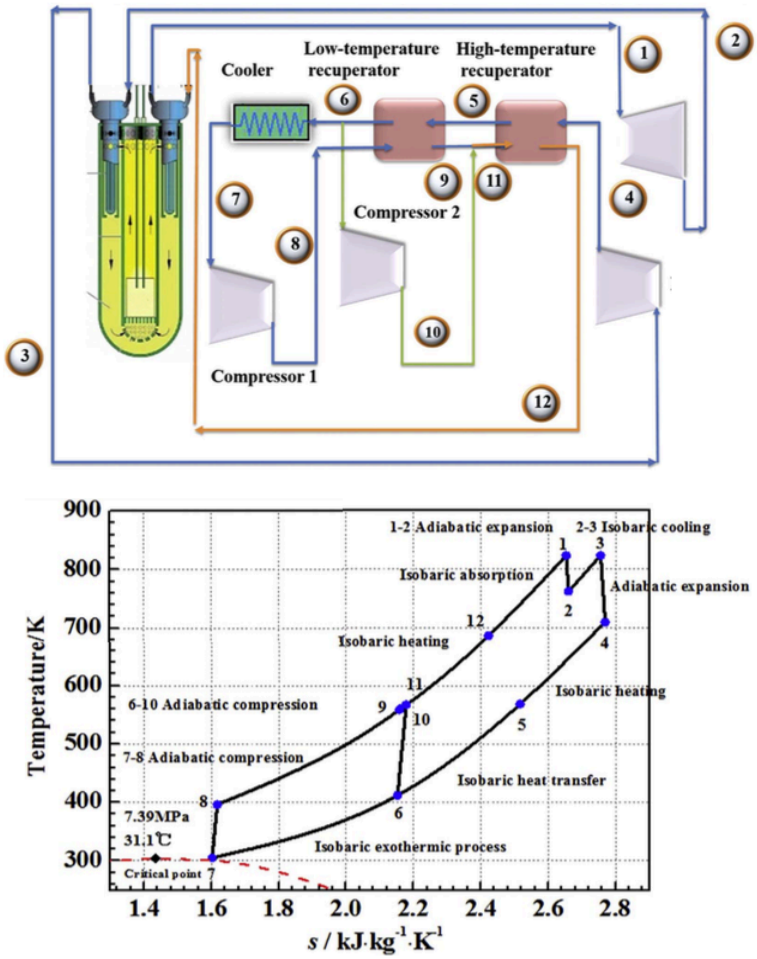

Figure 2.3 – Schematic layout and T-s diagram of a Recompression supercritical CO_2 Brayton cycle with reheating for nuclear application [42]

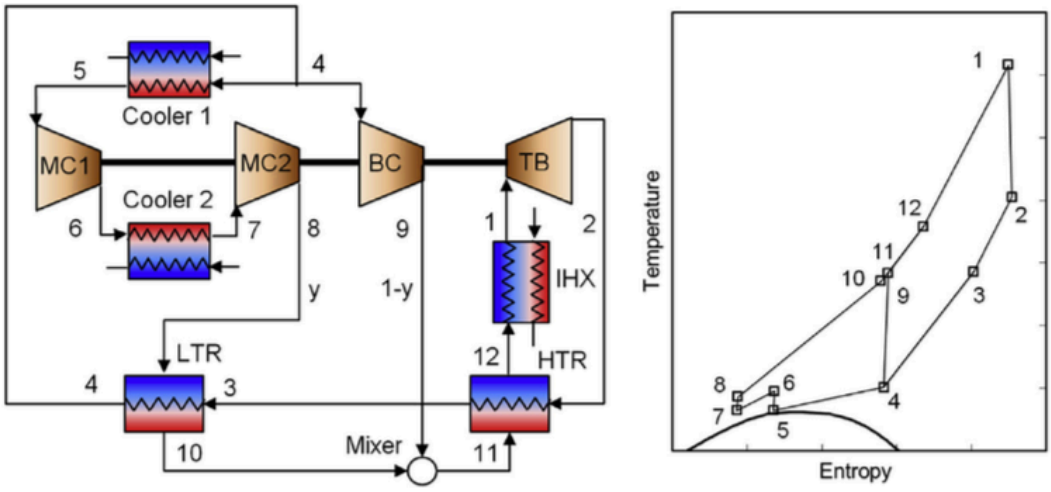

Figure 2.4 – Schematic layout and T-s diagram of a Recompression supercritical CO_2 Brayton cycle with intercooling for nuclear application [43]

2.1.3 Heat recovery unit

The cycle could be direct or indirect. In the direct cycle the s-CO_2 is at the same time the coolant of the reactor and the working fluid. Although a s-CO_2 cycle would most likely be an indirect power conversion system for nuclear application, in the the study presented by Edwin et al. [44] a direct cycle for HTGR was analyzed. The CO_2 enters the reactor where it is heated before expanding in the turbine, so that the cycle performance could be optimized and compared with results from other direct power conversion cycles without the added complication of an interface between the power cycle and a primary helium cooling loop. Even in the LFR it is possible to eliminate the intermediate cooling circuit, anyway the cycles studied in the literature are mainly indirect so there is the need to have an intermediate heat exchanger between the heat source (the reactor) and the working fluid (CO_2). The fluid that is used as the heat transfer fluid for the power cycle and the cooling fluid for the reactor depends on the type of reactor.

The Sodium-cooled Fast Reactor utilizes molten sodium metal as the reactor coolant and its operating temperature range is 500-550°C. The system's use of liquid metal provides a multitude of advantages due to the physical properties of the molten metal coolant. For example, the metal's high thermal conductivity and heat capacity creates a large thermal inertia against overheating if coolant flow is lost. In addition, sodium-based systems do not serve as neutron moderators, unlike water, which allows the use of fast neutrons. Lastly, sodium can be operated at near atmospheric pressure since its boiling point is higher than the reactor's operating temperature [45].

Disadvantages: sodium is highly reactive with air and water. A sodium leak could lead to the production of toxic sodium-oxide aerosols and explosions caused by sodium fires due to the lack of the water-fail safe that current nuclear reactors utilize. Early SFRs, constructed before, have also suffered from corrosion and sodium leaks that resulted in runaway nuclear reactions and sodium explosions. Furthermore, the fast neutrons in the core can activate sodium, causing it to become radioactive. However, the half-life of activated sodium is only 15 hours [46].

The Lead-cooled Fast Reactor is characterized by a high degree of safety, as it is based on the use of liquid lead as heat transfer fluid. Temperature range is 400-470°C. Unlike other fluids, lead requires no pressurization (the boiling temperature of lead at atmospheric pressure is 1743°C); nor does its use accidentally produce hydrogen or other explosive gases. The use of lead allows the introduction of decay heat removal systems in the primary circuit [47].

Due to the low hydraulic friction inside the core and the thermodynamic properties of lead, the LFR owns the potential to transport the reactor power totally via effective natural circulation. LFR has great safety performance under steady and transient conditions. At the same time, the coolant of LFR has stable chemical characteristics and does not react with water or air. Its feature makes the LFR system possible to eliminate the intermediate cooling circuit, which is needed in the sodium fast reactor system. As we all know, higher core outlet temperature means higher turbine inlet temperature, which could help produce very high power conversion efficiency. However, coolant lead at high temperature will bring corrosion problems for the core materials, which is still not solved for LFR development [48].

The High Temperature Gas Cooled Reactors uses Tri-Structural ISOtropic Particle Fuel (TRISO) that consists of a fuel kernel composed of uranium and oxygen in the center, coated with four layers of three isotropic materials deposited through fluidized chemical vapor deposition, full ceramic core structure, and helium as coolant. The defining characteristic of this reactor is its very high operating temperature (650-850°C), capable of running an efficient power cycle. Fuel, core structure, and coolant in HTGR can all withstand high temperature and can provide inherent safety features [49].

Pressurized water reactor is a typical commercial nuclear reactor where the coolant is pressurized water so it can not boil, are able to provide operating temperatures in the range 250-350°C.

2.1.4 Optimization Methodology

Thermodynamic optimization

The type of thermodynamic optimizations in the literature are mainly single objective with the aim to maximize the cycle first law efficiency and performed by Yichuan He et al. [41], Edwin A. Harvego and Michael G. McKellar [44], Ho Joon Yoon et al. [50], Joo Hyun Park et al. [51] and Pan Wu et al. [52].

Yichuan He et al. [41] studied the thermodynamic properties of s-CO_2 Brayton cycle for CiADS (Chinese Initiative Accelerator Driven System, heat available of 7.74 MW_{th}). The layout studied is the recompression supercritical CO_2 Brayton cycle. The influence of pressure ratio (PR), minimum temperature of the cycle, TIT and terminal temperature difference of regenerators on cycle performances were investigated and optimized to increase as high as possible the cycle thermal efficiency. Pressure drops were neglected and the constraints conditions for the cycle are the following: maximum pressure between 15 MPa and 25 MPa, minimum pressure of the cycle between 7.38 MPa and 12 MPa, outlet temperature of condenser between 31.2°C and 50°C, turbine inlet temperature (TIT) between 200°C and 370°C and the terminal temperature difference of both regenerators between 3°C and 50°C. Two algorithms were used in parameter optimization of the cycle: the genetic algorithm (GA) and the pattern search algorithm, however GA needs longer calculation time with the higher requirement of parameter setting. Compared with other nuclear power plants of s-CO_2 Brayton cycles does not have the best thermal efficiency that resulted 35.97%, but if the reactor outlet temperature increases (optimized TIT resulted 370°C, its maximum value respecting the constrains) the thermal efficiency can be improved.

Edwin A. Harvego and Michael G. McKellar [44] performed an analysis using the UniSim process analyses software to evaluate the performance of the supercritical CO_2 recompression Brayton cycle for HTGR (heat available 600 MW_{th}). The optimization is carried out studying the effect on the cycle efficiency of different TITs, recompression fractions and PRs. Main assumptions are that the highest pressure of the cycle is limited to 20 MPa and that the pinch point of heat exchangers is conservatively assumed 20°C. Results show that high power cycle thermal efficiencies can be achieved for turbine inlet temperatures in the range of 550°C to 850°C, up to 51% for the cycle efficiency and 49.2% for the net efficiency of the system.

Simplicity and compactness of the power conversion system design make this an attractive option for high temperature reactor applications.

Ho Joon Yoon et al. [50] considered SMART (System-integrated Modular Advanced ReacTor), a 330 MW_{th} integral reactor developed by KAERI as a potential candidate for applying the s-CO_2 recompression Brayton cycle. A SMR water-cooled nuclear reactor has been gaining interest due to its wide range of application due to its small size. Therefore, the combination of a s-CO_2 Brayton cycle with a SMR can reinforce any advantages coming from its small size because the s-CO_2 Brayton cycle has much smaller size components, and simpler cycle layout compared to the currently considered steam Rankine cycle. In consideration of SMART condition, the turbine inlet pressure and size of heat exchangers are analyzed by using in-house code developed by KAIST–Khalifa University joint research team. According to the cycle evaluation, the maximum cycle efficiency under 310°C optimizing the PR (even if it is observed that the cycle efficiency is not significantly influenced by the pressure ratio when the performance of turbomachinery is fixed), the SR and the length of heat exchangers (recuperators and precooler) is 30.05% at 22 MPa with 82 m^3 of total heat exchanger volume while the total volume of turbomachinery which can afford 330 MW_{th} of SMR is less than 1.4 m^3 without casing.

Joo Hyun Park et al. [51] performed the optimization of a supercritical carbon dioxide recompression Brayton cycle for three types of 300 MW_{th} small modular reactors: PWR, SFR and HTGR. The parameters PR and SR were examined for sensitivity analysis and optimization of the cycle. The inlet temperature and pressure of the compressor were fixed for all the cases and set 32°C and 7.69 MPa, while the TITs for the three cases were different and equal to 310°C, 500°C and 650°C respectively. A thermodynamic analysis model RCAM (Recompression Cycle Analysis Model) was developed in Fortran coupled with NIST-REFPROP. The optimized cycle efficiencies of PWR, SFR, and HTGR were 30.6%, 46.38%, and 50.04% respectively. PCHE are assumed in this study with an effectiveness higher than 95% and with the constrain of 5°C pinch point temperature difference to avoid damaging to component materials. Based on cycle optimization results, the required volume and length of zigzag type PCHE were estimated and also the design of turbomachinery. Moreover, the effect of channel shape of PCHE were investigated to improve cycle thermal efficiency. The study indicates that using airfoil fin type PCHE has the potential to increase the cycle thermal efficiency by nearly 1.0% in comparison with using zigzag type PCHE. These results confirm the feasibility of using s-CO_2 Brayton cycle as a power conversion system for SMRs with different turbine inlet temperatures.

Pan Wu et al. [52] developed a thermodynamic analysis solver named SACOB to provide the analysis tool. The solver includes turbomachinery models for compressor and turbine, and heat exchanger models for recuperator and precooler. The optimal design of simple Brayton cycle and recompression Brayton cycle for the LFR under water-cooled and dry-cooled conditions (main compressor inlet temperatures assumed 32°C and 55°C respectively) are carried out. The TIT is fixed at 460°C and optimization of compressor inlet pressure (CIP), turbine inlet pressure and UA coefficient of recuperators are performed leading to optimal cycle efficiencies of 40.48% and 35.9% for the recompression Brayton cycle and simple Brayton cycle under water-

cooled condition while optimal cycle efficiencies of 34.36% and 32.6% can be achieved for the recompression Brayton cycle and simple Brayton cycle under dry-cooled condition. Increasing the dry cooling flow rate will be helpful to decrease the compressor inlet temperature. Every 5°C decrease in the compressor inlet temperature will bring 1.2% cycle efficiency increase for the recompression Brayton cycle and 0.7% cycle efficiency increase for the simple Brayton cycle.

In the literature there are also few multi-objectives optimizations. The result of a multi-objective optimization is a Pareto curve if the objectives of the optimization have a conflicting relation. Every point on the curve is an optimum solution. Multi-objective optimizations are performed by Q.H. Deng et al. [53] with net power output and exergy efficiency as its objectives and by H.S. Pham et al. [43] with cycle first law efficiency and recuperation power as its objectives.

Q.H. Deng et al. [53] in their work studied the influences of some key parameters on supercritical CO_2 recompression Brayton cycle (RBC) thermodynamic performance for nuclear applications. The exergy destruction of the main components and the multi-objective parameter optimization with net power output and exergy efficiency as its objectives of s-CO_2-RBC are carried out and performed by Non-dominated sorting Genetic Algorithm (NSGA-II). The optimization variables are the TIT (that varies in the range 450-650°C) and the pressure ratio (that varies in the range 1.2-8). Main assumptions are the minimum temperature and pressure of the cycle set to 32°C and 7.7 MPa. Main findings are that the Pareto optimal relation curve indicates a conflicting relation between the cycle net power output and exergy efficiency, that result 37-42 MW_e and 63%-72% respectively. At different cycle heat source temperature, the optimal pressure ratio rise with cycle heat source temperature increasing, the exergy destruction of heater, cooler, turbine and main compressor rise while HTR exergy destruction decrease.

H.S. Pham et al. [43] investigated two typical nuclear applications: low temperature and medium-high temperature. A SMR featuring a current generation PWR has been chosen as an example of a low temperature range case. Parametric studies of a recompression cycle featuring a TIT of 275°C have guided investigations regarding optimal operating conditions depending on a balance between cycle efficiency and recuperation power. Options for performance improvement such as reheat have been investigated for a maximum cycle pressure of 20 MPa and compressor inlet temperature of 35°C. The optimization was carried out with CYCLOP (CYCLe Optimization) the CEA tool for power conversion cycle modeling allowing all cycle parameters to be modified and optimized using the deterministic Nelder-Mead algorithm, coupled with NIST-REFPROP. The highest thermal efficiency (29.3%) was found for the recompression cycle with single reheat optimizing the split ratio and compressor inlet pressure. Moving to a higher temperature range, the s-CO_2 cycles has been studied at a TIT of 515°C for a test case application to SFR. The recompression cycle operating at a compressor inlet temperature of 35°C provides a maximum efficiency of 43.9% and features an optimal IHX inlet temperature of 347.8°C. However the considered application requires that this temperature should be kept below 330°C. Work has been carried out to optimize the cycle with regard to this specific constraint through several options including the modification of the operating

conditions and the investigation of other cycle configurations. The recompression cycle with intercooling is finally identified as the most interesting one since it achieves the same efficiency of the optimized recompression cycle and features an optimal IHX inlet temperature of 330°C even though it has a smaller recuperation power (1.77 MW_{th} vs 1.66 MW_{th}).

Thermo-economic studies

There is a lack in the literature about thermo-economic optimizations. This is mainly due to the fact that the s-CO_2 cycles are studied to be applied to the IV Generation nuclear reactors, that are not in commercial market yet, so there is still a lack of information about the cost of the reactor (they are prospected to be commercially available in 2030-2040). There is an important economic analysis performed by Ming-Jia Li et al. [54] that provide a comprehensive thermodynamic study and cost-benefit analysis on the miniaturized LFR system comprising s-CO_2 power cycle and the feasibility of its commercial operation. According to the wide application of miniaturized LFR system, a right decision from the economic perspective needs a detailed thermodynamic investigation as well as the cost-benefit analysis. Main parameters of thermodynamic analysis and economic analysis were based on the National Standards of Chinese Industry and the realistic financial and cost estimating assumptions in China. There are some conclusions drawn from the study that are summarized as follows. First, the optimization performance of thermodynamic model of the LFR power generation system comprising reheating recompression s-CO_2 Brayton cycle has been obtained primarily. The main results obtained with GA demonstrate that optimizing TIT, pressure ratio, split ratio and RPR, resulted in a TIT of 465°C, pressure ratio of 3.18 and RPR of 0.4 the thermal efficiency of the reheating recompression s-CO_2 Brayton cycle is 43.72% while the maximum pressure of the cycle and the minimum temperature of the cycle are fixed and respectively 25 MPa and 32°C. The efficiency of the LFR generation system comprising reheating recompression s-CO_2 Brayton cycle is 41.53%. Finally, the electricity production costs (EPC) and cost-benefit analysis are analyzed based on the thermodynamic models. The EPC of LFR generation system is 0.0536 $/kWh, which is lower than the average electricity price in China (0.0632 $/kWh), therefore the reheating recompression s-CO_2 Brayton cycle is the primary choice of the miniaturized LFR system, and the investment for commercialization of the system is feasible.

Optimized cycles layout, efficiencies and costs

The most studied layout for the nuclear application is the Recompression Brayton cycle. This is because it has the benefits of the Simple cycle, in particular low complexity and components but huge gains in terms of efficiency as demonstrated by H.S.Pham et al. [43]. The main parameter that influences the cycle first law efficiency is the TIT even if in most of the studies in the literature is constrained as a fixed parameter depending on the particular nuclear reactor assumed in the analysis. For the nuclear reactors characterized by lower TITs such as PWR, SMART and CiADS the first law efficiency of the cycle varies from 29.3% to 36%, while for higher TITs an efficiency close to 50% is achievable as demonstrated by Edwin et al. [44] and Joo Hyun et al. [51]. The recompression cycle shows its very high performance also in terms

of exergy efficiency as by reported by Q.H. Deng et al. [53] (63.57-73% for TITs 450-650°C) in their two-objectives optimization. To further increase the performance of the cycle it is possible to add a single reheating, and, as demonstrated by Ming-Jia Li et al. [54] it seems also to be economically feasible at least for SMR (net power 10 MW_e) resulting in an electricity production cost of 0.0536 $/kWh, which is lower than the average electricity price in China (0.0632 $/kWh).

Research projects

Reactor cores in nuclear power plants still generate 'decay heat', even once their fuel's chain reaction has stopped. This radioactive residual heat has to be transferred to a heat sink. Removal systems usually depend on external power supplies, active triggers and water availability. The EU-supported sCO2-HeRo project (coordinated by Universitaet Duisburg-Essen) avoids these dependencies, making its heat removal process more efficient, more reliable and safer. Powered by the decay heat itself, independent of external power supplies, sCO2-HeRo is automatically activated and self-sustaining. Additionally, as the highly compact cooling system uses supercritical carbon dioxide and air for the heat sink, it doesn't rely on water. Putting the system through its paces sCO2-HeRo's innovative idea was to actually harness the waste heat from power plants to enable its own removal. Project partners were assigned system elements to build and test. The compact heat exchanger, turbomachine and sink heat exchanger were all finished, tested and validated, using numerical simulation tools to ensure component quality. One challenge which the team addressed was how to start the system without battery power. They did so by using a pressurised reservoir which stores CO_2. Release of the pressure turns the turbomachine, which drives the cycle. For further testing, the components were integrated into a demonstrator glass model, with positive results. Additionally, to investigate the system's ability to deal with accident scenarios, the project started to apply the German ATHLET nuclear code, which simulates the flow of heat and steam in a nuclear power plant. While nuclear power offers a promising energy pathway that could significantly reduce CO_2 emissions, acceptance will be determined in part by public confidence in its safety. sCO2-HeRo's heat removal activation, independent of reactors, helps build this. Furthermore, the team is confident that the system will extend the period of safe heat removal during a station blackout, with its ability to also generate electricity proving extremely valuable. To take the technology forward, team members are currently undertaking a follow-up project, sCO2-4-NPP (selected for funding by the European Commission) started in September 2019 until the end of 2022, which will improve thermal hydraulic system codes. A highlight will be the use of a nuclear plant simulator of a pressurised water reactor, which is a 1:1 copy of the control room of a nuclear power plant, with all signals in real time. A virtual model of the sCO2-HeRo will be attached to a pressurised water reactor to evaluate heat removal. Although the team have so far applied the system to existing reactors, its design allows for integration into future (Generation 4) reactors. "Once we have demonstrated the system's ability during accidents, we will work with national safety authorities and nuclear power plant operators for implementation," says project coordinator Prof. Brillert. "There is a long way to go, but our iterative approach means that we have already integrated stakeholder feedback, saving time later."[55][56]

2.1.5 Typical assumptions

All the papers and the studies in the literature make several assumptions for modeling the s-CO_2 cycles. Many of these assumptions are about components performances such as turbomachinery efficiencies or effectiveness of recuperators, pinch point temperatures and pressure drops (sometimes neglected for simplicity) in heat exchangers. All these assumptions are obviously reasonable depending on the case study, size of the plant, application, mass flow rates, operating pressures and temperatures. The main assumptions in the papers analyzed for nuclear application are:

Turbine efficiency: in the analyzed papers the turbine efficiency is assumed in the range 87-93%. The lowest efficiency value (87%) is assumed by Yichuan He et al. [41], the characteristcs of the turbomachines are not specified in the paper but this value is probably correlated to the small size of the system (2.78 MW_e, the smallest size among the paper studied). Higher value of efficiency (90%) is assumed by Edwin A. et al. [44], Q.H. Deng et al. [53] and Ho Joon et al. [50], considering an axial turbine and the larger size of the plants (respectively about 300 MW_e, 37-42 MW_e and about 100 MW_e.) The highest values 92-93% are adopted by Joo Hyun et al. [51], Ming-Jia Li et al. [54] in the first case according to higher size of the plant and in the second case according to the two stage expansion (reheating). Distribution of the values show an average around 90%. Lower values should be adopted for small size plant while higher values for larger size plant or a multi-stage expansion.

Compressor efficiency: in the analyzed papers the compressor efficiency is assumed in the range 80-89%. The lowest efficiency value (80%) is assumed by Q.H. Deng et al. [53], the characteristcs of the turbomachines are not specified in the paper but this value is probably correlated to the very high compression pressure ratio 4.33-5.34 (the highest among the papers studied). Higher value of efficiency (88-90%) is assumed by Edwin A. et al. [44],Ming-Jia Li et al. [54], Pan Wu et al. [52], H.S. Pham et al. [43] and Ho Joon et al. [50],considering a much lower pressure ratio of 2.3-3.2.

HTR effectiveness: in the papers studied the HTR effectiveness is assumed in a small range of 92-96%, very high values of effectiveness but this is consistent with the fact that usually the HTR is balanced in terms of capacitance of the hot and cold stream. In any case the smallest value of effectiveness (92%) is assumed by H.S. Pham et al. [43] according to the constraint to have a minimum pinch point temperature in recuperators higher or equal than 10°C, while the highest values of effectiveness are assumed by Joo Hyun et al. [51] assuming Zig Zag type PCHE (very compact and efficient heat exchangers) constraining the pinch temperature in recuperators at 5°C.

LTR effectiveness: in the papers studied the LTR effectiveness is assumed in the range of 88-95%, the effectiveness is slightly lower with respect to HTR. The smallest value of effectiveness (88%) are assumed by Ming-Jia Li et al. [54] that assumes Shell&Tubes heat exchangers, while the highest values of effectiveness are assumed by Joo Hyun et al. [51] assuming Zig Zag type PCHE (very compact and efficient heat exchangers) constraining the pinch temperature in recuperators to be 5°C.

2.2 Coal

2.2.1 Introduction to the Energy Source

Coal is abundant (economic), secured (widespread all over the world) and easy to integrate on existing electricity networks. However, coal contributes to global warming (coal combustion released 30% of world CO_2 emissions nowadays). In this context, developing efficient and economic methods to reduce CO_2 emissions represents a challenge in the coal power engineering field. The next two methods are considered as the most promising ways to reduce coal combustion CO_2 emissions:

- reducing flue gas CO_2 content with Carbon Capture and Storage (CCS) systems,
- reducing the coal consumption of a given fleet of power plant (and thus CO_2 emission levels) by improving global power plant efficiency [57].

As no other technologies can significantly reduce emissions from fossil fuel power generation systems, which are predicted to play an important role in the future electricity portfolio, CCS is seen as crucial to decarbonising the power sector. Regardless of significant reductions in the energy intensity of mature CO_2 capture and separation technologies, integration of CCS to fossil fuel fired power plants is still expected to reduce the net efficiency of the entire system by at least 7.2% points. Importantly, reduction in the net efficiency and the capital cost associated with CCS have been shown to lead to at least 60% increase in the electricity cost. The higher the plant efficiency the lower the energy penalty induced for capturing CO_2. Therefore, to provide incentives for CCS deployment in the power sector, less energy- intensive technologies, such as solid looping cycles, are currently being developed. Carbonate looping (CaL), which is based on the reversible carbonation reaction of CO_2 with a metal oxide, such as calcium oxide, is regarded as an emerging technology for decarbonisation of fossil-fuel-fired power generation systems. This is because it has the potential to reduce the net efficiency penalties to 2.4% points. The main reason behind such an improvement, when compared to the mature CO_2 capture and separation technologies, is the high temperature operation of CaL (600–900°C) [58].

In the past decades, the s-CO_2 Brayton cycle has attracted lots of scholars' attention due to compact components and excellent power conversion efficiency. The net efficiency of a coal-fired s-CO_2 Brayton cycle is more than 48% at a turbine inlet temperature of 650 °C, while that of a steam Rankine cycle is only 45% approximately. Unfortunately, due to the limitation of high temperature resistant materials, it is very difficult to further improve the efficiency of current coal-fired station. Recent research to improve overall coal power plant efficiency have led to conceptual design of Advanced Ultra-Supercritical (A-USC) power units that require new nickel-based superalloys to reach water-steam operating conditions up to 35-37.5 MPa and 700-720°C. A-USC power plant theoretically leads to about 50%-Lower Heating Value (LHV) net efficiency (without CCS system). Currently, A-USC systems are not seen as economical especially because of components manufacturing costs (nickel-based superalloys). The s-CO_2 Brayton cycle has been shown to have significant efficiency benefits, especially when the

operating temperature is above 600°C, therefore it has a great potential for newly built coal fired power plant due to its high efficiency, simple system and less carbon emission [57].

There are many types of coal-fired boilers such as pulverized coal fired boiler, fluidized bed boiler, pressurized boiler etc. The available studies focused on pulverized coal fired boiler to drive s-CO_2 cycle and Pressurized Fluidized Bed Combustion (PFBC) boiler, theoretically able to provide heat power in the range 600-2000 MW_{th}, while the operating TITs for this application are 600-700°C.

2.2.2 Cycle layouts studied and analyzed

Recompression supercritical CO_2 Brayton cycle

Studies concerning the integration of s-CO_2 cycles within coal-fired power plants (SCPP), with a focus on power cycle configuration and performance evaluation, have begun in the last few years. System optimizations and evaluations are based on recompression s-CO_2 Brayton cycle. The basic scheme of coal-fired power plant integrated with a recompression s-CO_2 cycle and its T-s diagram are shown in Fig. 2.5. The heat exchangers of the boiler include gas wall (GW), high-temperature superheater (HSH), low-temperature superheater (LSH), economizer (ECO), and air preheater (APH). The low-temperature and low-pressure s-CO_2 is pressurized in the MC, enters the LTR and the HTR to recover the heat of the high-temperature exhaust gas of the turbine (TU), and is sequentially heated by the ECO, GW, LSH, and HSH in the boiler. The high-temperature and high-pressure s-CO_2 expands to generate power in the turbine. The turbine exhaust gas is sequentially cooled in the HTR and the LTR. It then splits into two parts: one cools in the precooler and the other mixes with s-CO_2 at the cold side outlet of the LTR [59].

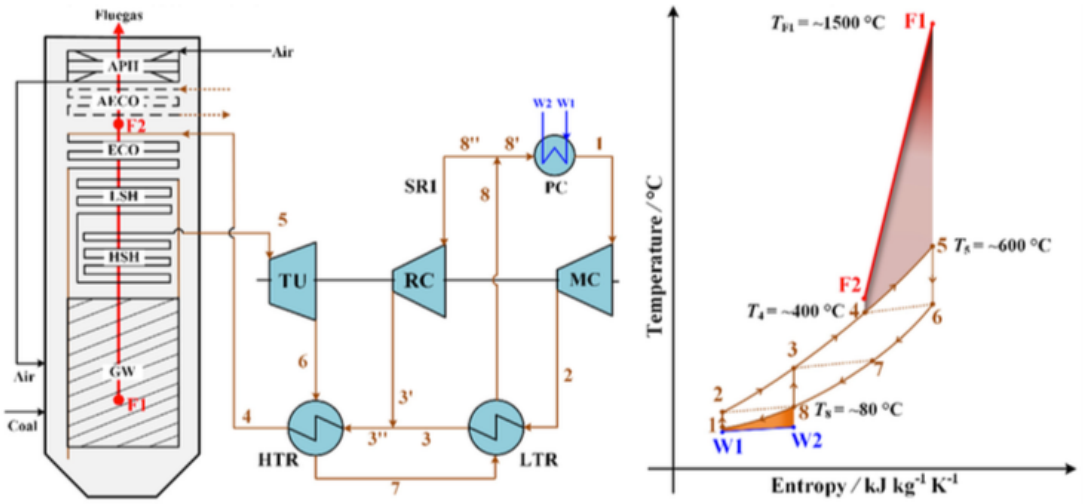

Figure 2.5 – Schematic layout and T-s diagram of a Recompression supercritical CO_2 Brayton cycle for coal application [59]

Recompression supercritical CO_2 Brayton cycle with single or double reheating

The fluegas of coal-fired boiler is a variable-temperature heat reservoir, and its available heat exits in a large temperature range from about 1,500°C to 100°C. The highest temperature of s-CO_2 cycle (TIT) is restricted by the material selected to construct the power plant, which is about 650°C. Therefore, the fluegas exothermic curve and the s-CO_2 endothermic curve are not well matched, causing a large irreversibility of heat transfer. Single or multiple stage reheats (Fig. 2.6) is an effective way to address this issue. An important investigation of the performance gains of the recompression cycle with single or double reheat is performed by Mecheri and Moullec [57]. They also highlighted that a recompression cycle is mandatory for this application, the difference between this option and a Simple cycle is more than 4.5% points of efficiency. This gain of efficiency is directly linked to the reduction of the recuperator "pinch-problem'' as already explaned before for nuclear application. A first reheat in the cycle increases the efficiency by 1.5% points at the optimal pressure ratio, regardless of the maximal temperature of the power cycle. This modification is therefore very interesting. Adding a second reheat in the cycle increases the efficiency by 0.5% at the optimal pressure ratio and for a 600°C turbine inlet temperature. This improvement decreases while the turbine inlet temperature increases, leading to no improvement when the TIT reaches 800°C. Another interesting study on the efficiency improvement with reheat stages (up to four) is performed by Ming Liu et al. [59] where the huge efficiency gains thanks to single reheat (1,77%) and second reheat (0,5%) for a TIT and TIP of 600°C and 30 MPa respectively are demonstrated.

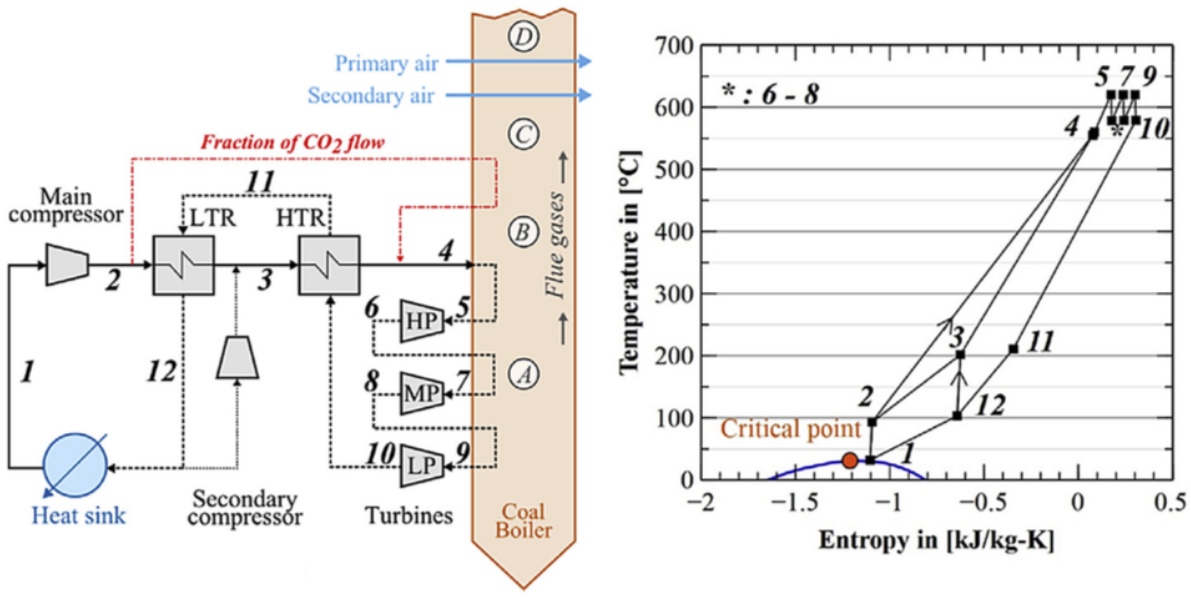

Figure 2.6 – Schematic layout and T-s diagram of a Recompression supercritical CO_2 Brayton cycle with double reheating for coal application [57]

Recompression supercritical CO_2 Brayton cycle with double reheating and intercooling

The cycle in Fig. 2.7 it is a recompression cycle, for which all the main characteristics have already been described before but it presents the addition of both double reheat and intercooling increasing at the same time the performances and the complexity of the layout.

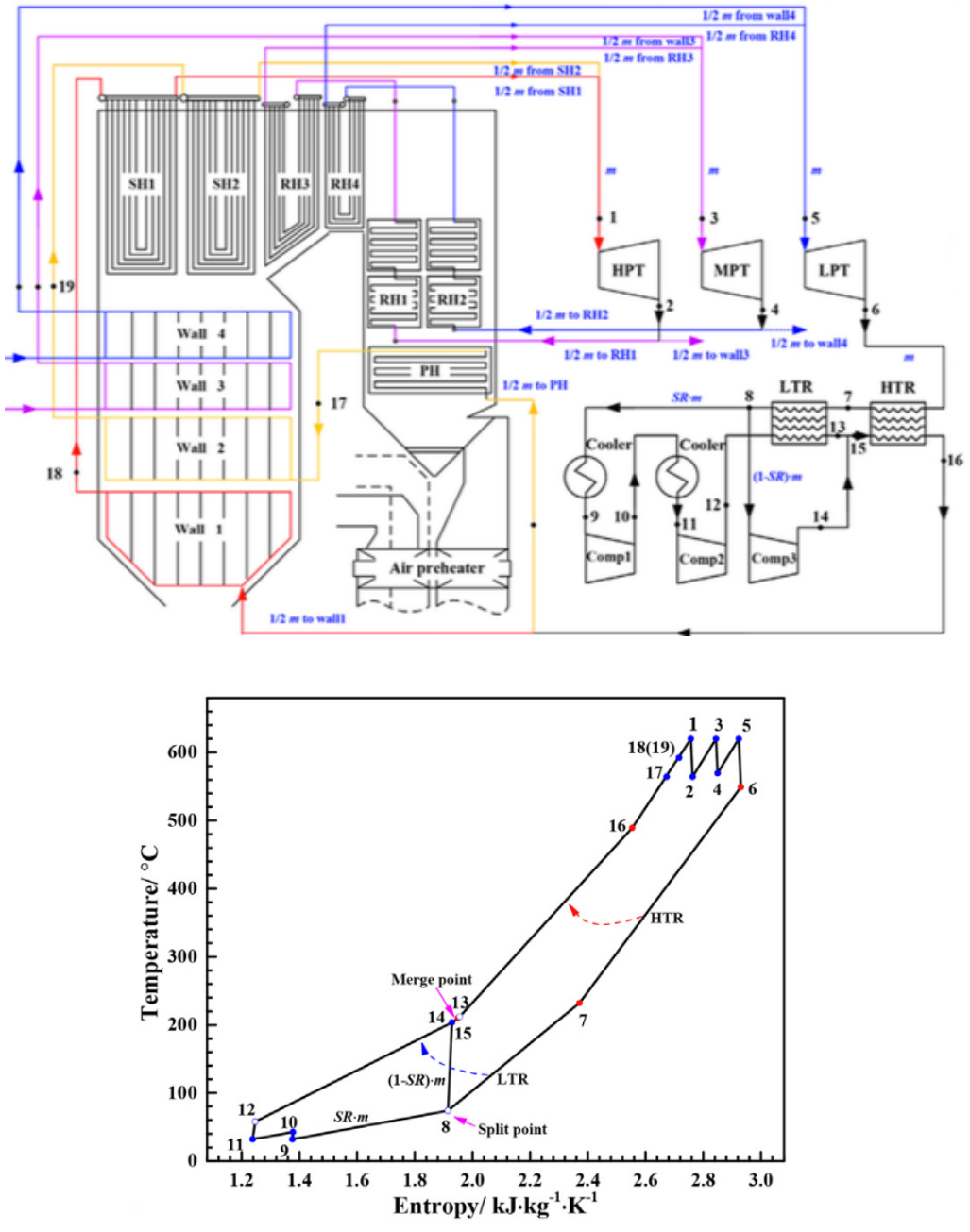

Figure 2.7 – Schematic layout and T-s diagram of a Recompression supercritical CO_2 Brayton cycle with double reheating and intercooling for coal application [60]

2.2.3 Heat recovery unit

The heat recovery unit for coal application is the boiler. The boiler includes the Gas cooling wall and Superheater (GSH), optional First-stage Reheater (FRH), optional Second-stage Reheater (SRH), ECO, Medium-Temperature Economizer (MTE), and APH. A s-CO_2 flow is split and send to the MTE (it is called in different ways in the papers such as split economizer or low temperature economizer but it is always a second economizer for the recuperation of medium heat due to a split fraction that could be placed in different locations in the cycle such as after the RC, after the MC, before the HTR, etc.) to cool the fluegas. This arrangement is necessary to further cool the fluegas in the MTE to a suitable temperature to enhance the boiler efficiency and ensure the suitable operation temperature of selective catalytic reduction denitrification. Then, the feed s-CO_2 is heated in ECO and GSH successively, and high-temperature and high-pressure s-CO_2 is sent to high-pressure turbine (HPT) to generate power. The exhaust s-CO_2 of HPT and medium-pressure turbine (MPT) (if it is present) are all sent back to the boiler for the optional reheating in FRH and SRH. There could be more that a split fraction of the mass flow rate to enhance the heat recuperation and to increase the boiler efficiency (even up to four). The split ratios (proper mass flow rate is set, so that the required heat duty of the s-CO_2 cycle matches with the distribution of the capacity of the flue gas from the boiler), the layout of the boiler, the air preheater (that has to be adapted to the boiler) and the cycle layout (with its split ratios) are also optimized, often as a preliminary step of the study focused on the optimization of the parameters of the cycle.

Jia-Qi Guo et al. [60]in their work firstly pointed out the differences between the conventional steam boiler and s-CO_2 boiler. Three layouts of the water-cooling wall are compared in the aspect of the hydrodynamic characteristic and structural parameters to select the suitable one coupled to the s-CO_2 cycles. To reduce pressure drops of the s-CO_2 boiler and improve the thermal efficiency of the s-CO_2 coal-fired power plant, the split flow strategy and module design of vertical tubes are applied. Furthermore, the differences between the conventional steam boiler and the s-CO_2 boiler are revealed and the following conclusions were drawn: once-through layout of water-cooling wall is no longer suitable for s-CO_2 boiler. The s-CO_2 boiler has about 8 times larger mass flow rate of working fluid than the conventional steam boiler, resulting in fatter s-CO_2 boiler with larger diameter and more water-cooling tubes when the once-through layout of the water-cooling wall is used. In conclusion, the s-CO_2 boiler is not economic competitive when using the once-through water-cooling wall layout. The vertical tubes layout of water-cooling wall with module design method is beneficial to design an economic s-CO_2 boiler. The split flow strategy is helpful in decreasing the diameter and number of the water-cooling wall tubes with mass flow rate through each part of the water-cooling wall reduced by 1/2 to the total mass flow rate of the system. The vertical tubes of the water-cooling wall with the split flow strategy applied is more suitable for the s-CO_2 boiler for its reasonable structural parameters and higher thermal efficiency of cycle.

2.2.4 Optimization Methodology

Thermodynamic optimization

The kind of thermodynamics optimizations in the literature are mainly single objective for the coal application with the aim to maximize the plant first law efficiency, performed by Ziwei Bai et al. [61], Hongzhi Li et al. [62], Ming Liu et al. [59] and Mounir Mecheri and Yann Le Moullec [57], Yifan Zhang et al. [63].

Ziwei Bai et al. [61] investigated a novel supercritical carbon dioxide Brayton cycle (starting from a recompression cycle with intercooling) with a bleeding anabranch used in coal-fired power plants. The anabranch flow can, first, deliver part of the s-CO_2 flow with a proper temperature to utilize the medium temperature heat in the boiler, and then, decrease the mass flow rate of the HTR cold side to minimize the temperature difference in the recuperators. Main assumptions are that the minimum temperature difference in recuperators is set at 6°C and the compressor inlet temperature and pressure are fixed respectively at 32°C and 7.4 MPa. Starting from a reference layout, varying the maximum pressure of the cycle and the TIT it is shown with a simulation of the plant with Aspen Plus that the cycle can achieve higher efficiencies (52.33% gross cycle efficiency and 49.5% net low heat value efficiency with 29.6 MPa/650°C). A further increment of 1% in gross cycle efficiency can be achieved with the decrement of 5°C pinch temperature difference or 0.07 MPa pressure loss in the recuperators. The simulation indicates that an increment of 2.14% in gross cycle efficiency can be further achieved with 37 MPa/700°C. Besides, the parameter of the bleeding anabranch does not affect the cycle performance. The cycle performance remains constant with variable flue gas inlet temperature of the air preheater but affects the proportion of the medium-temperature heat of the flue gas on the contrary. Therefore, the novel cycle configuration is suitable for the s-CO_2 cycle to utilize the medium-temperature heat in flue gas and for the boiler to design its air preheater. The feasibility of this novel s-CO_2 cycle coupled with a coal-fired power plant is demonstrated.

Hongzhi Li et al. [62] in their study evaluated the coal-fired s-CO_2 power cycle in terms of both the whole thermodynamic cycle layout and the preliminary assessment of key components. The effect of several key factors such as turbine inlet parameters, compressor inlet parameters and two split flow ratios were analyzed by an in-house code developed in Fortran for the purpose of optimization design of a 300 MW_{th} commercial scale coal fired power plant. The proposed recompression and reheat cycle with two split ratios (one split to the recompression compressor and one to MTE) tailored for coal-fired power plants can achieve 50.2% net efficiency assuming the key components could be carefully designed to meet the high standard requirements optimizing the split ratios, the low turbine inlet pressure and the inlet temperature of recompressor. The two split ratios have great effect on cycle performance. It is consistent with previous studies that there exists an optimum split ratio to RC for a given working condition and the optimum value is decreased with the increase of the pressure ratio. However, due to the unbalance of heat capacity between the HTR cold side and hot side, there exists an optimum range not a fixed value of split ratio to MTE. As the mass flow rate of s-CO_2 sent to MTE is sufficient to cool down the flue gas to a reasonable value, the net efficiency achieves maximum and remains unchanged for a certain range. The compressors and turbines are required to

achieve the high industry level with compressors efficiency of 89% and turbines efficiency of 94%, the turbine inlet temperature and pressure are set at 600°C and 32 MPa, while the main compressor inlet temperature and pressure are set as 32°C and 7.6 MPa. The counter flow PCHE with semicircular straight channels has been chosen for the HTR, LTR and PC due to simplicity and highly effective compact heat exchangers with pinch temperature as low as 5°C.

Ming Liu et al. [59] based on a benchmark coal-fired power plant integrated with a recompression s-CO_2 power cycle, calculated and compared quantitative efficiency enhancements of system improvements of the hot end and cold end for s-CO_2 power cycle. The optimized efficiency of benchmark coal-fired plant integrated with recompression s-CO_2 power cycle is performed with GA and obtained working on four key parameters: MC inlet temperature and pressure and turbine inlet temperature and pressure. The efficiency resulted 50.66% for the cycle and 45.43% for the plant. The optimization ranges of parameters are chosen similar to traditional coal-fired power plants with water as working fluid: TIT in the range 500-600°C, TIP in the range 20-30 MPa, compressor inlet temperature (CIT) in the range 35-42°C and CIP in the range 7.4-8.4 MPa. Then efficiency enhancement by reheats and intercooling are evaluated and both increase cycle and overall the plant efficiency, especially reheat. The power plant efficiency can be increased by 1.77% and 2.24% by single reheat and double reheats, respectively. To maintain the simplicity of the cycle the recompression with a single reheat layout is chosen as the most appropriate for this application and reaches the efficiency of 52.6% for the cycle and 48.52% for the net plant efficiency.

Mounir Mecheri and Yann Le Moullec [57] in their work investigated the supercritical CO_2 cycles performance. Main findings are the following: a recompression cycle is mandatory for this application, the difference between this option and a standard Brayton cycle is more than 4.5% in terms of efficiency. Compared to no-reheated cycle, single reheat is an effective configuration with 1.5% efficiency increase at the optimal pressure ratio, regardless of the maximal temperature of the power cycle. Another process improvement such as double reheat cycle, double recompression cycle and an advanced flue gas economizer configuration induce efficiency gain between 0.3 and 0.5%. Influence of the heat sink temperature stability has been quantified: 1.5% reduction for 5°C increase with a minimal cycle pressure of 7 MPa; however, performance stability could be improved by adapting the main compressor inlet pressure. As expected for a Brayton cycle, the component pressure drop in the cycle has a critical impact on efficiency, especially for low pressure ratio configurations. From the first estimation of 0.9 MPa pressure drop in the cycle, doubling cycle pressure drop decreases the efficiency by 1.2% for a pressure ratio of 2.7. This efficiency drop is damped while the cycle pressure ratio grows. Recuperator temperature-pinches have a significant impact on power cycle efficiency. Getting from a conservative 10°C pinch, reducing it respectively to 6°C then 3°C induces 0.7% and 1.2% net efficiency rise. However, low temperature pinch heat exchangers are bigger and more expensive, so their design will result in a compromise between efficiency, size and cost. It is also interesting to mention that the optimal pressure ratio also increases as global cycle pressure drop increases. As a conclusion, CO_2 supercritical coal-fired power plant theoretically offers interesting performances, of 47.8%-LHV efficiency for turbine inlet temperature conditions

620°C/30 MPa and recompression cycle with double reheating, with existing materials at current operating conditions in a relatively near timeframe.

Yifan Zhang et al. [63] built at first an in-house code in Fortran of s-CO_2 Brayton cycle tailored for coal-fired power plant. Then, three improved cycles are proposed, all based on a low temperature economizer (LECO). All the three improved cycles can reduce the exhaust gas temperature and increase the net efficiency. With the turbine inlet parameters of 31 MPa/600°C/620°C, the maximum net efficiencies of the three improved cycles are 49.83%, 48.55% and 50.71%, respectively, which are much higher than that of the based cycle layout (Basic coal-fired recompression s-CO_2 Brayton cycle, 45.96%), and also higher than that of a state-of-the-art USC steam power plant (about 46%-47%). The s-CO_2 Brayton cycle with a second split flow to boiler is proved to be the most efficient one. Finally, the effects of the second split flow ratio on net efficiency were analyzed, and the equations to calculate the optimal range of second split flow ratio was derived.

Thermo-economic optimizations and economic considerations

Sebastian Michalski et al. [58] performed a thermo-economic optimization aimed to maximize the cycle efficiency and minimize the break-even price of electricity, while Jia-Qi Guo et al. [60] performed a single objective maximization of a coal power plant efficiency with considerations on the thermo-economic performances of three different layouts.

Sebastian Michalski et al. [58] in their study aimed to assess the techno-economic feasibility of the coal-fired power plant based on calcium looping combustion for carbon capture and storage with different advanced Brayton cycles. These included single power cycles, such as recompression supercritical CO_2 with reheating, simple supercritical CO_2 cycle, and xenon cycle, as well as combined power cycles based on helium, nitrogen and recompression supercritical CO_2 cycles. The net efficiency and break-even electricity price, which was estimated using the net present value method, were used as the key techno-economic performance indicators. A parametric study was also conducted to assess the impact of the key thermodynamic parameters and an optimization of TIT, compressor outlet pressure (COP) and the pinch point temperature difference in recuperators has been performed. This study showed that the case based on a single recompression supercritical CO_2 cycle with reheating had the best overall techno-economic performance. The former was characterised with a net efficiency of 38.9% for the turbine inlet conditions 665°C/30 MPa, which is higher than that of the reference coal-fired power plant without CO_2 capture (38.0%). Such performance was achieved at a break-even electricity price of 71.2 €/MWh, corresponding to a cost of CO_2 avoided of 16.3 €/t_{CO2}.

Jia-Qi Guo et al. [60] in their work firstly pointed out the differences between the conventional steam boiler and s-CO_2 boiler. Based on the optimized water-cooling wall layout, the energy, exergy and economic analysis models of the integrated s-CO_2 coal-fired power systems are further developed. The systematic comparison was performed among three configurations of s-CO_2 coal-fired power plants, namely the partial-cooling, the recompression cycle with double reheat and the recompression cycle with double reheat and intercooling, with considerations on

the thermo-economic performances. The conceptual design of key components is also provided. Among the three s-CO_2 cycle layouts studied, the s-CO_2 coal-fired power system with the intercooling yielded highest efficiency and was the most economic configuration. The thermal efficiency of the s-CO_2 coal-fired power plant composing the intercooling cycle resulted 47.69–49.09% with total thermal conductance of recuperators changed from 120 MW_{th}/K to 180 MW_{th}/K while the turbine inlet parameters were 620°C/620°C/30 MPa, displaying an advantage over the ultra-supercritical steam Rankine power plant. The optimized variables using GA were the SR, the ratio of HTR thermal conductance to the UA, the pressures of reheating and intercooling. The system LCOE resulted 0.0397 $/kWh showing great commercial potential.

Optimized cycles layout, efficiencies and costs

The Recompression layout is mandatory for this application to reach high efficiencies, the difference between Recompression and Simple cycle is higher than 4.5% in terms of efficiency [57]. In the literature some efficiency enhancements strategies are analyzed, especially single reheating, double reheating and intercooling. Single reheat and double reheats are very interesting because they can increase the cycle efficiency from 1.77% to 2.24% at the working conditions typical for coal application [59]. Finally, the recompression cycle with double reheats and eventually also with intercooling lead to the highest net plant first law efficiency 47.6-49.8%. These plant configurations show also a great commercial potential as demonstrated by Jia-Qi Guo et al. [60] that estimated an LCOE equal to 0.0397 $/kWh for the double reheat recompression cycle with intercooling. All the proposed cycle layouts in the literature have at least two split ratios, one aimed to recover the medium-low temperature heat in the boiler. All the components have to be carefully designed to meet the high standard requirements, because the split ratios have great effect on the plant performance [62].

Research Projects

Current fossil-fuel power plants have been designed to operate in base-load conditions, to provide constant power output. However, their role is changing, due to the growing share of renewables, both in and outside European Union (EU). Fossil-fuel plants will increasingly be expected to provide fluctuating back-up power, to foster the integration of intermittent renewable energy sources and to provide stability to the grid. However, these plants are not fit to undergo power output fluctuations. In this context, s-CO_2-Flex consortium addresses this challenge by developing and validating the scalable/modular design of a 25 MW_e Brayton cycle using supercritical CO_2, able to increase the operational flexibility and the efficiency of existing and future coal and lignite power plants. sCO_2-Flex will develop and optimize the design of a 25 MW_e s-CO_2 Brayton cycle and of its main components (boiler, HX, turbomachinery, instrumentation and control strategies) able to meet long-term flexibility requirements, enabling entire load range optimization with fast load changes, fast start-ups and shuts-downs, while reducing environmental impacts and focusing on cost-effectiveness. The project, bringing the s-CO_2 cycle to TRL6, will pave the way to future demonstration projects (from 2020) and commercialization of the technology (from 2025). Ambitious exploitation and dissemination

activities will be set up to ensure proper market uptake. sCO_2-Flex is an industry-based consortium made up of 10 recognised and experienced key players from 5 different EU member states led by Electicite de France. The Consortium includes Zabala Innovation Consulting, Fives Cryo, large technology companies such as Baker Hughes, Centro Sviluppo Materiali, Ujv Rez, and Centrum Vyzkumu Rez and academic istitutions: Politecnico di Milano (Dario Alfani, Marco Astolfi, Paolo Silva, Marco Binotti, Stefano Campanari and Francesco Casella), Universitaet Stuttgart and Universitatet Duisburg-Essen. This project is awarded by the European Commission with a Horizon 2020 Programme and will run for three years.[64][65] Politecnico di Milano had an important role in the project, its assignments were the optimization of system design at nominal point, definition of optimal part-load operation strategy, evaluation of system dynamic and cycle applications to other energy fields.[66]

2.2.5 Typical assumptions

All the papers and the studies in the literature make several assumptions for modeling the s-CO_2 cycles. Many of these assumptions are about components performances such as turbomachinery efficiencies or effectiveness of recuperators, pinch point temperatures and pressure drops (sometimes neglected for simplicity) in heat exchangers. All these assumptions are obviously reasonable depending on the case study, size of the plant, application, mass flow rates, operating pressures and temperatures. The main assumptions in the papers analyzed for coal application are:

Turbine and compressor efficiencies: in the analyzed papers the turbine efficiency is assumed in the range 92-94%, while compressor efficiency is assumed 89-90% for all the studies. These are very high values of turbine efficiency. Only Hongzhi Li et al. [62] specified that they assumed an axial turbine with an efficienty of 93%, all the other papers do not enter in the detailed analysis of the turbine but the very high efficiencies assumed could be correlated to the very high large size of the plants (500-1,000 MW_e), moreover all the studies assumed al least one reheat, meaning a multi-stage and more efficient expansion.

Pinch point temperature difference in recuperators: pinch point temperature difference in recuperators is assumed for all the papers analyzed 5-6°C (a reasonable value for PCHE often correlated to the s-CO_2 cycle application).

HTR and LTR hot side pressure: HTR and LTR hot side pressure drops in the papers are assumed in the range 0.08-0.1 MPa The smallest value is assumed by Sebastian Michalski et al. [58] while the higher value of 0.1 MPa is assumed by by Ziwei et al. [61] and Xuwei et al. [59]. This diffence could be correlated to the different size (and also mass flow rate), of these studies 566 MW_e and about 1,000 MW_e respectively.

HTR and LTR cold side pressure drops: HTR and LTR cold side pressure drops in the papers are assumed 0.15 MPa by Ziwei et al. [61] and Xuwei et al. [59], this is constistent with the similar maximum pressure of the cycle 32.8 and 30 MPa respectively and a very similar mass flow rate 7,630 kg/s versus 7,723 kg/s.

2.3 CSP

2.3.1 Introduction to the Energy Source

Solar energy is green, ubiquitous and readily accessible. Despite that, it is criticized for low power density, intermittency and maldistribution. Empirical models are generally used in theoretical calculations to predict the irradiance which take the latitude, solar altitude angle, azimuth angle and sunshine hours into consideration. CSP continues with providing service after sunset and before sunrise as long as a Thermal Energy Storage (TES) is built in. Moreover, TES is low-cost and more efficient when compared with electric storage. State of the art CSP is able to deliver dispatchable renewable energy while still remains stable all day around which is favored in the grid part. Power capacities in the range of 10–150 MW_e are anticipated for CSP application, heat power available 20-220 MW_{th} and TITs that could be reached vary from 500°C to 700°C. Nevertheless, several aspects still remained unclear regarding the concept of adopting the s-CO_2 based systems for CSP application. The ability to accommodate dry cooling and daily cycling, as well as the compatibility with the TES system were emphasized when performing the optimal design of s-CO_2 based systems for CSP application in the literature.

Typical CSP applied in power plants focuses the diluted sun flux into a small area through the sophisticated-designed optical mirror. The small area is known as a receiver where the heat transfer fluid (HTF) absorbs the radiation and transfers the energy to the power cycle. A TES system served as an energy bumper is usually accompanied which mitigates the environmental fluctuation factor and extends the availability. CSP equipped with TES presents an economic improvement for the reason that frequent starts and stops can be alleviated or even eliminated. Currently, four CSP technologies are available, which can be categorized by the way to concentrate the beam and the technology to receive the sun's energy. These four CSP technologies are Parabolic Trough Collector (PTC), Solar Power Tower (SPT), Linear Fresnel Reflector (LFR) and Parabolic Dish System (PDS) illustrated in Figure 2.8. Despite the fact that the PTC technology is currently the most mature one and contributes more than 90% power generation of all the installed operational CSP plants, the SPT system is seen as the most promising technology in the near future due to the expected performance improvements and cost reductions associated with technology innovations in the three main components, i.e., heliostat, solar receiver and power block. In comparison to other three technologies, the SPT has the following advantages:

1. High operating temperature up to 1,000°C and therefore superior cycle thermal efficiency for the power block
2. The capability of hybridization with fossil power
3. High annual capacity factors with TES integrated
4. Great potential for further significant cost reduction and cycle efficiency improvement

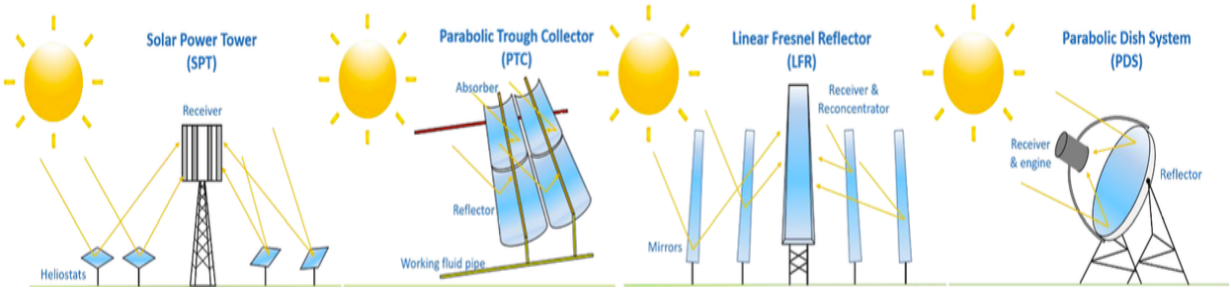

Figure 2.8 – CSP current technologies to receive sun's energy [11]

2.3.2 Cycle layouts studied and analyzed

Recompression supercritical CO_2 Brayton cycle and Recompression supercritical CO_2 Brayton cycle with single reheating

The characteritstics and benefits of Recompression cycle (Fig. 2.9) already explained for nuclear and coal application are also valid for CSP and therefore it still one of the layout more studied also for this application. This is consistent with the fact that for all these applications the thermodynamic goal is the maximization of thermal efficiency of the cycle.

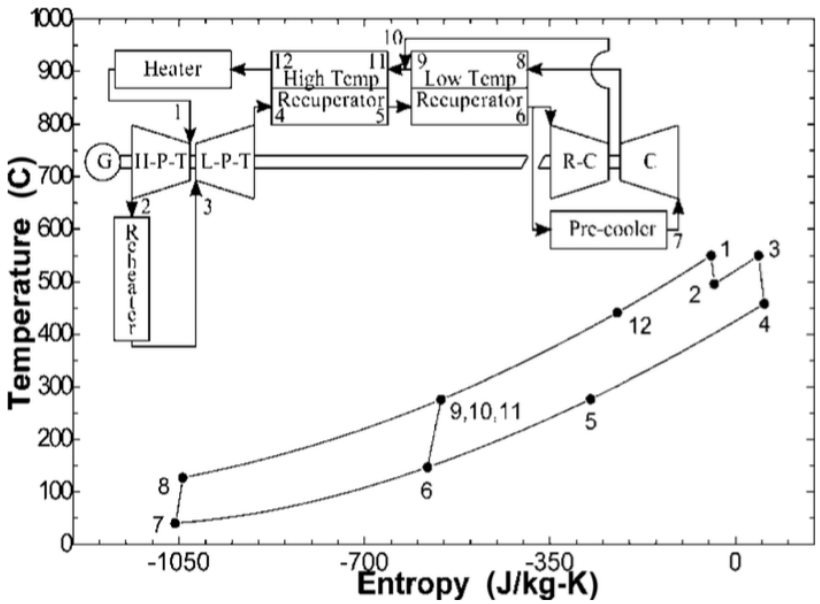

Figure 2.9 – Schematic layout and T-s diagram of a Recompression supercritical CO_2 Brayton cycle with reheating for CSP application [67]

Partial cooling supercritical CO_2 Brayton cycle with reheating

One possible intercooling recompression configuration splits the stream after the precompressor (Fig. 2.10). Dostal refers to this as the "Partial cooling" cycle [10]. In this cycle configuration, the turbine exhaust flow (6) is cooled in a precooler before entering the precompressor (7). Flow exiting the precompressor (8) is split. One path flows to the

recompressor, while the other path flows to the intercooler and main compressor (9). After the precompressor, the inlet pressure to the recompressor is at an intermediate pressure and thus the recompressor operates over a fraction of the turbine pressure ratio. The cycle also accommodates large turbine pressure ratios and provides better performance for reheating operation. One important benefit of intercooling for CSP applications is the larger temperature differential that can be accommodated across the primary heater. CSP systems with sensible heat thermal storage are more cost effective with a large temperature differential because this reduces the required amount of thermal storage media. If sensible thermal energy storage, e.g., molten salt power towers, is to be used with s-CO_2 power systems, a cycle with a larger temperature differential across the primary heater and thermal storage system will be favored. [68]

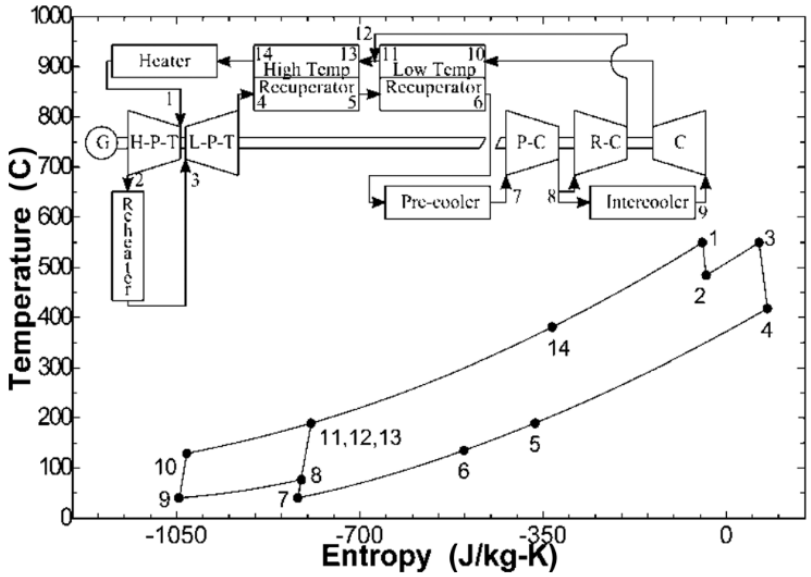

Figure 2.10 – Schematic layout and T-s diagram of a Partial cooling supercritical CO2 Brayton cycle with reheating for CSP application [67]

Recompression supercritical CO_2 Brayton cycle with main compressor intercooling

A common way to introduce intercooling is to have the precooler located after the recompression split (Fig. 2.11). This cycle is referred to as the "Recompression with main-compression intercooling" cycle. In this configuration, the inlet pressure to the recompressor (6) is the turbine outlet pressure and thus the recompressor operates over the entire pressure ratio. The similarity between this and the partial cooling cycle is that they have both multistage compression with intercooling. The difference is the position of recompression flow split. [68] The inlet temperatures of the compressors are not required to be equal, but since only one cold sink is likely to be used, the temperatures will typically be equal.

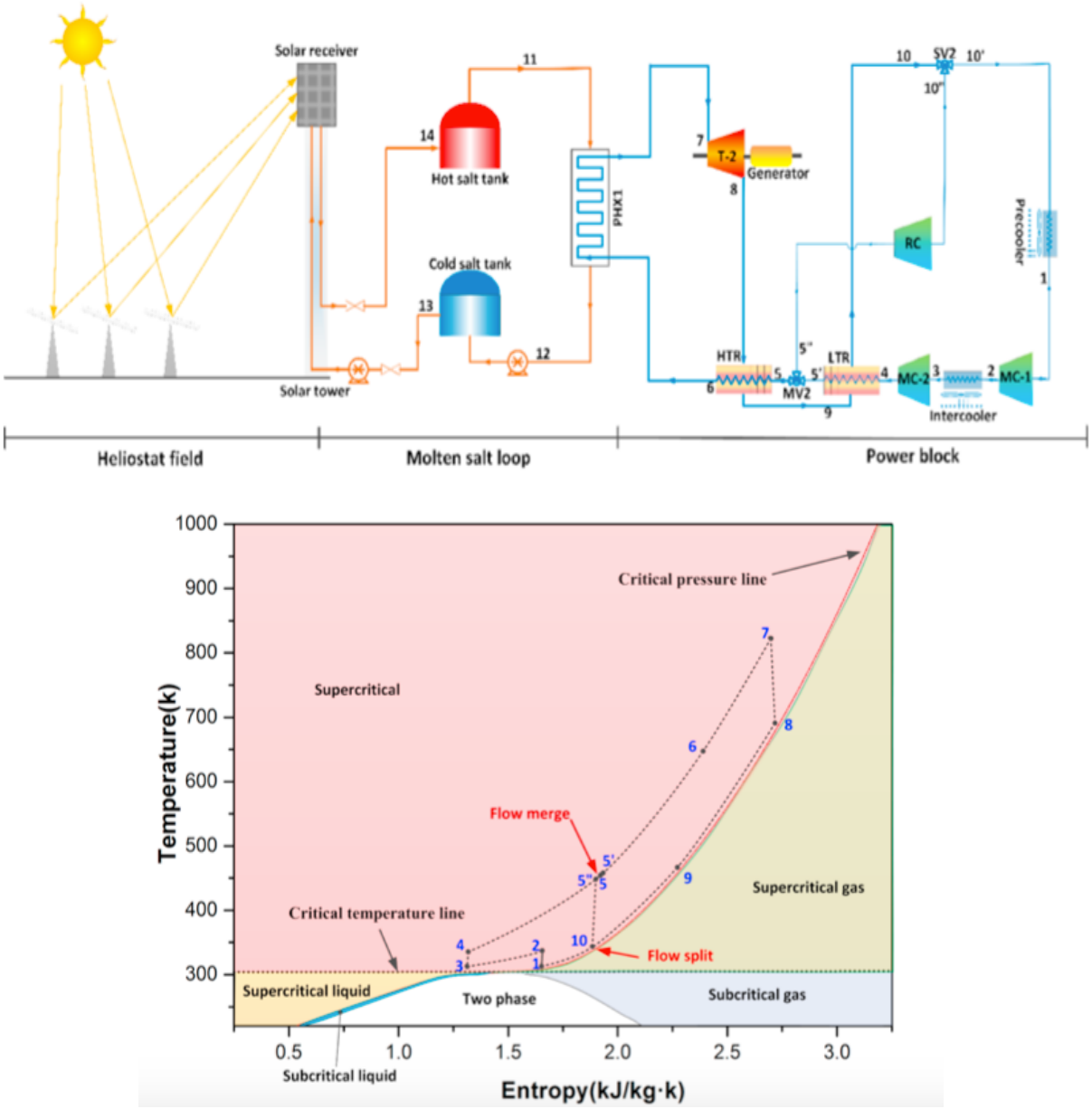

Figure 2.11 – Schematic layout and T-s diagram of a Recompression supercritical CO_2 Brayton cycle with intecooling for CSP application [69]

Recompression supercritical CO_2 Brayton cycle with single reheating and intercooling

The cycle in Fig. 2.12 it is a recompression cycle, for which all the main characteristics have already been described before but it presents the addition of both reheat and intercooling increasing at the same time the performances and the complexity of the layout.

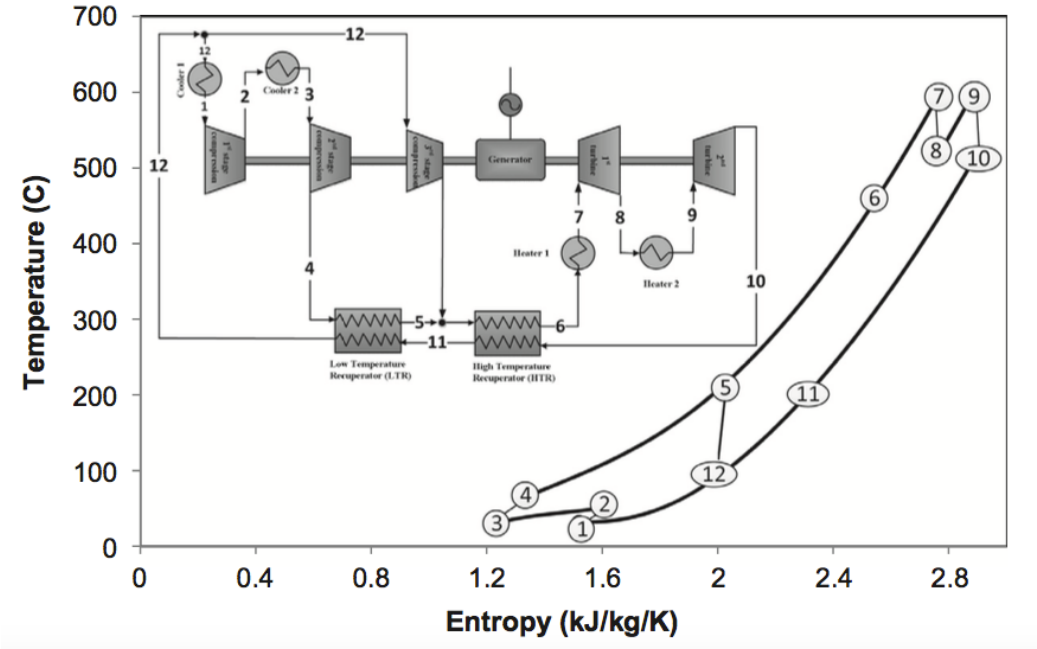

Figure 2.12 – Schematic layout and T-s diagram of a Recompression supercritical CO_2 Brayton cycle with reheating and intercooling for CSP application [70]

2.3.3 Heat recovery unit

There are two technical options to integrate a s-CO_2 based system in a CSP plant, which were known as direct-heated and indirect-heated systems, represented in Fig. 2.13 and 2.14. In the direct-heated system, the CO_2 fluid is directly heated by the concentrated sun rays in the pipes of solar receiver. In the indirect-heated the heating media through the receiver is also used as the storage media in the TES system, which then flows through the PHX to heat the CO_2 working fluid in the hot end of the cycle. These two approaches to integrating the s-CO_2 cycle in a CSP system result in two different receiver designs. The direct system requires s-CO_2 gas receiver while the indirect-heated system can be designed with the commercialized liquid receiver using molten salt or oil. Despite the capability of achieving high temperature and relative flexible construction, the gas receiver has deficiencies of high thermal loss, flow instability and challenges in material durability. By contrast, the indirect-heated system is less challenging in design and has similar solar components to the already commercialized CSP plants.

The two-tank thermal storage still remains the only commercialized TES technology currently. The most representative TES system adopted in the CSP plant is the two-tank system using "solar salt", a molten nitrate salt consisting of 60% sodium nitrate ($NaNO_3$) and 40% nitrate of potash (KNO_3) as HTF. The applicable temperature range for the solar salt is between 238°C–585°C, bounded by the freezing and decomposing temperature of this mixture. Novel salts are being developed to enlarge the applicable range of temperature, increase the energy density of salts, and lower the capital costs of the TES system.

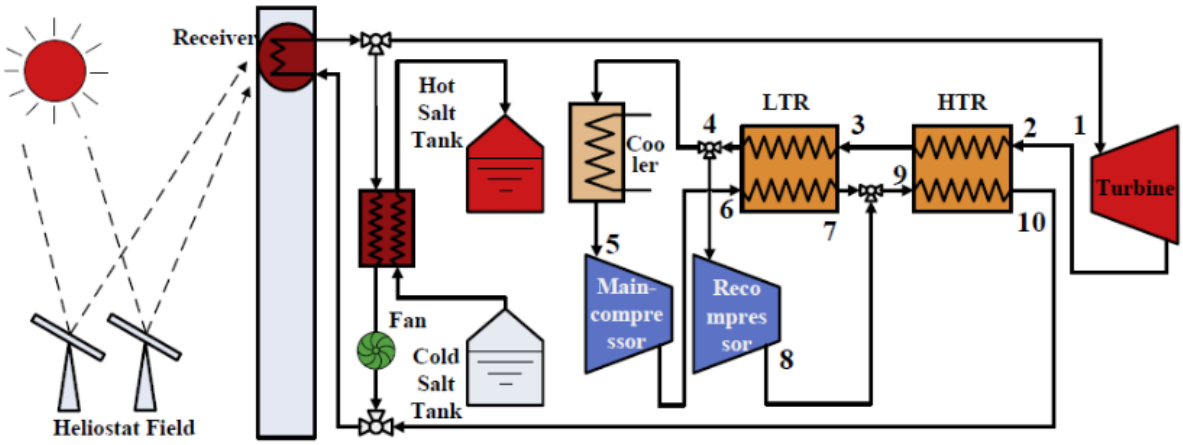

Figure 2.13 – CSP plant with s-CO_2 cycle integration based on a direct-heated system [11]

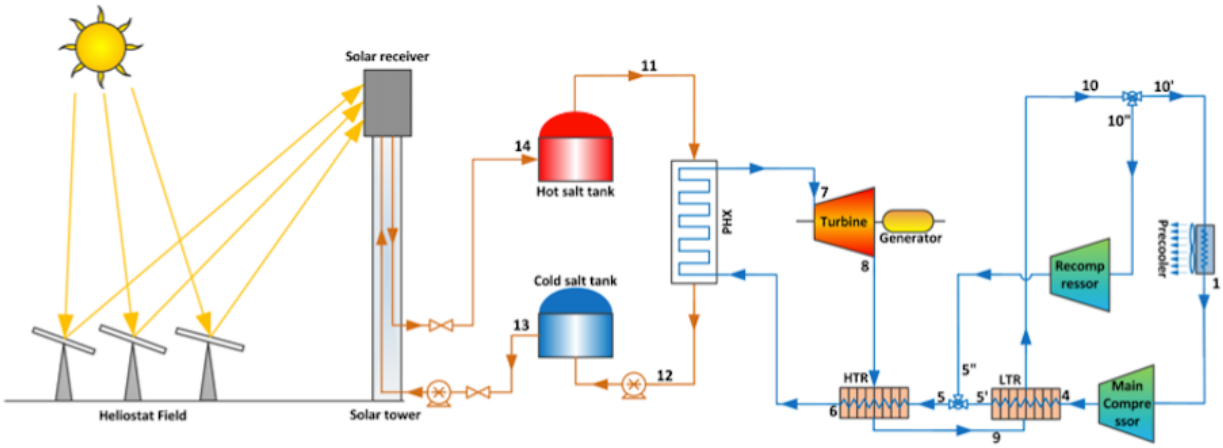

Figure 2.14 – CSP plant with s-CO_2 cycle integration based on a indirect-heated system [11]

2.3.4 Optimizations Methodology

Thermodynamic optimization

The kind of thermodynamic optimizations in the literature are mainly single objective for the CSP application with the aim to maximize the cycle first law efficiency, performed by Craig S. et al. [68], T.Neises and C.Turchi [71], M.A. Reyes-Belmonte et al. [72], Dia Milani et al. [70], Yuegeng Ma [11] and Astolfi M. et al. [73] or to maximize second law efficiency performed by R. Vasquez Padilla et al. [74].

Craig S. et al. [68] explored s-CO_2 Brayton cycle configurations that have attributes desirable from the perspective of a CSP application. Four s-CO_2 cycle configurations are studied: simple cycle, recompression cycle, recompression with precooling, recompression with main-compression intercooling. The study is based on the National Renewable Energy Laboratory (NREL) model using the Engineering Equation Solver (EES). The main goal is the optimization of the cycle efficiency and the optimized parameters are: PR, SR and RPR while all the other parameters are fixed. Main assumptions are that the pressure losses in the pipes and heat

exchangers are negligible and that the maximum temperature and pressure of the cycle are fixed at 700°C and 25 MPa. Main findings are that the simple s-CO_2 configuration has limited advantage over the steam power system while recompression cycles combined with intercooling and turbine reheat are able to hit the efficiency target of 50% or higher even with dry cooling.

T.Neises and C.Turchi [71] investigated the performances of simple, recompression and partial cooling cycles under design point conditions relevant to CSP applications with two approaches: the effectiveness approach and the conductance approach, where to describe the recuperators characteristics the effectiveness and the conductance are fixed respectively. Main assumptions are that the turbine inlet temperature and pressure are set at constant values 650°C and 25 MPa respectively, the compressor inlet temperature is fixed at 50°C and the pressure drops are neglected. All the optimizations were completed using the "Variable Metric" method build into EES with the goal of maximizing the cycle efficiency. The optimized variables are the PR, the RPR and the fraction of total conductance allocated to the HTR (not applicable for effectiveness approach) while the other parameters are fixed. Results show that when specifying effectiveness to model the recuperators the performance of the recompression and partial cooling were similar (the cycle efficiency results for both close to 50%), while when specifying conductance to model recuperators, the partial cooling cycle outperformed the recompression cycle until large quantities of conductance were modeled. Another key benefit of the partial cooling cycle for CSP is a larger temperature differential across the primary heat exchanger, which allows for more cost efficient sensible thermal energy storage systems and possible more thermally efficient receivers as well that translates in a better integration for CSP applications.

M.A. Reyes-Belmonte et al. [72] in their study have optimized a recompression s-CO_2 for a solar central particle receiver for a CSP plant. The optimization variables to maximize the cycle first law efficiency were recuperators effectiveness, TIT and the SR, the parameters that mostly affect the cycle thermal efficiency. Governing equations and thermodynamic relations used for power cycle modelling have been encoded in MATLAB coupled with NIST-REFPROP. The main assumptions are that the temperature at the receiver outlet of heat transfer fluid is 700°C, so the maximum temperature of the cycle varies in the range 630-680°C, the compressor inlet temperature and pressure are fixed at 40°C and 7.8 MPa respectively and the maximum pressure of the cycle is limited to 24.84 MPa. As a result, a cycle thermal efficiency closed to 50% can be achieved, even with dry cooling and moderate temperature range.

Dia Milani et al. [70] introduced a unique model for a small-scale decentralized solar-assisted s-CO_2 closed Brayton cycle. They analyzed the most common cycle configurations and selected the cycle that showed the highest values for the proposed key performance indicators (KPIs): thermal efficiency, CSP compatibility, and water demand for cooling. For a case-study of 10 MW_e CSP-assisted power plant, the recompression with single reheating and intercooling was the cycle with the better values of the proposed KPIs. They have optimized the key manipulated variables (SR, compression ratio of the main compressor and expansion ratio of the first turbine for a fixed TIT of 600°C) with Aspen PLUS software to reach the highest thermal efficiency and demonstrated the significance of thermal efficiency vs HX area on the techno-economic nexus. Results show that the cycle can reach a 52.7% thermal efficiency, 25.9% solar

penetration and up to 80% of water saving in heat-rejection units with hybrid water and air cooling while concerning the total heat transfer area of the cycle it was found that accepting a minor reduction in thermal efficiency (by 1.7%) could save up to 25.5% (when split ratio and compression were manipulated) or 34.8% (when split ratio and expansion ratio were manipulated) from overall HX area.

Yuegeng Ma [11] in his thesis performed an optimal design of the s-CO_2 cycle based system for the CSP application. The design optimization begins with the selection of the intercooling configuration for the compressors. The results of the design-point study show that the main compression intercooling (MCIC) is the optimal intercooling configuration for the recompression cycle and an optimization of the cycle efficiency varying the pressure ratio in the range 2-5, the split ratio in the range 0.5-1, the RPR of the main compressor and the RPR of recompressor in the range 0-1, is performed with genetic algorithm. TIT, turbine inlet pressure (TIP) and CIT are fixed at 500°C, 25 MPa and 45°C respectively and the cycle efficiency after optimization resultes 45.27%.

R. Vasquez Padilla et al. [74] performed an energy and exergy analysis of a supercritical CO_2 recompression Brayton cycle with and without reheat scenarios for CSP applications. The energy, mass and exergy balance were written in Python 3.2 and REFPROP was used to obtain the thermodynamic properties of carbon dioxide under supercritical conditions based on the model developed by Span and Wagner while Sequential Least Programming (SLSQP) is used for the optimization. Main assumptions are that pressure drops are neglected and that the maximum pressure of the cycle is fixed at 25 MPa. The optimization of TIT and PR were carried out and main results show that adding reheat improves both energy and exergy efficiency. The fist law efficiency increases monotonically with the high temperature of the cycle and the maximum value corresponds to 52% at 850°C for reheat configuration, while the exergy efficiency has a parabolic tendency and the maximum value of 35.1% is reached at 600°C due to the exergy losses in the solar receiver.

Astolfi M. et al. [73] discussed a preliminary thermodynamic assessment of three different s-CO_2 power cycles applied to a high temperature solar tower system, namely the partial cooling, the recompression and the recompression cycle with main compression intercooling with maximum temperatures up to 800°C. The thermal power is transferred from the solar receiver to the power block through KCl-$MgCl_2$ molten salts used as HTF, therefore an indirect cycle configuration is considered assuming a surrounded field as the one of Gemasolar plant. The most promising cycle configuration in terms of solar-to-electric efficiency is selected, optimizing the cycle TIT to achieve the best compromise between cycle and receiver performance: the highest efficiency at design conditions is achieved by the Recompression with Main Compression Intercooling (RMCI) configuration with a solar to electric efficiency of 24.5% and a maximum temperature of 750°C. A preliminary design of the turbine has been also carried out, leading to a three-stage configuration, thus demonstrating the technical feasibility of a machine with smaller weight and volume, lower complexity and thermal mass with respect to Rankine steam cycle turbines.

Thermo-economic studies

There is a lack in the literature of thermo-economic optimization but there are some interesting studies that give us information, data and references for the cost of a CSP plant integrated with s-CO_2 cycles like the studies of Josè I. Linares et al. [75], Yuegeng Ma et al. [76] and Yuegeng Ma et al. [69].

Josè I. Linares et al. [75] proposed a novel supercritical CO_2 Brayton cycle for power tower concentrating solar plants. Different options based on the recompression layout with intercooling and reheating have been investigated in both dry and wet cooling scenarios (where the main difference is the inlet temperature in the main compressor, 35°C for wet cooling and 50°C for dry cooling). Reheating is recommended for wet cooling, optimization process in EES environment for TIT, SR, TIP and pressure of reheating (TIT resulted above 600°C and TIP 30 MPa) and economic analysis resulted in 54.6% of cycle efficiency and an investment of 8,662 $/$kW_e$; while intercooling with reheating is the best option for dry cooling, reaching 52.6% of cycle efficiency and an investment of 8,742 $/$kW_e$.

Yuegeng Ma et al. [76] propose in their study a novel recompression supercritical CO_2 Brayton cycle integrated with an absorption chiller (RSBC/AC) for air-cooled concentrated solar power plants where the residual heat of CO_2 in the cold end of the cycle is utilized to drive the absorption chiller, which chills the CO_2 exiting the precooler further before it enters the main compressor. Main assumptions are that pressure drops are neglected, TIT is fixed at 565°C and the maximum pressure of the cycle is limited to 25 MPa. Parametric analysis and optimization of PR (in the range 2.2-4), recuperators effectiveness (in the range 85-98%), temperature approach in the absorption chiller and the concentration variation of the solution LiBr-water are performed with GA to improve cycle exergy and thermal efficiencies. Economic evaluations of the CSP plant integrated with RSBC/AC are performed to investigate its feasibility as an alternative to the stand-alone s-CO_2 cycle. Results show that the optimized thermal and exergy efficiencies of RSBC/AC (45.84% and 76.67% respectively) are 5.19% and 6.12% higher than those of the stand-alone s-CO_2 cycle. The exergy destruction/loss in the high-temperature recuperator and precooler of RSBC/AC are significantly reduced. The levelized cost of electricity and payback period for the plant integrated with RSBC/AC (13.72 $/kWh and 14.44 years) are reduced by 0.46-0.77 $/kWh and 0.67-5.27 years, respectively, with an annual full-load hour ranging from 5,000 to 8,500.

Yuegeng Ma et al. [69] studied the optimal integration of the recompression s-CO_2 Brayton cycle with MCIC in the SPT system with the exergoeconomic approach. The thermodynamic and exergoeconomic models of the SPT plant integrated with the recompression s-CO_2 Brayton cycle with MCIC were established. The comparison between the exergoeconomic optimization cases and the thermodynamic optimization case performed with GA was carried out. Optimization parameters were the PR of MC, SR, effectiveness of recuperators and RPR of the compressors (TIT, TIP and CIT fixed at 550°C, 25 MPa and 45°C respectively). Results indicated that the total of unit costs of system production obtained by exergoeconomic optimization using the proposed models is reduced by 8.94% than that obtained by the thermodynamic optimization from 12.41 $/kWh to 11.30 $/kWh. The integration of reheating

is not justified for the cycle due to the significant decreased temperature change across the primary heat exchanger and the consequent reduction in the exergoeconomic performance of the SPT plant.

Optimized cycle layout, efficiencies and costs

T. Neises and C.Turchi [71] compared the performances of the simple, recompression and partial cooling cycle, demonstrating that recompression and partial cooling have higher performances with respect to the simple cycle. Intercooling process is highly recommended for this application as demonstrated by Astolfi M. et al. [73] and Yuegeng Ma [11] that performed a selection of the best intercooling configuration for the compressor demonstrating that the main compression intercooling is the optimal intercooling configuration for the recompression cycle and for CSP application often integrated with a dry cooling system. Also reheating has the power to improve the performance of the cycle as shown by R. Vasquez Padilla et al. [74], indeed Craig S. et al. [68] explored the performances of simple, recompression, recompression with partial cooling and recompression with main compression intercooling all with single reheating finding that simple s-CO_2 configuration has limited advantage over the steam power system while recompression cycles combined with intercooling and turbine reheat are able to hit the efficiency target of 50% or higher (52.2-52.6%) even with dry cooling. The recompression cycle with reheating and main compression intercooling has also other beneftis. Dia Milani et al. [70] in their study analyzed the most common cycle configurations and selected the cycle that shows the highest values for the proposed KPIs: thermal efficiency, CSP compatibility, and water demand for cooling. For a case-study of 10 MW_e CSP-assisted power plant, the dynamic model shows that the recompression with single reheating and intercooling is the cycle with the better values of the proposed KPIs. Results showed that the cycle can reach a 52.7% thermal efficiency, 25.9% solar penetration and up to 80% of water saving in heat-rejection units with hybrid water and air cooling. Final conclusions are that reheating is recommended for wet cooling, optimization and economic analysis resulted in 54.6% efficiency and an investment of 8,662 \$/kW_e; while intercooling with reheating is the best option for dry cooling, reaching 52.6% efficiency and an investment of 8,742 \$/kW_e [75], LCOE: 12-13 \$/kWh [69] and the net efficienty (solar to electricity) of the plant: 28.5-31% [49][56].

Research projects

According to the JRC CSP platform, with an increased efficiency of component and price reduction, it could be feasible that 11% of EU electricity will be produced by solar thermal electricity by 2050. S-CO_2 is globally attracting more and more industrial interest, but also EU stakeholders haven't had the opportunity to test MW scale turbomachinery on real EU operating plants yet. For this reason, the main objective of SOLARSCO2OL project is to demonstrate an innovative, economically viable and easily replicable s-CO_2 power block that, also coupled with fast reactive electric heater and efficient heat exchangers, will enable the operation and design of a novel integrated power plant layout in order to un-tap CSP plant potential flexibility and reduce their LCOE to values below 0.010 €/kWh. The project started in October 2020 and

RINA is the Project Coordinator. Project Consortium is made up of 15 international partners and 1 extra-EU (Morocco). Main activities of the project are the support to s-CO_2 turbomachinery design, manufacturing and material selection via CFD/FEM analysis, Health & Safety procedures, SOLARSCO2OL demonstration and replication, regulatory and non-technical assessment of SOLARSCO2OL solutions and techno-economic Roadmap towards TRL9. In conclusion, SOLARSCO2OL project Consortium will collect all the technological and nontechnological evidences to unlock the potential of integrating s-CO_2 in all kinds of CSP plants towards higher efficiency and higher responsiveness to grid flexibility requests, demonstrating them on the field and planning next steps towards technical maturity and marketability within 2030.[78]

Another development project that is taking place is the Gen 3 Particle Pilot Plant (G3P3). The objectives of the Gen 3 Particle Pilot Plant (G3P3) project are to design, construct, and operate a multi-MW_{th} falling particle receiver system that can operate for thousands of hours, provide six hours of energy storage, and heat a working fluid to temperatures higher than 700°C while demonstrating the ability to meet SunShot cost and performance goals. G3P3 development is taking place at the National Solar Thermal Test Facility the only test facility of its type in the United States. The team of the project is composed of Georgia Institute of Technology, King Saudi University, Australian Solar Thermal Research Initiative, German Aerospace Center, EPRI and other companies. Preliminary models of a commercial 100 MW_e particle power-tower system using the System Advisor Model (SAM) and EES have shown that particle-based CSP systems can meet the SunShot goal of 0.06 $/kWh using recently published capital costs for particle-based components with a receiver efficiency as low as 85% if the storage costs are reduced from 22 $/kWh to 15 $/kWh. In addition, results show that the G3P3 technology can be used as a peaker plant with three to six hours of storage and LCOE < 0.10 $/kWh. Cost advantages in the particle receiver and storage can result from eliminating costly high-temperature metal alloys to hold and convey fluids. Direct storage of the particles also provides cost advantages over gas-based systems, which require additional heat exchangers and storage media. This project is funded by the U.S. Department of Energy Solar Energy Technologies Office as part of Gen 3 Concentrating Solar Power initiative [79].

Finally, in the STEP Pilot Project, a team led by GTI, Southwest Research Institute (SwRI), and General Electric Global Research, along with the University of Wisconsin and Natural Resources Canada, is executing a project to design, construct, commission, and operate an integrated and reconfigurable 10 MW_e s-CO_2 Pilot Plant Test Facility located at SwRI's San Antonio, Texas campus. This project is a significant step toward commercialization of s-CO_2 cycle based power generation and will inform the performance, operability, and scale-up to commercial power plants. The pilot plant design, procurement, fabrication, and construction are ongoing. By the end of this six-year project, started in 2016, the operability of the s-CO_2 power cycle will be demonstrated and documented starting with facility commissioning as a simple recuperated cycle configuration initially operating at a 500°C turbine inlet temperature and progressing to a recompression closed Brayton cycle technology configuration operating at 715°C [27].

2.3.5 Typical assumptions

All the papers and the studies in the literature make several assumptions for modeling the s-CO_2 cycles. Many of these assumptions are about components performances such as turbomachinery efficiencies or effectiveness of recuperators, pinch point temperatures and pressure drops (sometimes neglected for simplicity) in heat exchangers. All these assumptions are obviously reasonable depending on the case study, size of the plant, application, mass flow rates, operating pressures and temperatures. The main assumptions in the papers analyzed for CSP application are:

Turbine and compressor efficiencies: in the analyzed papers the turbine efficiency is assumed in the range 90-93%, while the compressor efficiency is assumed for all the studies 88-89%.The lowest value of turbine efficiency (90%) is assumed by Yuegeng Ma et al. [69], for a power output of about 60 MW_e and two stage expansion. Higher efficiency (93%) is assumed by Craig S. et al. [68], T.Neises and C.Turchi [71] and Yuegeng Ma [11] for axial turbine and large size plants (30-100 MW_e). As for the coal application most of the studies proposed reheating, splitting the expansion that results more efficient.

HTR effectiveness: in the papers studied HTR effectiveness is assumed in a small range of 96-97%, very high values, but this is consistent with the fact that usually the HTR is balanced in terms of capacitance of the hot and cold stream and their additional constrains or assumptions about the pinch point temperature to be 5°C.

LTR effectiveness: in the papers studied LTR effectiveness is assumed in the range of 88-97%. The higher values of effectiveness (95-97%) are assumed by T.Neises and C.Turchi [71], Yuegeng Ma [11], R.Vasquez Padilla et al. [74], M.A. Reyes Belmonte et al. [72]. These very high values of effectiveness are in according to their additional constrains or assumptions about the pinch point temperature to be 5°C. Lower effectiveness is used by Craig S. et al [67] probably assumed due to the much higher or much lower minimum pressure of the cycle with respect to the other studies.

Pressure losses in the primary heat exchanger: in the analyzed papers are assumed in the range 50-80 kPa. The higher value 80 kPa is assumed by Dia Milani et al [70] for a small-scale decentralized solar plant of 10 MW_e while a lower value of 50 kPa is assumed by Yuegeng Ma [11] and Yuegeng Ma et al [59] for a larger size plants of 100 MW_e and about 60 MW_e respectively.

Pressure losses inside the cooler: the pressure losses inside the cooler in the analyzed papers are assumed in the range 20-80 kPa. The lower value is assumed by Yuegeng Ma [11], this very low value is correlated by the higher value of minimum pressure of the cycle (9.26 MPa) with respect to the other studies, the higher the pressure, the lower are the pressure drops. A slightly higher value (40 kPa) is assumed by Josè I.Linares et al [75] and Yuegeng Ma et al [69] correlated to a lower minimum pressure of the cycle (8-8.5 MPa). The highest value of pressure losses in the cooler is assumed in the work of Dia Milani et al [70] correlated to even lower minimum pressure of the cycle (7.5 MPa).

2.4 Medium and High Temperature Waste Heat Recovery

2.4.1 Introduction of the Energy Source

The recovery of waste heat for mechanical and electrical power generation is among the key strategies to reduce the consumption of fossil fuels and limit CO_2 emissions. Forman et al. [80] assessed the waste heat potential in the electricity generation sector and in the most common sectors of end use. The authors showed that, globally, 38% of the waste heat in the industrial sector, 36% in the commercial sector, and 54% in the transportation sector are available at temperatures higher than 300°C. When the waste heat is available at intermediate to high temperatures, the heat-to-power conversion is highly fostered due to the high thermal efficiency of the bottoming thermal engine. The state-of-the-art system for Waste Heat Recovery (WHR) from gas turbine exhaust is the three-pressure level steam Rankine cycle. It combines high cycle thermal efficiency with excellent capability in heat extraction from the exhaust, yet at the expense of staging the evaporation and expansion processes due to the thermodynamic properties of water. While this complexity in plant layout and equipment design is accepted for large heavy-duty gas turbines, it is hardly tolerated for aero-derivative gas turbines and internal combustion engines, where simpler bottoming cycle layouts based on single/dual pressure steam cycle or ORC are generally preferred. Thus, simple heat recovery steam/vapor generators and turbine designs are put before high efficiency in presence of small system sizes. This shift towards simpler and cheaper bottoming cycles is even more pronounced when the topping thermal engine operates at low-capacity factors, which is not uncommon in view of the wider deployment of renewables. In this context, the s-CO_2 power cycle does represent a promising bottoming cycle option to overcome, on the one hand, the complexity of bulky steam Rankine cycles and, on the other hand, the thermodynamic limitations of ORC dictated by the low limit of thermal stability of the organic fluids. In the literature the heat power from the exhaust gases is available at temperatures from 400 to 800°C and vary from 1 to 40 MW_{th}.

2.4.2 Cycle layouts studied and analyzed

Pre-heating supercritical CO_2 Brayton cycle

The distinctive feature of the WHR architectures is the maximization of the waste heat utilization of the hot source and, in turn, of the electrical net power output produced instead of the maximization of the first or second law efficiency of the cycle. Among them, the least complex cycle scheme is the Pre-Heating (Fig 2.15). The total CO_2 at the outlet of the compressor is split into two streams that are heated in parallel to an intermediate temperature. The first stream (m_1) is heated to state 3 by the external heat source in heater 1, whereas the second stream (m_2) is heated to state 4 in the recuperator by recovering internally the heat at the turbine exhaust. After mixing (state 5), the total CO_2 flow is heated by the external heat source in the heater 2 (5-6) up to turbine inlet temperature. The turbine exhaust is cooled in the recuperator (7-8) and in the cooler (8-1) in sequence down to the desired compressor inlet state.

This arrangement allows to have a better matching between the working fluid temperature glide and the hot source such that a greater heat utilization is achieved.

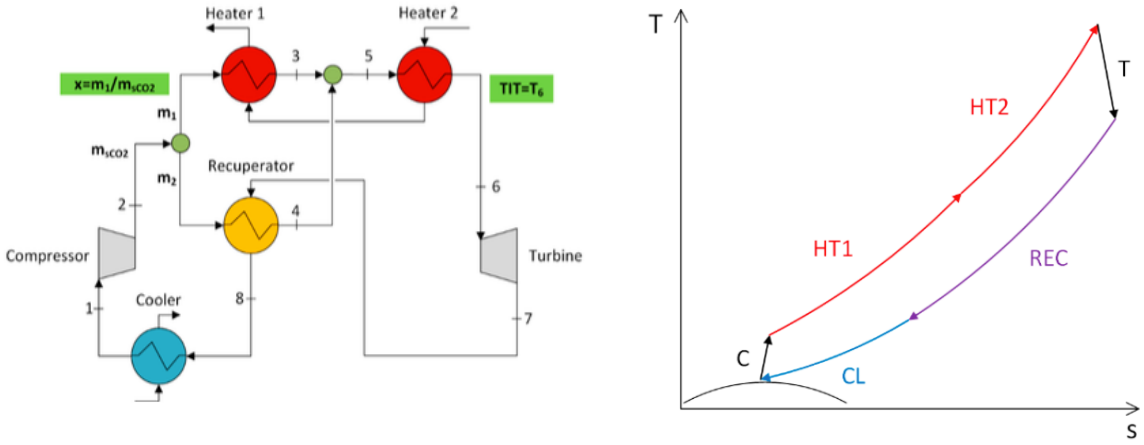

Figure 2.15 – Schematic layout and T-s diagram of a Pre-heating supercritical CO_2 Brayton cycle for High and Medium WHR application [81]

Pre-heating supercritical CO_2 Brayton cycle with Split Expansion

With respect to the Pre-Heating architecture, the Pre-Heating with Split Expansion (Fig. 2.16) is characterized by greater complexity. In fact, the flow is split downstream the compressor, heated up separately in two parallel branches and eventually expanded in two turbines at different inlet temperatures [40].

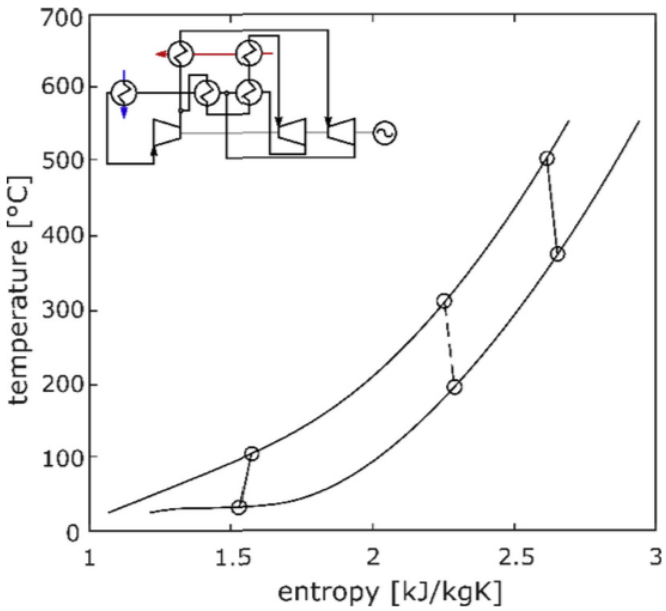

Figure 2.16 – Schematic layout and T-s diagram of a Pre-heating supercritical CO_2 Brayton cycle with split expansion for High and Medium WHR application [40]

Pre-heating supercritical CO_2 Brayton cycle with Pre-compression

Pre-Heating with Pre-Compression (Fig. 2.17), with respect to the Pre-Heating architecture embeds only an additional compressor and a gas cooler [40].

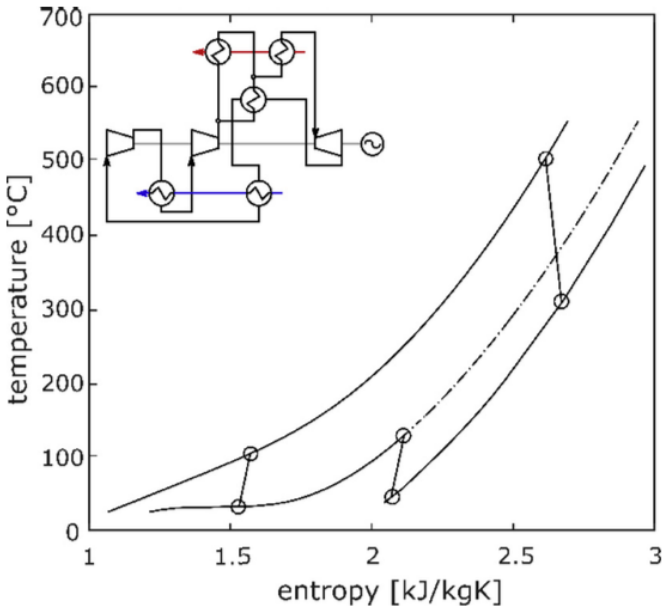

Figure 2.17 – Schematic layout and T-s diagram of a Pre-heating supercritical CO_2 Brayton cycle with Pre-compression for High and Medium WHR application [40]

Single Flow split with Dual Expansion s-CO_2 Brayton cycle

The Single Flow split with Dual Expansion s-CO_2 Brayton cycle (Fig. 2.18) is the most interesting and more studied cycle layout for High and Medium temperature WHR [30][58][59]. The total CO_2 flow at the outlet of the compressor is split into two streams. The first stream is heated to the maximum cycle temperature in the heater and expanded in the high temperature turbine (HTT). The second stream is heated to the low temperature turbine (LTT) in two recuperators in sequence. The s-CO_2 flow leaving the HHT is cooled in the HTR and mixed with the exhaust from LTT. The total CO_2 flow is cooled in the LTR and cooler down to the desired compressor inlet state.

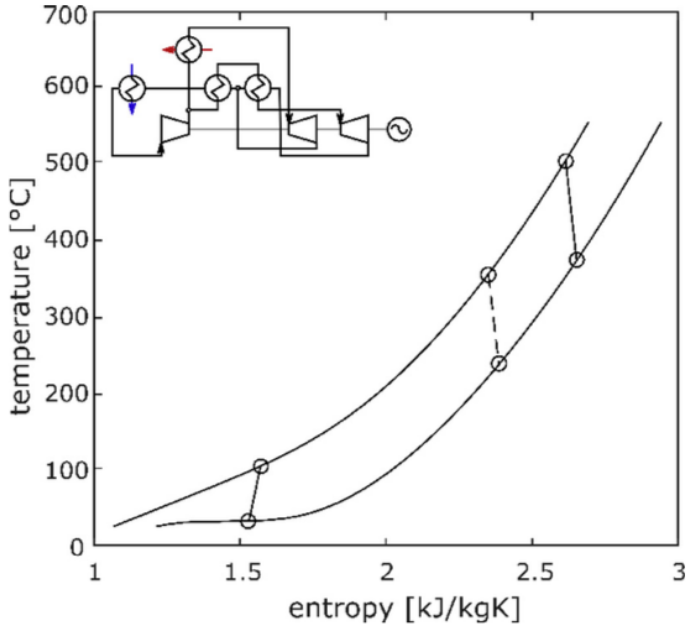

Figure 2.18 – Schematic layout and T-s diagram of a Single flow split with dual expansion supercritical CO_2 Brayton cycle for High and Medium WHR application [40]

Dual Flow split with Dual Expansion s-CO_2 Brayton cycle

After two compression processes, a portion of compressed fluid flows to one heater and the other portion flows to the recuperator, as we can see in Figure 2.19. Each flow goes to different turbine for the expansion process. Since the dual heated and flow split cycle has two flow splits unlike other cycle layouts, it can increase both heat absorption from the exhaust gas waste heat as well as the recuperated heat. Due to these reasons, the dual heated and flow split cycle is considered among the most promising one in the later studies [59][60].

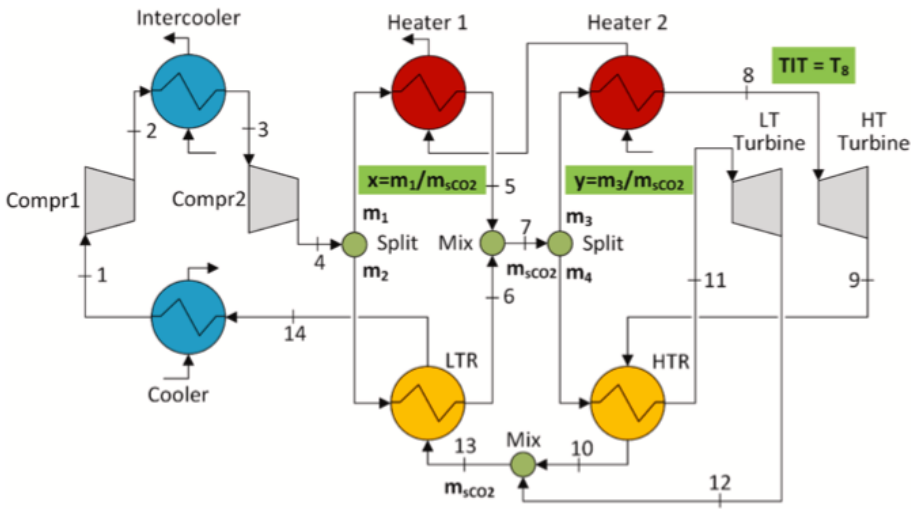

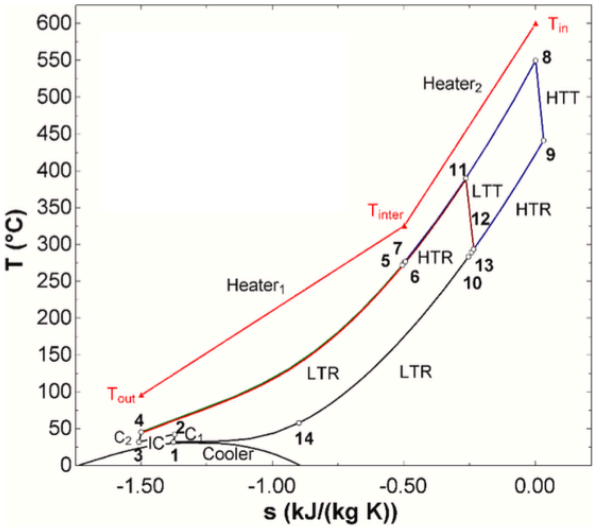

Figure 2.19 – Schematic layout and T-s diagram of a Dual flow split with dual expansion supercritical CO_2 Brayton cycle for High and Medium WHR application [82]

Dual Recuperated s-CO_2 Brayton cycle

This particular layout is proposed by Giovanni Manente and Mario Costa [81] in their work and is represented in Fig 2.20. The CO_2 flow at the outlet of the compressor is split into two streams that are sent to HTR and LTR in parallalel. The first stream (m_1) is heated in the LTR by the exhaust of the LTT and, subsequently, in the heater by the external heat source before expansion in the HTT. The second stream (m_2) is heated in the HTR by the exhaust of the HTT before expansion in the LTT. After heat recovery in HTR (5-6) and in LTR (8-9), the two heat depleted exhaust streams are mixed, and the residual heat is rejected to the environment in the cooler (10-1) down to the desired compressor inlet state.

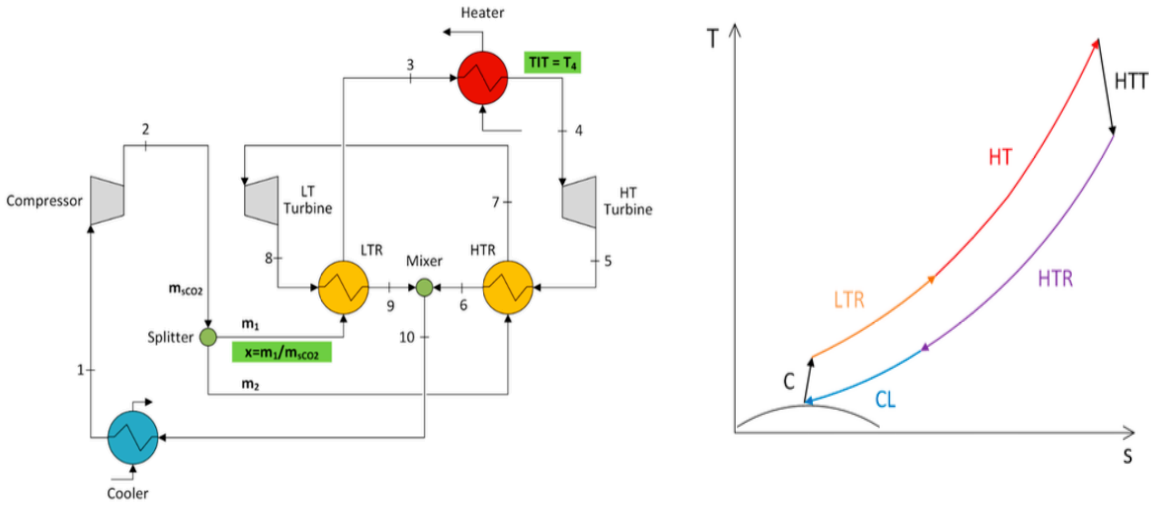

Figure 2.20 – Schematic layout and T-s diagram of a Dual recuperated supercritical CO_2 Brayton cycle for High and Medium WHR application [81]

Dual turbine-alternator-compressor recompression s-CO_2 Brayton cycle

This particular layout (a modified recompression cycle) was proposed by Pengcheng et al. [84] to recover the waste heat from the main engine exhaust gas of an ocean-going 9000 TEU container ship. Fig. 2.21 shows the schematic diagram of the dual TAC s-CO_2 RBC system. The components of this cycle are the main compressor, re-compressor, LTR, HTR, gas heat exchanger, turbines, generator and precooler. In the cycle process, the working fluid is divided into two parts by the splitter at the state point 9 before entering the precooler. A part of the working fluid flows into the bypass loop, is pressurized in the re-compressor, and then joins the cold stream from the entry point between the LTR and HTR. Therefore, the cold stream mass flow rate through the LTR is lower than the working fluid mass flow rate in the HTR because the outlet working fluid from LTR and recompression compressor are mixed together in the mixer at the state point 10. The dual TAC s-CO_2 RBC system is equipped with two turbines, the splitter separates the working fluid into two parts at the state point 6. The working fluid has the same temperature at the outlet of the two turbines and mixed together before entering the hot stream in the HTR. The whole working fluid will be cooled in the LTR where heat is transferred to preheat the cold stream CO_2. Finally, the working fluid is cooled close to its critical temperature in the precooler where the heat is rejected to the surroundings.

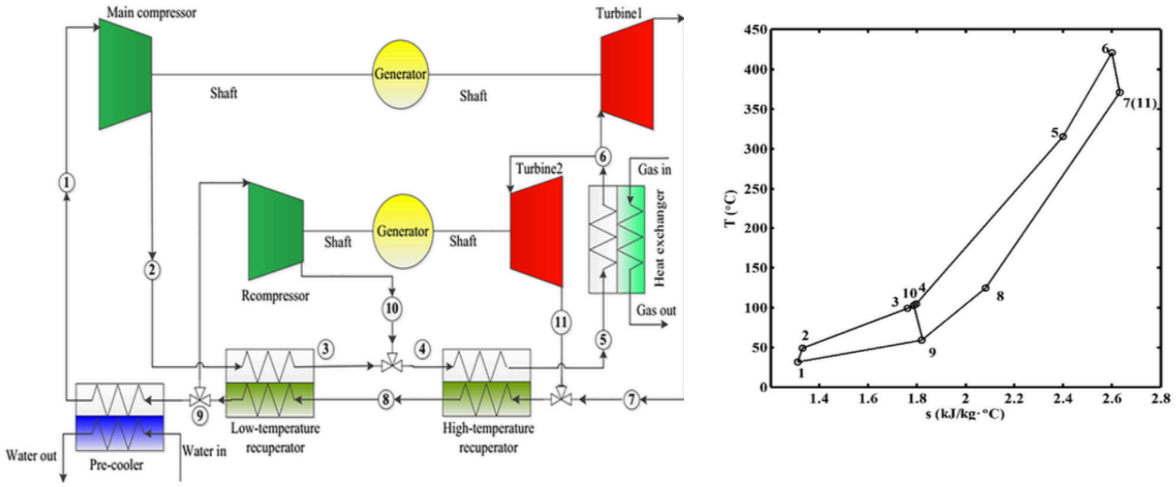

Figure 2.21 – Schematic layout and T-s diagram of a Dual turbine-alternator-compressor recompression supercritical CO_2 Brayton cycle for High and Medium WHR application [84]

2.4.3 Optimization Methodology

Thermodynamic optimization

The kind of thermodynamics optimizations in the literature are mainly single objective for the high and medium temperature waste heat recovery application with the aim to maximize the cycle net power output performed by Marchionni et al. [40], the total heat recovery efficiency (the product between the cycle efficiency and heat recovery efficiency) performed by Giovanni Manente and Mario Costa [81] or exergy efficiency performed by Min Seok Kim et al. [83].

Giovanni Manente and Mario Costa [81] concentrated their work on some novel layouts of s-CO_2 Brayton cycles, aimed at increasing the heat extraction from the heat source while preserving as much as possible the inherently high thermal efficiency. Among these, the most promising ones feature dual expansion, partial heating and dual recuperated for waste heat recovery application. In this work a systematic approach based on the superimposition of elementary thermodynamic cycles to identify the building blocks for the achievement of high performance in the utilization of waste heat sources is used. A thermodynamic optimization is set up in EES environment to compare the performance of these novel layouts. The two optimization variables are the TIT and the SR. The inlet temperature of the heat source is fixed and set at 600°C, also the inlet and outlet pressure of compressor and its inlet temperature are fixed for all the cycles and equal to 7.63 MPa, 20 MPa and 32°C respectively. Main results show that the total heat recovery efficiency for dual expansion cycle is 22.3%, for the preheating cycle is 21.63% and for dual recuperated cycle id 19.39%, while the optimized TITs result 550°C, 390°C and 520°C respectively.

Min Seok Kim et al. [83] studied the thermodynamic analysis and sensitivity analysis of various s-CO_2 power cycles in conjunction with 5 MW_e Landfill Gas Firing (LFG) turbine to investigate which s-CO_2 cycle is the most suitable to maximize the net power output produced. The most suitable cycle layout for this application resulted the dual heated and flow split cycle, the other layouts studied are the partial-heating, simple recuperated, recompression, pre-compression, single and dual heated cascade, single and dual heated cascade with intercooling and some new cycles proposed such as triple heating cycle, a combination of recompression and partial heating cycle, partial recuperation and dual expansion cycle. The optimization was performed with an in-house code, KAIST-CCD developed by KAIST research team. The optimization variables were the mass flow rate, flow splits ratios, turbine outlet pressure and first compressor outlet pressure, while the TIT and the maximum pressure of the cycle were fixed at 503.17°C and 27.6 MPa respectively. It was found that a recompression cycle is not suitable for the bottoming cycle application, while the partial heating cycle has relatively higher net produced work with a simple layout and small number of components. Although the dual heated and flow split cycle had the highest net produced work, it has disadvantages of having numerous components and complex process which requires more sophisticated operational strategies. This study identified that the recuperation process is much more important than the intercooling process to the s-CO_2 cycle design for increasing the thermal efficiency and the net produced work.

Marchionni et al. [40] have presented a tecno-economic analysis of eight variants of s-CO_2 Joule-Brayton cycles, in particular, four layouts originally developed for CSP and nuclear applications: the simple regenerative, re-heating, recompression and recompression with reheating, have been compared to architectures more oriented to waste heat recovery and conversion uses, such as pre-heating, pre-heating with split expansion, split-heating with split expansion and pre-heating with pre-compression (PCPH). Main assumptions of the study were: all the pressure losses neglected, the compressor inlet and outlet pressure fixed at 7.4 MPa and 20 MPa. The analysis was carried out with the software CycleTempo with the goal to maximize the net power output varying the TIT and split ratio with reference to a heat source gas flow rate of 1.0 kg/s and 650°C. The waste heat recovery and conversion architectures have been

found to be able to generate a much higher net power output in comparison to the more conventional layouts, due to the higher amounts of waste heat they can recover. The novel PHPC architecture was found to be able to achieve the highest net power output 171 kW_e. Nonetheless, the investment cost analysis revealed that the Simple Recuperative plant scheme, which is characterized by the lowest complexity, provides the highest economic effectiveness (SC=1,500 \$/kW_e and LCOE=0.014 \$/kWh).

Thermo-economic optimization

The thermo-economic optimizations are obviously at least two-objectives, the ones present in the literature are performed by Alperen Tozlu et al [85] with minimization of total cost rate and maximization of exergy efficiency as its objectives, Giovanni Manente e Francesca Maria Fortuna [82] with maximization of total heat recovery efficiency and minimization of specific investment cost as its objectives and Pengcheng Pan et al [84] that performed a multi-objective optimization with maximization of net power output, energy and exergy efficiency and minimization of LCOE as its objectives.

Alperen Tozlu et al. [85] performed a thermodynamic and thermo-economic analyses as well as optimization of a simple supercritical CO_2 cycle with intercooling. The exhaust gas of an actual solid waste power plant is used as heat source of the cycle (mass flow rate of exhaust gas is 16 kg/s and 566.7°C). A multi-objective thermo-economic optimization was carried out using the NSGA-II developed in MATLAB software. The PR of the cycle, the inlet pressure of the turbine, the dead state temperature and the logarithmic mean temperature difference are selected as decision parameters in order to maximize the exergy efficiency and to minimize the total cost rate of the system while the other parameters ate fixed (TIT 546.7°C; CIT 40°C). The net power, the energy and exergy efficiencies, the total cost and the total capital cost rates of the gas turbine cycle are optimized by +1.73%, +3.21%, +2.45%, -1.11% and -1.64%.

Giovanni Manente e Francesca Maria Fortuna [82] investigated the potential of two novel layouts, namely the single and dual flow split with dual expansion, in the recovery of waste heat in a wide temperature range between 400 and 800°C compared to the more traditional single recuperated and recompression layouts. The results of the thermodynamic optimization performed in EES environment showed that the novel layouts markedly improve the total heat recovery efficiency (i.e., the ratio between net power output and heat available from the heat source) compared to the traditional layouts, optimizing the TIT and the split ratios (while the minimum pressure and temperature and maximum pressure of the cycles are fixed at 7.63 MPa 32°C and 20 MPa respectively). Both the traditional cycles achieved a maximum total heat recovery efficiency between 12.0 and 18.5%, the improvement varies from 3.0 to 7.7% points for the single flow split with dual expansion cycle and from 5.8 to 9.5% points for the dual flow split with dual expansion cycle. The improvement in total heat recovery efficiency is mainly the consequence of a more effective heat extraction from the heat source, whose outlet temperature is no more constrained by the recuperators. The multi-objective optimization (maximization of total heat recovery efficiency and minimization of specific investment)

showed that the marked increase in performance is obtained at the expenses of only a limited increase of 5.0–6.2% in specific investment cost compared to the traditional cycles.

Pengcheng Pan et al. [84] proposed a modified s-CO_2 RBC system, namely the dual TAC s-CO_2 RBC system, which to be used to recover the waste heat from the main engine exhaust gas of an ocean-going 9000 TEU container ship. Multi-objective optimization based on the Imperialist Competition Algorithm to investigate the optimal performance of the proposed system was conducted with the net power output, energetic efficiency, exergetic efficiency, heat exchanger area per unit power output and LCOE as objective functions, while the main compressor inlet temperature (in the range 32-40°C) and pressure (in the range 8-9 MPa), main compressor outlet pressure (in the range 14-24 MPa), flow split ratio between compressors, turbine required mass flow rate (in the range 10-15 kg/s), TIT (in the range 400-435°C) and flow split ratio between turbines were selected as decision variables The results showed that the performance of the modified system is strengthened significantly, whose highest net power output, energetic efficiency and exergy efficiency were 452.2 kW_e, 24.53% and 41.47%, approximately 26.58%, 16.67% and 16.90% higher than that of the s-CO_2 RBC system. Compared with the s-CO_2 RBC system, the modified system is more compact because its heat exchanger area per unit power decreased by 44.08%. The modified system can contribute to decreasing the ship auxiliary engine fuel consumption. The results of this study can provide theoretical support for the application of the dual TAC s-CO_2 RBC waste heat recover system on ships.

Optimized cycle layouts, efficiencies and costs

Giovanni Manente and Mario Costa [81] compared some novel layouts of s-CO_2 Brayton cycles, namely dual expansion, partial heating and dual recuperated, aimed at increasing the heat extraction from the heat source (maximizing the total heat recovery efficiency defined as the product between cycle efficiency and the heat recovery efficiency). Among these, dual expansion was the most promising one. Ming Seok Kim et al. [83] and Marchionni et al. [40] studied the performances of different cycle layouts aiming at maximize the net power output and the most promising layouts resulted the dual heated and flow split cycle (also called dual flow with dual expansion cycle that resulted with a total heat recovery efficiency of 22.3%) and the pre-heating with pre-compression cycle (with a cycle first law efficiency of 29%, specific cost 2,000 \$/kW_e and LCOE of 0.016 \$/kWh). As we can observe by the different conclusions of these different studies there is a lack on consensus of the best CO_2 cycle layout in the literature for WHR application, however all the cycle mentioned show higher performance in terms of net power output produced and total heat recovery efficiency with respect to traditional layouts. Giovanni Manente e Francesca Maria Fortuna [82] performed an interesting thermo-economic optimization (aiming at maximizing the total heat recovery efficiency and minimizing the specific investment cost) and compared some traditional layouts such as the simple recuperated and recompression cycle against the single and the dual flow with dual expansion that showed a high enhancement of total heat recovery efficiency (3-9.5%) and only a limited increase in specific investement cost (5-6.2%).For a waste gas termperature varying

from 600°C to 800°C, total heat recovery efficiency resulted 20.62-26.45% and the specific investment cost of 2,025-2,430 \$/kW_e.

Research projects

Waste heat recovery is the process of capturing heat from waste streams of an existing industrial process and using this heat directly, upgrading it to a more useful temperature, and/or converting it to electrical power or cooling. The energy generated from heat recovery, if not required by the process or industrial site can be exported to neighboring facilities or to electrical or heat distribution networks, offering significant energy savings and substantial greenhouse gas emission reductions. The main aim of the I-ThERM project (coordinated by Brunel University London) is to investigate, design, build and demonstrate innovative plug and play waste heat recovery solutions and the optimum utilization of energy within and outside the plant perimeter for selected applications with high replicability and energy recovery potential in the temperature range 70°C-1000°C for process heating and heat to power conversion [86]. This project has received funding from the EU and has many partners (Spirax-Sarco Limited, Tata Steel UK Limited, Enogia, E-4 Experts GMHB, Avanzare Innovacion Tecnologica SL, and other European companies from Spain, France, Germany, United Kingdom, Cyprus and Greece) among which the Italian society Synesis Società Consortile a Responsabilità Limitata. The innovation of this project is the development of an on-line monitoring, evaluation and control optimization system to maximize energy conversion efficiency of heat recovery and heat to power conversion technologies. EINSTEIN Expert system tool has been upgrated to incorporate the I-ThERM heat recovery and heat to power conversion technologies. Hardware and software tools are being developed to enable real-time communication between monitorning and control system and EINSTEIN tool. Development and demonstration of a 50 kW_e supercritical CO_2 high temperature heat to power system has been carried out and also development and demonstration of flat heat pipe technology for high temperature heat recovery from steel manufacturing plant while future activities aim to implement monitoring and control system to demonstration technologies, use web based monitoring and evaluate, in real-time, performance of the I-ThERM technologies at the specific demonstration sites and to assemble and demonstrate a high temperature (about 700°C) heat source s-CO_2 prototype heat to power conversion system integrated with the heat source evaluating its performance [87][88].

2.4.4 Typical assumptions

All the papers and the studies in the literature make several assumptions for modeling the s-CO_2 cycles. Many of these assumptions are about components performances such as turbomachinery efficiencies or effectiveness of recuperators, pinch point temperatures and pressure drops (sometimes neglected for simplicity) in heat exchangers. All these assumptions are obviously reasonable depending on the case study, size of the plant, application, mass flow rates, operating pressures and temperatures. The main assumptions in the papers analyzed for high and medium temperature WHR application are:

Turbine efficiency: in the analyzed papers the turbine efficiency is assumed in the range 85-90%. The lowest efficiency value (85%) is assumed by Marchionni et al. [40], Giovanni Manente and Mario Costa [81] and Giovanni Manente and Francesca Maria Fortuna [82] the characteristcs of the turbomachinery are not specified in all the papers (Giovanni Manente and Francesca Maria Fortuna [82] assumed radial turbine) but this value is probably correlated to the very small size of the system (120 kW_e-1 MW_e). Higher value of efficiency (90%) is assumed by Min Seok et al. [83] and Abubakr Ayub [89] , considering a larger size of the plants (3.23-10 MW_e).

Compressor efficiency: in the analyzed papers the compressor efficiency is assumed in the range 70-85%. The lowest efficiency value (70%) is assumed by Marchionni et al. [40], due to the very small size of the system (124-174 kW_e), while higher values of efficiency (80-85%) are assumed by Min Seok et al. [83], Giovanni Manente and Mario Costa [81], Giovanni Manente and Francesca Maria Fortuna [82] and Abubakr Ayub [89] , considering a larger size of the plants (1-10 MW_e).

Recuperators effectiveness: in the papers studied the recuperators effectiveness is assumed in a small range of 92-95%. The smallest value of effectiveness (92%) are assumed by Alperen Tozlu et al. [85] according to the constraint of LMTD in the range 9-13°C to be optimized and the use of Shell&Tube heat exchangers. Highest value (95%) of effectiveness are assumed by Giovanni Manente and Francesca Maria Fortuna [82], Giovanni Manente and Mario Costa [81] according to the assumption of using PCHE.

Pressure losses in the primary heat exchanger: pressure losses in the primary heat exchanger in the analyzed papers are assumed in the range 140-200 kPa. The lower value 140 kPa is assumed by Min Seok Kim et al. [83] for a higher maximum pressure of the cycle 27.6 MPa and the higher value 200 kPa is assumed by Giovanni Manente and Francesca Maria Fortuna [82] correlated to a lower value of maximum pressure of the cycle 20 MPa. The higher pressure of the cycle is the same of the working fluid in the primary heat exchanger, so the higher the maximum pressure of the cycle the lower are the pressure losses.

Pressure losses inside the cooler: when not neglected are always assumed 0.5% in the cooler. All the studies have similar minimum temperature of the cycle (7.63 MPa [82] or 7.67 MPa [83]) resulting about 40kPa.

2.5 Low to Medium Temperature Waste Heat Recovery with Transcritical CO_2 Cycles

2.5.1 Introduction of the Energy Source

Increasing energy efficiency is a way to future energy sustainability. Significant part of energy input through fuel is lost as waste heat in industrial processes. Recovery of waste heat may be a possible option to increase energy efficiency. Low grade waste heat accounts for more than 50% of all the waste heat generated by the industry, but the lower the temperature, the more difficult it is to recover the waste heat. Generation of power using CO_2 cycle is a prospective option for recovery and utilisation of low temperature industrial waste heat, as it may not be economically viable using conventional technologies. The typical temperature range in the literature for transcritical CO_2 cycles is 145°C-500°C while the heat power available is 1-80 MW_{th}.

2.5.2 Cycle layouts studied and analyzed

Pre-heating transcritical CO_2 cycle

The layout and components of the Pre-heating transcritical CO_2 cycle (Fig. 2.22) are the same of the Pre-heating supercritical cycle. The only difference is that the compression of the working fluid is operated in the liquid phase and not in the supercritical region so there is pump instead of the compressor.

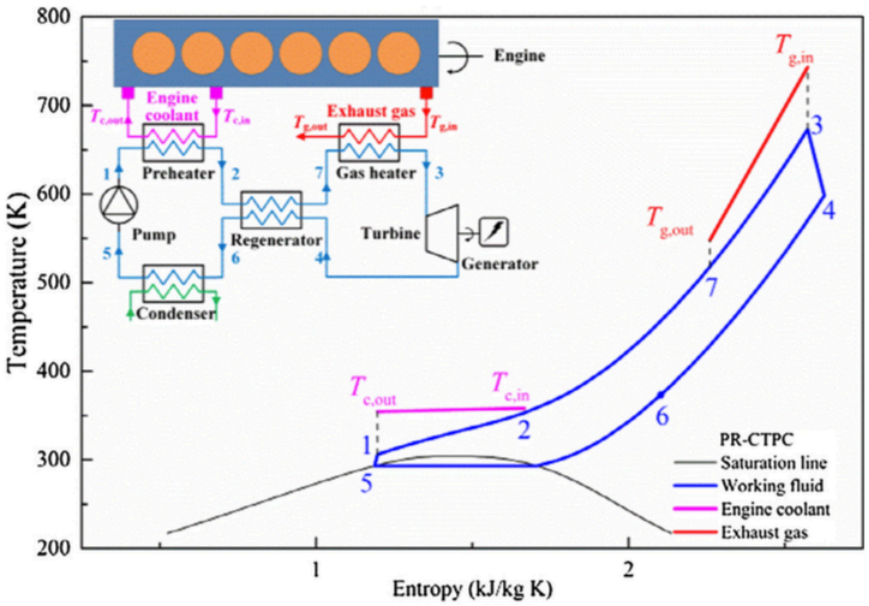

Figure 2.22 – Schematic layout and T-s diagram of a Pre-heating transcritical CO_2 Brayton cycle for Medium and Low WHR application [90]

Single pressure with Dual and Triple Expansion transcritical CO_2 cycle

As for the Pre-heating cycle, the Single pressure with Dual Expansion transcritical CO_2 cycle has the same layout and components of the supercritical cycle with the except for the pump instead of the compressor. This cycle is interesting also for the medium-low temperature WHR, mainly studied by Chuang Wu et al [91] and Shun-sen Wang et al. [92] that compared the performances of Single pressure with Dual Expansion transcritical CO_2 cycle (Fig. 2.23) with those of Single pressure with Triple Expansion transcritical CO_2 cycle represented in Fig. 2.24 where three turbines and three regenerators are needed increasing the complexity of the cycle layout.

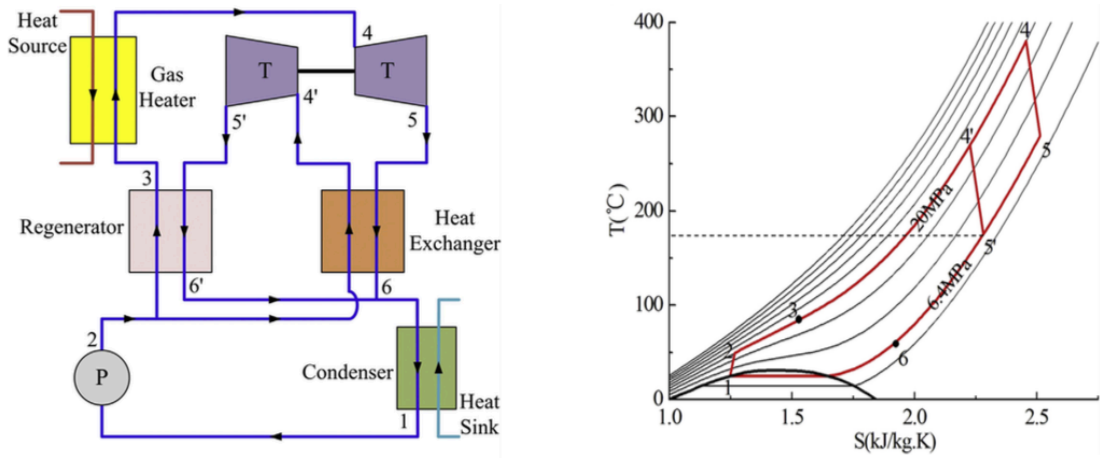

Figure 2.23 – Schematic layout and T-s diagram of a Single pressure with dual expansion transcritical CO_2 Brayton cycle for Medium and Low WHR application [91]

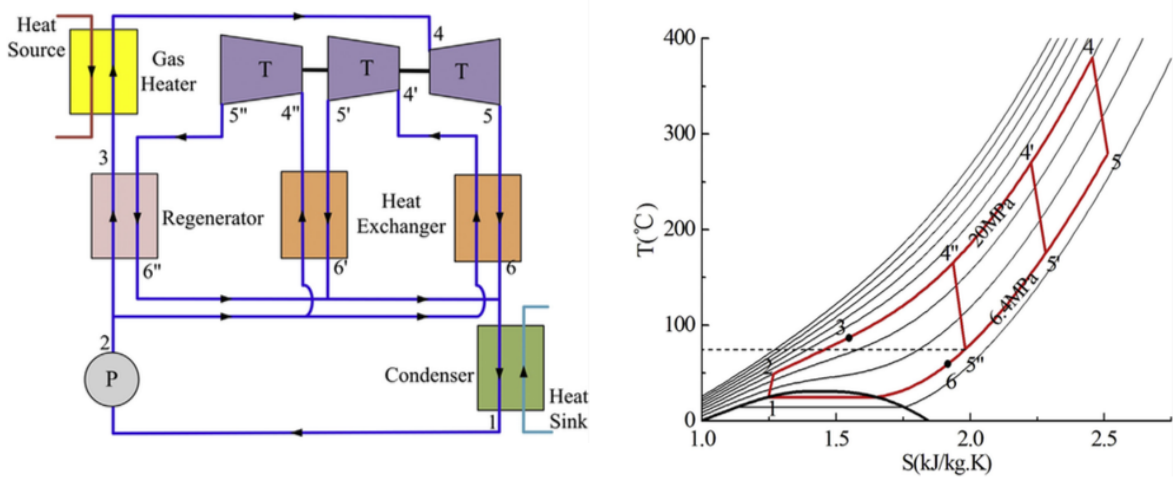

Figure 2.24 – Schematic layout and T-s diagram of a Single pressure with triple expansion transcritical CO_2 Brayton cycle for Medium and Low WHR application [91]

Simple transcritical CO_2 cycle with and without regeneration

The Simple transcritical CO_2 cycle presents the same conceptual configuration as the simple supercritical CO_2 cycle but turns out to be a pseudo-Rankine cycle. It is represented in Fig. 2.25 and 2.26 with and without regeneration respectively. It is studied for its simplicity and compactness and also as a base cycle to evaluate and compare the performances of more sophisticated layouts.

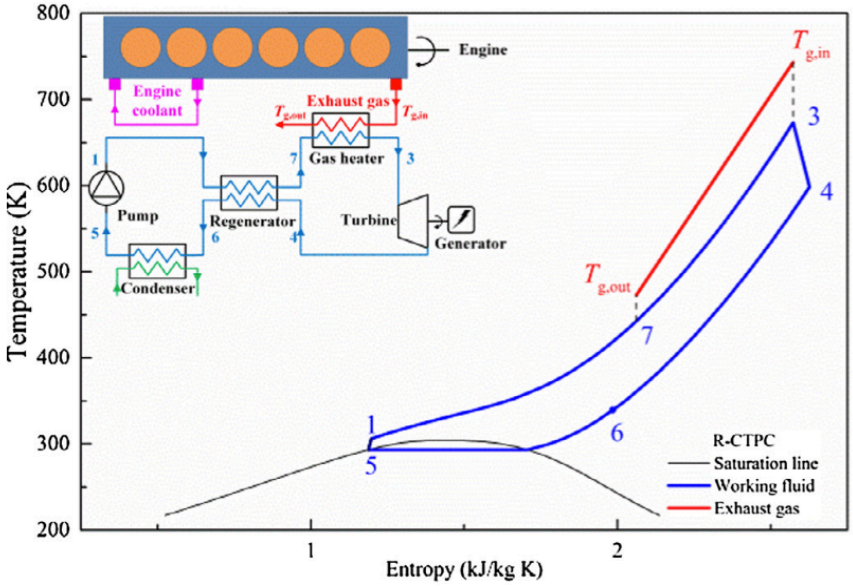

Figure 2.25 – Schematic layout and T-s diagram of a Simple transcritical CO_2 Brayton cycle for Medium and Low WHR application [90]

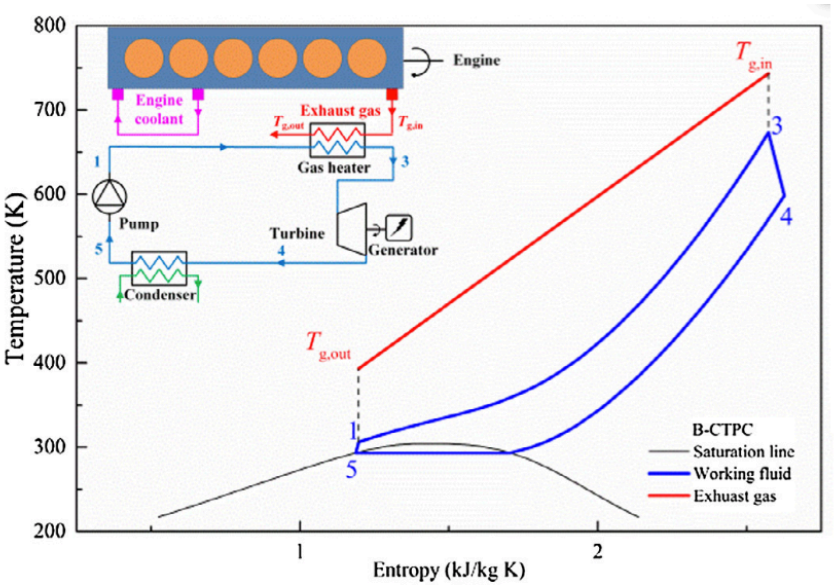

Figure 2.26 – Schematic layout and T-s diagram of a Simple transcritical CO_2 Brayton cycle without regeneration for Medium and Low WHR application [90]

2.5.3 Optimization Methodology

Thermodynamic optimizations

The kind of thermodynamics optimizations in the literature are mainly single objective for the medium-low temperature waste heat recovery application with the aim to maximize the cycle net power output performed by Chuang Wu et al. [91] and Shubham Banik et al. [93].

Chuang Wu et al. [65] in their work, proposed a novel type of single-pressure, multi-stage carbon dioxide transcritical power cycle (CDTPC) for waste heat of exhaust gas from gas turbines or internal combustion engines. System parameter optimization (TITs and TIPs) is carried out to achieve the maximum net power output using genetic algorithm. A comparative study between the existing (simple regenerative cycle) and the proposed novel type of cycles (single pressure with double and triple expansion) with the same exhaust gas temperature T_{gi} (250-500°C) at the inlet of the gas heater shows that the novel layouts can increase the net power output by 3.9-26.3% and decrease the optimum working pressure by 13.2-31.0%. Results show that waste heat can be utilized more effectively by the double-stage when 250°C<T_{gi} < 412°C and by the three-stage CDTPC when 412°C < T_{gi}<500°C.

Shubham Banik et al. [93] carried out a parametric optimization of a transcritical carbon dioxide (t-CO_2) power cycle which recompresses part of the total mass flow of working fluid before entering the precooler, thereby showing potential for higher cycle efficiency. Thermodynamic model for a recompression t-CO_2 power cycle has been developed for waste heat source of 2,000 kW_{th} and temperature of 200°C. The mathematical model described in this study predicts the calculated efficiencies from an Aspen simulation. Results obtained from this model are analysed to estimate effects on energetic and exergetic performances of the power cycle varying pressure and mass recompression ratio. Higher pressure ratio always improves thermodynamic performance of the cycle, both energetic and exergetic. Higher recompression ratio also increases exergetic efficiency of the cycle. However, it increases energy efficiency, only if precooler inlet temperature remains constant. Maximum thermal efficiency of the t-CO_2 cycle with a recompression ratio of 0.26 has been found to be 13.6%. To minimize total irreversibility of the cycle, an optimum ratio of 0.48 was found to be suitable. PC and HTR contributes to the maximum change in total irreversibilities.

Thermo-economic optimizations

Thermo-economic optimizations are obviously at least two-objectives, as the maximization of net power output and minimization of total bare module cost performed by Nima Mirkani et al. [94] or multi-objective such the as maximization of net power output and exergy efficiency and minimization of EPC [$/kWh] performed by Hua Tian et al. [90]. Generally, a representative subset of the Pareto optimal solutions better satisfying the preferences for double objectives can be obtained. It can be done focused tradeoffs within this set of solutions, rather than needing to consider all the Pareto solutions of the three-objective optimization.

Nima Mirkani et al. [94] investigated the thermo-economic performances of transcritical CO_2 Rankine cycles with and without reheat process in low-grade waste heat recovery applications.

Two reheating scenarios are proposed to evaluate the effect of bounded and unbounded reheats on the cycle. In the first method, the constant available heat flow is distributed between the evaporator and the reheater via an optimized ratio, while in the second, the required energy for the reheat process is provided with optimized additional fuel consumption. The proposed cycles are modeled and optimized for source temperatures ranging from 150 to 300°C at fixed flow rate of 1,000 kg/s. The results obtained from thermodynamic optimization indicate that reheat cycle with burning additional fuel leads to the largest power generations ranging from 14-57 MW_e depending on the source temperature, while the reheat cycle with heat stream division shows the weakest performance by producing 8-37 MW_e. In the thermo-economic optimization, the ratio of power output to the cycle total bare module cost has been maximized. Under these conditions, the reheat cycle with burners still shows the highest rate of power production, while economic indicators limit the power generation and introduce the simple Rankine cycle without regeneration as the best option as it has the highest benefit-to-cost ratio. The first scenario does not represent any powerful performance and has the least power output and benefit-to-cost ratio. Therefore, simple Rankine cycle is the most economical cycle for applying to heat recovery processes, if capital cost is the only variable taken into account. The second scenatio, is always the best cycle configuration in terms of power output generation. However, despite the higher power production, a slightly weaker performance when economic conditions are applied, compared to the simple Rankine cycle. Nonetheless, this scenario generates power outputs up to 50% higher than the simple cycle, and therefore, in cases where the additional capital and running costs associated with it are affordable for the project, it represents the best waste heat recovery option.

Hua Tian et al. [90] presented systematic multi-objective optimization methodology for the carbon dioxide transcritical power cycle with various configurations used in engine waste heat recovery to generate more power efficiently and economically. The parametric optimization was performed for the maximum net power output and exergy efficiency, as well as the minimum electricity production cost by using the genetic algorithm varying TIT in the range 165-430°C and TIP in the range 8-25 MPa. The layouts studied were the simple cicle with and without regeneration and the pre-heating cycle with and without regeneration. The comparison of the optimization results showed that the thermodynamic performance can be most enhanced by simultaneously adding the preheater and regenerator based on the basic configuration (simple transcritical brayton cycle without regeneration). On the condition of no additional preference, the optimum net power output, exergy efficiency and EPC for the referential optimal solution of simple regenerative cycle were 24.24 kW_e, 36.88% and 0.583 $/kWh, respectively. Pre-heating achieves 17.44% higher net power output and 4.98% higher exergy efficiency but at the expense of 4.11% more EPC, than those of simple regenerative cycle.

Another interesting thermodynamic and exergoeconomic study was performed by Shun-Sen et al. [92] that focused on the comparison between the novel single-pressure multi-stage and single-pressure single-stage carbon dioxide transcritical power cycles for engine waste heat recovery. Parametric studies were successfully conducted to evaluate the effects of the key thermodynamic parameters on the performances of the considered cycles, optimized by the GA. The main conclusions can be summarized as follows: the thermodynamic study indicates that

the double-stage cycle has the highest net power output (517.27 kW_e) for waste heat recovery from exhaust gas of a 2,928 kW_e engine at 470 °C, which is 21.53% and 9.21% higher than that of the single-stage and triple-stage cycle, respectively. The exergoeconomic study reveals that the single-stage CDTPC has the lowest total product unit cost when exhaust gas temperature is 300-600°C. The double-stage CDTPC is recommended when exhaust gas temperature is 530-600°C due to its highest net power output and comparable total product unit cost with that of single-stage cycle. Mean- while, the triple-stage CDTPC is not recommended when exhaust gas temperature is 300-600°C due to its highest total product unit cost and lower net power output than the double-stage. The multi-objective optimization for the case study shows that the optimal net power output and total unit product unit cost are 422.809 kW_e and 28.062 $/GJ for the single-stage, 516.667 kW_e and 28.266 $/GJ for the double-stage, and 473.647 kW_e and 31.250 $/GJ for the triple-stage, respectively. The parametric study and optimization results indicate that the multi-stage can obtain the optimal thermodynamic and exergoeconomic performances at lower maximum cycle pressure than single-stage.

Optimized cycle layout, efficiencies and costs

Chuang Wu et al. [91] in their study proposed two novel layouts (double and triple expansion) in comparison to the simple transcritical cycle to maximize the net power output and the double expansion seems the best layout for the WHR with an exhaust temperature varying from 250 to 500°C, increasing the power output and decreasing the optimum working pressure with respect to the simple configuration, resulting in a cycle efficiency 21.18-23.22% and net power output of 119-272 kW_e. The same conclusions were reached by Shun-Sen et al. [92] demonstrating that the double expansion cycle has the highest power output among the single, double and triple expansion cycles, and it also has benefit from the economic point of view because has a total product unit cost similar to the single expansion (efficiency resuted 30%, net power 516 kW_e and specific cost of 28.266 $/GJ for a mass flow rate and temperature of the exhaust of 4.35 kg/s and 470°C respectively). Another interesting thermo-economic study was the one performed by Hua Tian et al. [90] aimed to maximize the net power output and exergy efficiency and minimize the electricity production cost where the pre-heating cycle with regeneration is demonstrated to have the best performances with an exergy efficiency of 36.88%, net power output of 24.24 kW_e and an EPC of 0.583 $/kWh (for an exhaust mass flow rate of 0.381 kg/s and temperature 470°C).

2.5.4 Typical assumptions

All the papers and the studies in the literature make several assumptions for modeling the s-CO_2 cycles. Many of these assumptions are about components performances such as turbomachinery efficiencies or effectiveness of recuperators, pinch point temperatures and pressure drops (sometimes neglected for simplicity) in heat exchangers. All these assumptions are obviously reasonable depending on the case study, size of the plant, application, mass flow rates, operating pressures and temperatures. The main assumptions in the papers analyzed for medium to low temperature WHR application are:

Turbine efficiency: in the analyzed papers the turbine efficiency is assumed in the range 70-90%. The lowest efficiency values (70-75%) are assumed by Hua Tian et al. [90], Chuang Wu et al. [91] and Ali Amini et al. [95], the characteristcs of the turbomachinery are not specified in the papers but these values are probably correlated in the first and second case to the small size of the system (120-275 kW_e) and in the third case to the very small TIT (126°C). Higher value of efficiency (80%) is assumed by Shun-Sen et al. [92] due to the two or three stages for expansion. It still not a high value of efficiency because of the small size of the system (400-500 kW_e). The Highest value of efficiency (90%) is assumed by Nima Mirkhani et al. [94] because they assume a two-stage expansion (reheating) and a larger size of the plant with respect to the other studies (2-6.3 MW_e).

Pump efficiency: in the analyzed papers pump efficiency is assumed in the range 75-85%. Lowest value of pump efficiency (75%) is assumed by Chuang Wu et al. [91] according to the reduced size of the system (120-260 kW_e) while higher efficiency (80%) is assumed for centrifugal pump and larger power output by Nima Mirkhani et al. [94] and Ali Amini et al. [95] (2-6.3 MW_e). Highest efficiency of the pump (85%) is assumed by Shubham Banik et al. [93] probably due to the very low CIP (5 MPa) and low PR.

Pressure losses: the pressure losses in the analyzed studies are mainly always neglected both in pipes and heat exchangers.

3. Cost Correlations

The economic analysis and investment anlaysis are essential to assess the feasibility in the commercialization of a new to technology. Different applications require different layouts and devices to make the best integration between the s-CO_2 cycle and the heat source. When more than one solution seems valid from the thermodynamic point of view an economic investigation is mandatory to compare their benefits also from the thermo-economic perspective. Since the costs of pipelines possess a small proportion of the total investment in the system, the investment cost of the cycle is calculated merely considering main components such as turbines, compressors (or pumps) and heat exchangers. In all the thermo-economic optimizations, techno-economic studies or exergoeconomic investigations in the literature, some cost correlations for the components are assumed. These correlations are fuction on some component parameters from which depend its size and complexity. Generally, the more the parameters in the correlation, the more detailed and accurate is the economic evaluation. Obviously depending on the specific application other costs have to be taken into account, mainly concerning the heat souce and the introduction of the thermal power inside the power block such as reactor for nuclear application, boiler for coal application, receiver and heliostat field for CSP application. Moreover the costs of auxiliary components, fuel and operation and management costs have to be considered to evaluate some important economic indexes (LCOE, Pay Back Time, Net Present Value, etc.) useful to compare different technological solutions for the same application.

3.1. Turbine's Cost Correlations

As a thermal power conversion device, the turbine is the key component to ensure the system to run in a safe and effective way. The working fluid CO_2 expands in the turbine and converts heat energy into mechanical energy output through the kinetic energy of a series of moving blades. According to the flow direction of working fluid, turbines are classified into two types of axial flow and radial flow. The characterists and the detailed design of the turbine are not usually examined in depth in the papers analyzed, this is probably because this technology is not mature nowadays and the development of s-CO_2 turbomachinery is under research and development. The studies examined are mainly preliminary assessment of cycle layouts and theoretical stuctures aming to optimize the operating parameters of the plant as a whole. The correlations to compute a preliminary cost of the turbine are different and reported below:

$$C_T = 1000\dot{W}_T \quad [82] \quad (3.1)$$

$$C_T = 3880.5\dot{W}_T^{0.7}\left(1+\left(\frac{0.05}{1-\eta_T}\right)^3\right)(1+5exp\left(\frac{T_{T,i}-866}{10.42}\right) \quad [92] \quad (3.2)$$

$$C_T = 7790\dot{W}_T^{0.6842} \quad [96] \quad (3.3)$$

$$C_T = 479.34\dot{m}_T\frac{1}{(0.93-\eta_T)}ln(\beta_T)(1+\exp(0.036T_{T,i}-54.4)) \quad [40][85][52][76] \quad (3.4)$$

Where:

-$\dot{m}_T$ is the working fluid mass flow rate in the turbine [kg/s]

-η_T is the isentropic efficiency of the turbine [-]

-β_T is the pressure ratio of the turbine [-]

-$T_{T,i}$ is the turbine inlet temperature [°C]

-$\dot{W}_T$ is the power generated by the turbine [kW]

The correlations (3.2) and (3.3) keep valid in the shaft power range 1-10 MW. Correlation (3.2) is actually used to estimate the cost of steam turbines, so it can be considered valid for TITs in the range typical for steam turbines, about 300°C-650°C. The correlation (3.1) is proposed by Wright et al. [97] specifically developed for s-CO_2 power cycles for waste heat recovery application. Unfortunately the authors do not specify the power range applicability of such correlation, nor they clarified if these were obtained for a particular s-CO_2 power cycle layout. In spite of this lack information, I reported its graphical representation in the range 1-10 MW that is valid for (3.2) and (3.3). The last correlation (3.4) is actually developed for the evaluation of gas turbines cost. In the literature it is assumed to be valid also for s-CO_2 turbines and for the ranges of the operating parameters of this application.

The diagrams of total (C_1 and C_3) and specific (c_1 and c_3) cost correlations (3.1) and (3.3) are reported in Figures 3.1 and 3.2 respectively. These correlations depend only on the power generated by the turbine but their dependence on the shaft power is quite different. This difference could be clearly noticed in the Figure 3.2 that represents their specif costs. The specific cost of (3.1) is constant, while the specific cost of (3.3) decreases with the shaft power showing advantages increasing power production and lowering the costs (economy of scale).

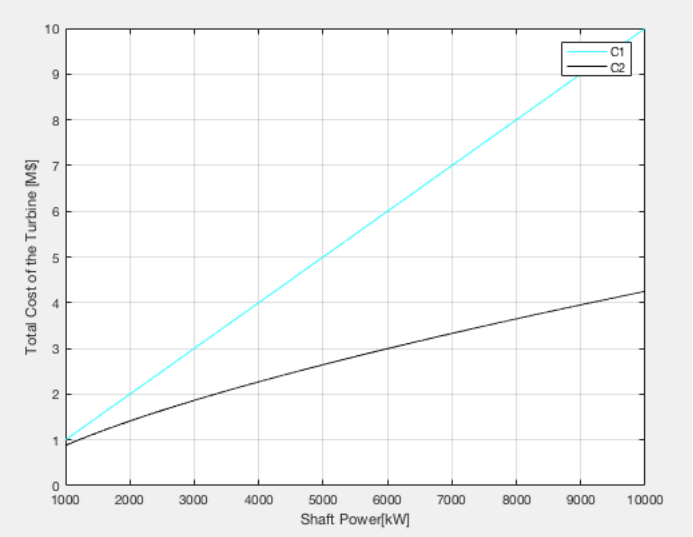

Figure 3.1 – Diagram of the Total Cost curves 3.1 and 3.3 for the turbine varying the Shaft Power

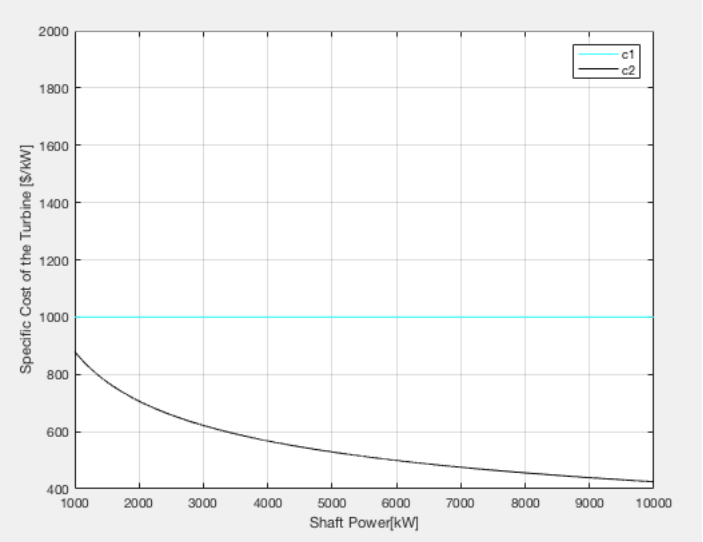

Figure 3.2 – Diagram of the Specific Cost curves 3.1 and 3.3 for the turbine varying the Shaft Power

The correlation (3.2) depends on three parameters: TIT, isentropic efficiency of the turbine and the power produced. From Figure 3.3 we can observe that the dependence on TIT (assuming a shaft power of 10 MW and an isentropic efficiency of 90%, an average and reasonable value for an axial 10MW turbine) in the range on interest for the s-CO_2 (400-800°C) is very small, apart for values in proximity of 800°C, where the trend of the correlation is no more valid. This is consistent with the considerations made previously (steam turbines operate at maximum temperatures of 650°C). In Figure 3.4 we can notice a marked dependence from the isentropic efficiency in the range of interest for this application 80-94%, especially for efficiencies higher than 90% (assuming a shaft power of 10 MW and a TIT 650°C, a value that it is deasiderable to reach for all the applications, not considering WHR). The cost of the turbine assuming an isentropic efficiency of 94% is about the double of that assuming an efficiency of 80%.

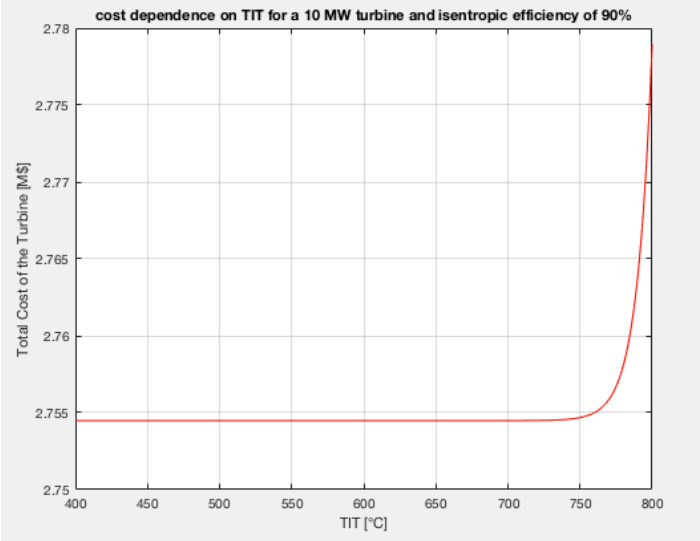

Figure 3.3 – Diagram of the dependence of correlation 3.2 from the TIT assuming a 10MW turbine and an isentropic efficiency of 90%

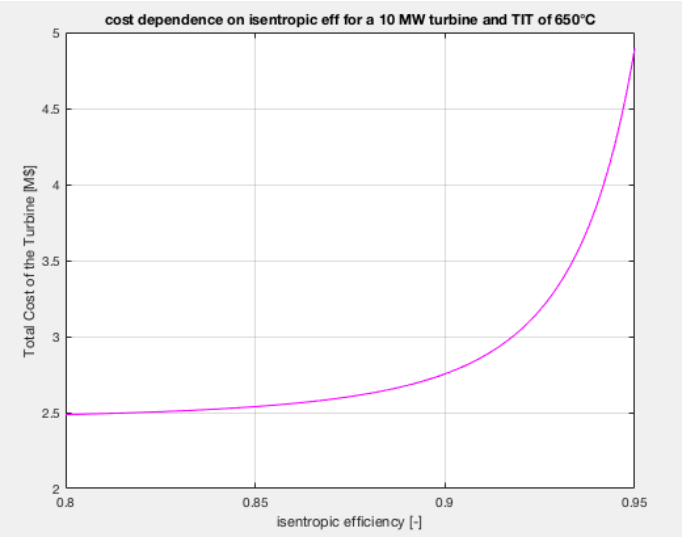

Figure 3.4 – Diagram of the dependence of correlation 3.2 from the isentropic efficiency assuming a 10MW turbine and a TIT of 650°C

The last correlation (3.4) does not depend on the shaft power but depends on other parameters that are chacteristics for the turbine: the mass flow rate, the expansion ratio, the TIT and turbine isentropic efficiency. The typical ranges of these parameters for the s-CO_2 application are mass flow rate in the range 10-8,000 kg/s, isentropic efficiency in the range 80-94%, TIT 400-800°C and expansion ratio in the range 2-4.5. This correlation is linearly proportional to the mass flow rate, so the higher the mass flow rate, the higher the cost of the turbine. It is also characterized by a logarithmic proportionality with the expansion ratio. In Figures 3.5 and 3.6 are represented the dependence of this correlation on the turbine efficiency and on the TIT assuming in the first case a TIT of 650°C, in the second case an efficiency of 90% and in both cases an intermediate

expansion ratio of 3 and a mass flow rate of 100 kg/s (the correlation is linearly proportional to this value, so the aim of this assumption is just to show the trend of the correlation. Assuming a higher value just increase the absolute value of the cost but doesn't change its trend). From the figures we can notice that this correlation is very sensitive to the turbine isentropic efficiency, while is shows mainly no influence on TIT unless temperatures higher than 1200°C are considered, however these values of temperature are never reached in this application.

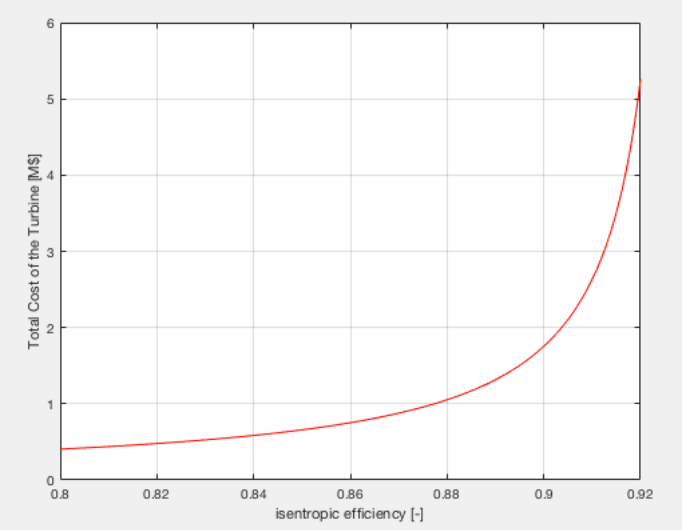

Figure 3.5 – Diagram of the dependence of correlation 3.4 from the isentropic efficiency assuming a TIT of 650°C, a mass flow rate of 100 kg/s and an expansion ratio of 3

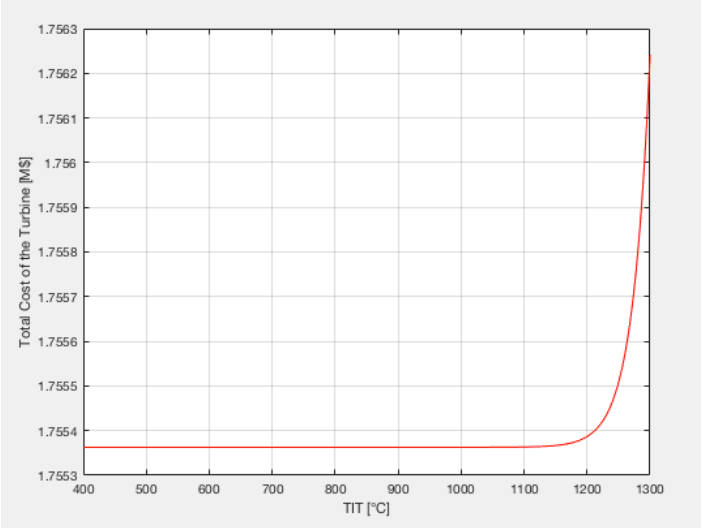

Figure 3.6 – Diagram of the dependence of correlation 3.4 from the TIT assuming an isentropic efficiency of 90%, a mass flow rate of 100 kg/s and an expansion ratio of 3

3.2 Compressor's Cost Correlations

The compressor is a key component in s-CO_2 cycles and its performance is crucial to the operation and efficiency of the whole system. The working fluid CO_2 is compressed in the compressor to raise the pressure of the fluid. According to the flow direction of the working fluid, compressors are classified into two types, namely, axial flow and radial flow. The axial compressor is characterized by large flow rate, high efficiency, long axial dimension, complex structure, while radial compressor by single stage pressure ratio, compact structure. The correlations in the literature to compute a preliminary cost of the compressor are different and reported below:

$$C_C = 6898\dot{W}_C^{0.7865} \text{ [96]} \tag{3.5}$$

$$C_C = 1000\dot{W}_C \text{ [82]} \tag{3.6}$$

$$C_C = 71.10\dot{m}_C \frac{1}{(0.92-\eta_C)} \beta_C ln(\beta_C) \text{ [40][76][84][85]} \tag{3.7}$$

Where:

-$\dot{m}_C$ is the working fluid mass flow rate in the compressor [kg/s]

-η_C is the isentropic efficiency of the compressor [-]

-β_C is the pressure ratio of the compressor [-]

-$\dot{W}_C$ is the power absorbed by the compressor [kW]

The structure of these correlations is very similar to those of the turbine. Correlation (3.5) keeps valid in the range of power absorbed by the compressor 1-10 MW, while correlation (3.6) as (3.1) is proposed by Wright et al [97] specifically developed for s-CO_2 power cycles for waste heat recovery application. Unfortunately the authors do not specify the power range applicability of such correlation, nor they clarified if these were obtained for a particular s-CO_2 power cycle layout. In spite of this lack information, I reported its graphical representation in the range 1-10 MW that it valid for (3.5). Correlation (3.7) is actually used to compute the cost of air compressors. In the literature it is assumed to be valid also to compute s-CO_2 compressors cost and for the ranges of the operating parameters of this application. For the correlations (3.5) and (3.6) represented in Figure 3.7, the same considerations made for the correlations (3.1) and (3.3) for the turbine can be made. The only difference is that in the case of the compressor the total costs are more comparable (in absolute values) and the cost estimated by (3.6) is lower than (3.5) until a power absorbed of about 8.5 MW is reached.

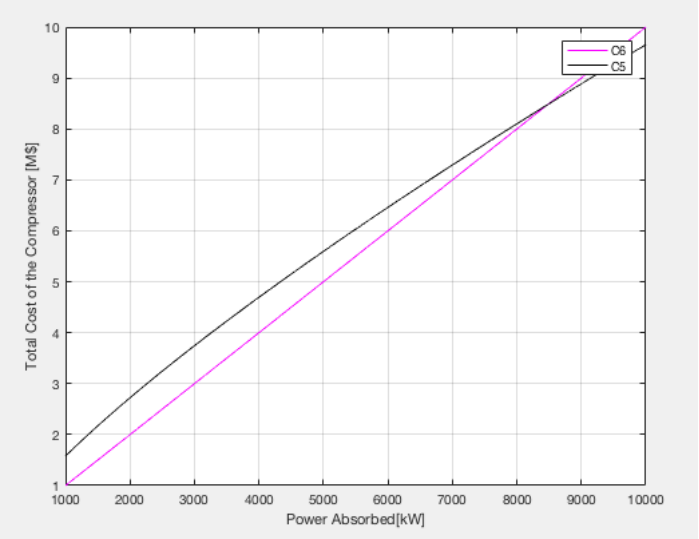

Figure 3.7 – Diagram of the Total Cost curves 3.5 and 3.6 for the compressor varying the Power Absorbed

The last correlation (3.7) does not depend on the shaft power but depends on other parameters that chacterize the compressor: the mass flow rate, the compression ratio and isentropic efficiency. The typical ranges of these parameters for the s-CO_2 application are the mass flow rate in the range 10-8,000 kg/s, isentropic efficiency in the range 80-89% and compression ratio in the range 2-5. The correlation is linearly proportional to the mass flow rate, so the higher the mass flow rate, the higher the cost of the turbine. In Figures 3.8 and 3.9 are represented the dependence of this correlation on the compressor efficiency and compression ratio, assuming in the first case a mean compression ratio of 3, in the second case a mean value of 85% for the compressor isentropic efficiency and in both cases a mass flow rate of 100 kg/s (as before the correlation is linearly proportional to this value, so the aim of this assumption is just to show the trend of the correlation. Assuming a higher value just increase the absolute value of the cost but doesn't change its trend). From the figures we can notice that this correlation is very sensitive to both the compressor isentropic efficiency and the compression ratio.

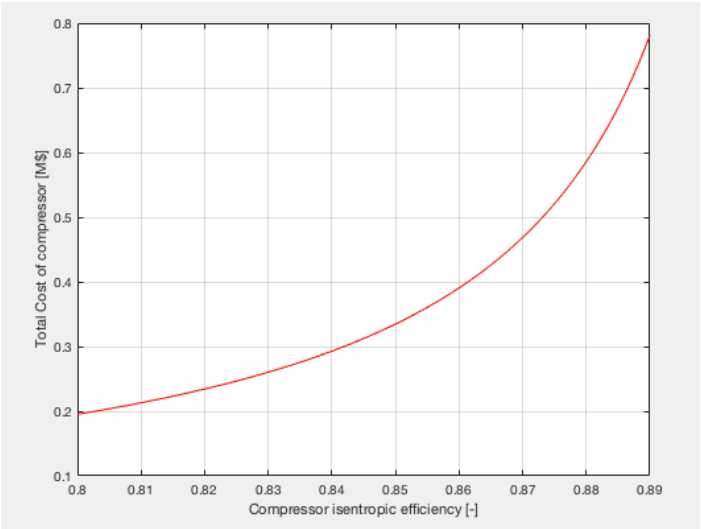

Figure 3.8 – Diagram of the dependence of correlation 3.7 from the isentropic efficiency assuming compression ratio of 3 and a mass flow rate of 100 kg/s

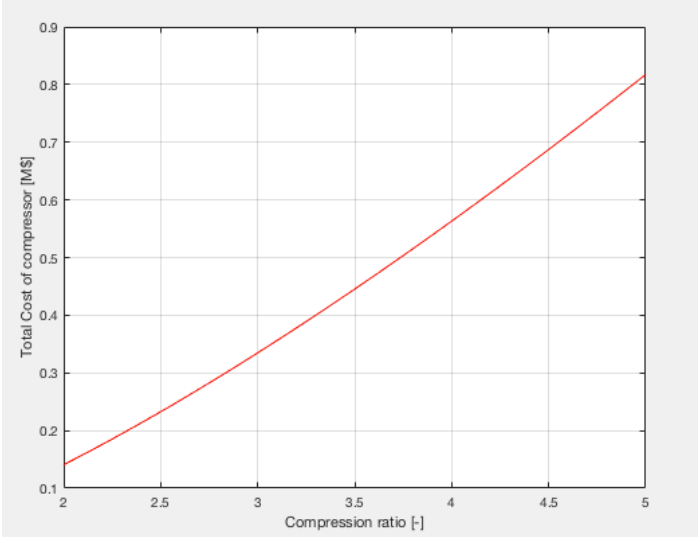

Figure 3.9 – Diagram of the dependence of correlation 3.7 from the compression ratio assuming an isentropic efficiency of 85% and a mass flow rate of 100 kg/s

3.3 Pump's Cost Correlation

Pump is a component used instead of compressor in trascritical cycles (where the compression process is performed in the liquid phase and no more in supercritical conditions). The power required to compress the fluid will be lower, increasing the net power output (this configuration is used for medium-low WHR where it is essential to maximize the power output, more difficult because this application is characterized by lower operanting temperatures with respect to other

applications). The cost correlation used for the pump in thermo-economic studies for trascritical cycles is the following:

$$C_P = 705.48\dot{W}_P^{0.71}\left(1+\frac{0.2}{1-\eta_P}\right)$$ [92]

Where:

-$\dot{W}_P$ is the power absorbed by the pump [kW]

-η_P is the isentropic efficiency of the pump [-]

This cost correlation is actually used to evaluate the cost of the pump in steam Rankine cycles but in the literature it is assumed to be valid also for t-CO_2 application. It depends on two parameters: the power required by the pump for the compression and the isentropic efficiency of the pump. A graphic representation of this correlation varying the power absorbed is represented in Figure 3.10 assuming a pump isentropic efficiency of 80% (an intermediate value from the range in the assumptions 75-85%). Its trend is obviously proportional with the power absorbed but not linearly, this means that also in this case the specific cost has a decreasing trend (economy of scale).

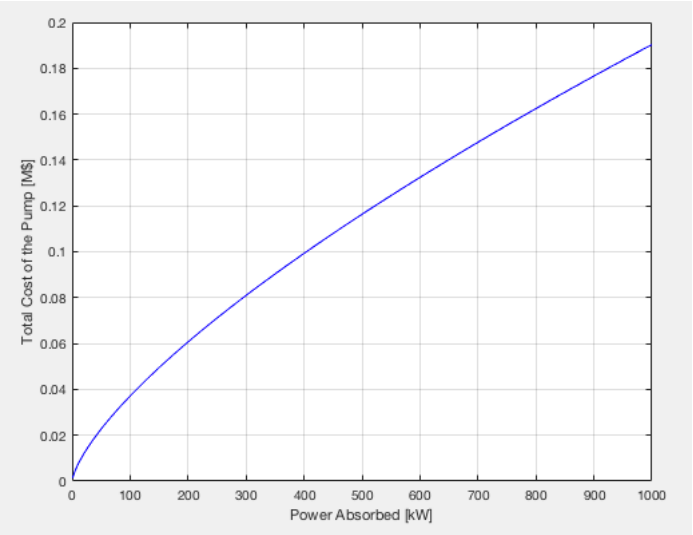

Figure 3.10 – Diagram of the Total Cost curve for the pump varying the Power Absorbed

3.4 Heat exchangers' cost correlations

Heat exchangers in a s-CO_2 are represented by intermiated heat exchanger (heater), reheater, recuperators, cooler, intercooler and condenser. As one of the compact heat exchangers, PCHE is known as an attractive option for this application due to its high heat transfer area and volume ratio (650 m^2/m^3) available at low temperature. The heat transfer characteristics of PCHE are influenced by shapes (straight shape, zigzag shape, s-shaped, airfoil…), cross-sections and structures of the flow channel [98]. The type of heat exchangers mostly assumed in the papers are PCHE or Shell&Tube heat exchangers are usually assumed for cooler or condenser. One of the most used correlation to evaluate heat exchangers cost is:

$C_{HX,j} = \lambda(UA)_j$ [30][55][58][70]

This correlation refers to a specific cost per heat transfer capacity (UA-value). Therefore, this approach allows an estimation of the costs without going into a detailed exchanger modelling.

Values of the λ coefficient depend on the type of heat exchanger considered and its technology (heater, recuperator or cooler):

-λ Heater: 5000 /3500 [$/UA] (Fin Tube primary Heater) [97]/(PFHE-Plate Fin Heat Exchanger) [99]

-λ Recuperators: 2500 [$/UA] (Advanced high pressure recuperators) [97]

-λ Cooler: 1700 [$/UA] (Shell and Tube heat exchangers with water) [97]

-λ Air-cooler: 856.67 [$/UA] [76]

There also other few correlations used in the papers to evaluate the cost of heat exchangers reported below.

Recuperators

$C_{rec} = 2681(A_{rec})^{0.59}$ [61][62][74]

$C_{rec} = 1.027(10)^3 V$ [96]

Where A_{rec} is the surface area of recuperator, the first correlation refer to Spiral Frame and Stainless Steel compact heat exchangerhers assuming a specif cost per unit area equal to 2,681 $/m^2$ [101], while the second one is valid only PCHE type of heat exchangers, assuming a cost of $1.027(10)^3$ $/m^3$. V represents the volume of recuperator.

Heater

$C_{Heater} = 2681(A_{heater})^{0.59}$ [61][62][74]

Where A_{Heater} is ther surface area of the heater. This correlation refer to Spiral Frame and Stainless Steel compact heat exchangerhers assuming a specif cost per unit area equal to 2,681 \$/m^2 [101].

Precooler, condenser and intercooler

$C_{pre} = 2143(A_{pre})^{0.514}$ [61][62][74]

$C_{cond} = 2143(A_{cond})^{0.514}$[61][62][74]

$C_{int} = 2143(A_{int})^{0.514}$[61][62][74]

Where A_{pre} is the surface area of precooler, A_{con} is the surace area of the condenser and A_{int} is the surface area of the intercooler. These correlations refer to a Shell&Tube heat exchanger made of Carbon Steel assuming a specific cost per unit area of 2,143 \$/m^2 [101].

4.Conclusions

While there has been increasing interest recently, the idea of using s-CO_2 in a power system is not new. A patent for a partial condensation CO_2 Brayton cycle was submitted by Sulzer Bros in Switzerland in 1948. The principle was reinvented two decades later in the works of Angelino and Feher, both authors agreed that the supercritical CO_2 cycle could achieve high efficiencies, close to 50%, higher than conventional Brayton cycles with moderate inlet temperatures and higher than Steam Rankine cycles for TITs higher than 600°C, but more interestingly, much smaller footprint. Despite the oversimplification of the thermodynamic calculations their contribution was fundamental to provide a very good initial to the topic. It was only in 2004, more than 30 years later that Dostal performed a systematic and detailed study with system design evaluation and multi-parameter optimization for nuclear application. His work led to research worldwide and development of s-CO_2 cycles. In this review work, all the thermodynamic and thermo-economic studies found in the literature are analyzed for the most interesting applications which can be applied to s-CO_2 cycles: nuclear, coal, CSP and WHR. The aim of this work is to give some important considerations and conclusions on the best suited cycle layout to every application, particularly referring to its performances and economic evaluations. This work coul be useful as guideline and a starting point for futher investigations and optimizations of s-CO_2 cycles. As a support of that, the typical assumptions found in the literature were summarized for all the applications with some explanations especially to give meaning to their values and understanding the reason of their dissimilarity in case of very different size of the plants or different operating parameters. What is relevant is that the results of optimization studies for nuclear, coal and CSP applications, despite their different assumptions and constraints, go in the same direction and often similar conclusions are reached. This confirms not only the validity and reliability of the studies, but also that the findings for each application sound solid, despite the different characteristics of the studies. Main conclusions are that the s-CO_2 power cycle can potentially be utilized for small and medium sized nuclear reactors, large size conventional water-cooled reactors and Fourth Generation Nuclear Reactors. Fourth Generation nuclear power implies a system of reactors and facilities that together may manage the weaknesses often associated with nuclear power of today, such as radioactive wastes or low cycle efficiency. The most studied layout for this application is the Recompression Brayton cycle, this is because it has the benefits of the Simple cycle, low number of components and low complexity enhancing at same time cycle efficiency. For turbine inlet temperatures equal or higher than 650°C a cycle efficiency close to 50% is achievable. Reheat is demonstated to be useful to increase cycle performances and seems to be economically feasible at lest for small modular reactors. Recompression layout is demonstrated to be mandatory also for coal and concentrated solar power applications, this is because the main goal of the thermodynamic optimizations found in the literature was mainly to increase the cycle first law efficiency as high as possible. For coal application all the cycle layouts

proposed have at least two split ratios, one to the recompressor and one aimed to recover the medium-low temperature heat in the boiler. The layout that is demonstrated to be the most suitable for coal application is the recompression cycle with double reheating and eventually with intercooling. Despite it seems a very complex layout, from thermo-economic evaluation it shows great commercial potential. For concentrated solar power intercooling is highly recommended and the main compression intercooling is demonstrated to be the optimal intercooling configuration for this application, often integrated with dry cooling system. The recompression layout with single reheat and main compression intercooling is able to hit the efficiency target of 50% even with dry cooling. Final conclusions on this application are that reheating is recommended for wet cooling while intercooling with single reheating is the best option for dry cooling demonstrated to affordable also from the economic point of view. The layouts proposed and studied for waste heat recovery are very different from the traditional layouts studied for all the other applications, aimed in this case to maximize the net power output or the total heat recovery efficiency. Many studies compared the performances of traditional layouts with the novel layouts proposed showing that some novel layouts have better performances in terms of net power output produced and heat recovered, but despite that there is a lack of consensous on the best layout for waste heat recovery application. The most promising configurations in the literature are found to be the single and the dual flow with dual expansion and the pre-heating with pre-compression cycle for high-medium temperature waste heat recovery with supercritical CO_2 cycle and the single flow with dual expansion and the pre-heating cycles for medium-low temperature waste heat recovery for transcritical CO_2 cycles. At the end of the work some considerations on the cost correlations for the main components of the cycle utilized to compute the economic or thermo-economic investigations in the literature are submitted highlighting their characteristics and their potential strengths and weaknesses, moreover the trends of their depencence on different operating parameters are graphically represented and interpreted.

Thanks to the important contribution of all the studies in the literature in recent years many projects and facilities have been demonstrated or are under construction. Sandia National Laboratory in 2012 explored the performance test of compressor near the CO_2 critical point that presented a stable and controllable operation. It also tested the performances of 2-TAC recompression cycle able to achieve theoretically a cycle efficiency of 31.5% at target conditions. A TIT of 342°C was reached but the target was 537°C. Issues of particular note were the heat rejection capacity, windage losses in the rotor cavity and thermal losses in the vicinity of the turbine and from piping. Betchel Marine Propulsion Corporation demonstrated a two-shaft recuperated Brayton cycle over a wide range of conditions, no inherent issues with the s-CO_2 Brayton cycle have been identified apart from electrical issues with the motor-generator controllers and mechanical issues with gas foil bearings that have limited the power output. These issues are a result of using equipment that is not typical of what would be used in larger system and for this reason cycle efficiency reached was only 7%. Similar conclusions were reached by Tokyo Institute of Technology and Kaeri-Kaist-Postech experimental loops where the main objectives were to accumulate experience on the s-CO_2 cycle including steady-state and transient operations, establish a system operational strategy for startup, normal

operation and shutdown, understand the underlying physical phenomena in component level and suggest an advanced concept for each component to improve the overall system performance in the future. These experimental loops demonstrated the operability of a s-CO_2 cycle but didn't demonstrate their potential high efficiency due to the low TITs and small scale of the facilities. More recent and advanced activities are ongoing such as STEP project, a six-year project started in 2018 led by a team composed of Gas Technology Institute, Southwest Research Institute and General Electric Global Research, that initiated this project to design, construct, commission and operate a versatile and reconfigurable 10 MW_e s-CO_2 Pilot Plant Test Facility located at SwRI's San Antonio, Texas campus. It is one of the largest scale and most comprehensive in the world, with the objective to study the aerodynamics and durability of turbomachinery, corrosion and fatigue of materials, design and fabrication of recuperators, performances of components and to demonstrate at least 700°C turbine inlet temperature, generating at least 10 MW_e to show the potential of thermodynamic efficiency greater than 50% at commercial scales with a lower cost of electricity. An important project started in October 2020 where RINA is the project coordinator is SOLARSCO2OL project. Its objectives are to demonstrate an innovative, economically viable and easily replicable s-CO_2 power block that, also coupled with fast reactive electric heater and efficient heat exchangers, will enable the operation and design of a novel integrated power plant layout in order to un-tap CSP plant potential flexibility and reduce their LCOE to values below 0.010 €/kWh. Main activities of the project are the support to s-CO_2 turbomachinery design, manufacturing and material selection via CFD/FEM analysis, health & Safety procedures for SOLARSCO2OL demonstration and replication, regulatory and non-technical assessment of SOLARSCO2OL solutions and techno-economic Roadmap towards TRL9. Another project that is taking place is the Gen 3 Particle Pilot Plant (G3P3). The objectives of G3P3 project are to design, construct, and operate a multi-MW_{th} falling particle receiver system that can operate for thousands of hours, provide six hours of energy storage, and heat a working fluid to a temperature higher than 700°C while demonstrating the ability to meet SunShot cost and performance goals. G3P3 development is taking place at the National Solar Thermal Test Facility, the only test facility of its type in the United States. Finally, s-CO_2-Flex consortium led by Electicite de France, with the participation of Politecnico di Milano, addresses the challenge of developing and validating the scalable/modular design of a 25 MW_e Brayton cycle using supercritical CO_2, able to increase the operational flexibility and the efficiency of existing and future coal and lignite power plants. sCO_2-Flex will develop and optimize the design of a 25 MW_e s-CO_2 Brayton cycle and of its main components (boiler, HX, turbomachinery, instrumentation and control strategies) able to meet long-term flexibility requirements, enabling entire load range optimization with fast load changes, fast load changes, fast start-ups and shuts-downs, while reducing environmental impacts and focusing on cost-effectiveness.

These projects demonstrate the importance of this technology and its potential in the power generation sector. Research and development are making great strides in these years, making the commercialization of this technology more and more closer.

Appendix

Tables filled with main information and data regarding all the papers and studies read and analyzed for the literature review.

General data			Study typology			Layout and main parameters of the cycle						Assumptions						Components characteristics		Results			
Author	Year	Journal	Optimizati on Y(single obj)Y(mul ti obj)	Objective function	Optimization algorithm	Thermodinamic s'economic'...	Optimization variables	Mass flow rate [kg/s]	Max temperatu re [°C]	Min temperatu re [°C]	Max pressure [Mpa]	Min pressure [Mpa]	Cycle layout	Turbomac hinery efficiencie s	Pressure drops [kPa]	Pinch point of recuperat ors [°C]	Heat transfer coefficient s	HTR effectiven ess [%]	LTR effectiven ess [%]	Net power [MW]	Axial or radial turbomac hinery	Heat exchangers typology	Pressure ratio	Cycle efficiency [%]	Split Ratio	Costs	Exergy efficiency [%]
Yichuan He, Aihua Dong, Min Xie and Yang Liu	2018	Science and Technology of Nuclear Installation	Single obj	Cycle efficiency	genetic algorithm and pattern search algorithm	Thermodynamic s	minimum temperature of the cycle, pressure ratio, minimum temperature difference in the regenerator; TIT	/	370	31,2	21,76	8	Recompressio n s-CO2 Brayton cycle	Turbine: 87% Compress or: 85%	Neglected	3 in both recuperat ors	/	not specified	not specified	/	not specified	Printed Circuit Heat Exchangers for recuperators and LBE-CO2 heat exchanger for heater	2,719	35,97	not specified	/	/
Edwin A. Harvego, Michael G. McKellar	2011	Science and Technology of Nuclear Installation	Single obj	Cycle efficiency	UniSim process analysis software	Thermodynamic s	TIT; recompression fraction; pressure ratio	2867 kg/s	750(refere nce case) /850	36	20	8,69	Recompressio n s-CO2 Brayton cycle	Turbine: 90% Compress or: 90%	20 kPa for all the heat exchangers for every CO2 stream	20	/	not specified	not specified	/	not specified	Shell and Tube	2,3	49,2/51	0,565/0,6	/	/
Q.H. Deng, D. Wang, H. Zhao, W.T. Huang, S. Shao, Z.P. Feng	2016	Applied Thermal Engineerin g	Multi obj	Exergy efficiency and Net power output	Simulation program written in FORSTRAN coupled with NIST REFPROP for CO2 properties; NGSA-II (non-dominated sorting genetic algorithm II	Thermodynamic s	TIT; pressure ratio	383,87 kg/s	516,15	32	40,88	7,7	Recompressio n s-CO2 Brayton cycle	Turbine: 90% Compress or: 80%	0,078 Mpa in both the high pressure and low pressure stream	8	/	not specified	not specified	42,24	not specified	not specified	5,26	41,35	0,716	/	63,57
Q.H. Deng, D. Wang, H. Zhao, W.T. Huang, S. Shao, Z.P. Feng	2016	Applied Thermal Engineerin g	Multi obj	Exergy efficiency and Net power output	Simulation program written in FORSTRAN coupled with NIST REFPROP for CO2 properties; NGSA-II (non-dominated sorting genetic algorithm II	Thermodynamic s	TIT; pressure ratio	319,31 kg/s	579	32	41,56	7,7	Recompressio n s-CO2 Brayton cycle	Turbine: 90% Compress or: 80%	0,078 Mpa in both the high pressure and low pressure stream	8	/	not specified	not specified	41,33	not specified	not specified	5,34	45,15	0,718	/	68,26
Q.H. Deng, D. Wang, H. Zhao, W.T. Huang, S. Shao, Z.P. Feng	2016	Applied Thermal Engineerin g	Multi obj	Exergy efficiency and Net power output	Simulation program written in FORSTRAN coupled with NIST REFPROP for CO2 properties; NGSA-II (non-dominated sorting genetic algorithm II	Thermodynamic s	TIT; pressure ratio	266,48 kg/s	650	32	33,65	7,7	Recompressio n s-CO2 Brayton cycle	Turbine: 90% Compress or: 80%	0,078 Mpa in both the high pressure and low pressure stream	8	/	not specified	not specified	36,93	not specified	not specified	4,33	49,42	0,689	/	72,95
Ho Joon Yoon, Yoonhan Ahn, Jeong Ik Lee, Yacine Addad	2012	Nucear Engineerin g and Design and ScienceDir ect	Single obj	Cycle efficiency	In-house code developed by KAIST Khalifa University coupled with NIST-REFPROP	Thermodynamic s	PR (pressure ratio); SR (split ratio); lenght of heat exchangers (recuperators and precooler)	/	310	32	22	7,7	Recompressio n s-CO2 Brayton cycle	Turbine: 90% Compress or: 89%	Neglected	10	/	/	/	/	axial turbine and axial compress ors	Printed Circuit Heat Exchangers	2,85	30,05	0,64	/	/
Joo Hyun Park, Hyun Sun Park, Jin Gyu Kwon, Tae Ho Kim, Moo Hwan Kim	2018	Energy and Science Direct	Single obj	Cycle efficiency	A thermodynamic analysis model RCAM (Recompression Cycle Analysis Model) was developed in FORTRAN coupled with NIST-REFPROP	Thermodynamic s	PR (pressure ratio); SR (split ratio)	2085 kg/s	310	32	19,828	7,69	Recompressio n s-CO2 Brayton cycle	Turbine: 92% Compress or: 85%	Hot side LTR: 0,011 Mpa;Hot side HTR: 0,031 Mpa; Cold side HTR: 0,087 Mpa; Cold side LTR: 0,11 Mpa;	3,7	/	>95	>95	93,68	radial turbine and radial compres ors	Zig Zag type Printed Circuit Heat Exchangers	2,6	30,6	0,59	/	/
Joo Hyun Park, Hyun Sun Park, Jin Gyu Kwon, Tae Ho Kim, Moo Hwan Kim	2018	Energy and Science Direct	Single obj	Cycle efficiency	A thermodynamic analysis model RCAM (Recompression Cycle Analysis Model) was developed in FORTRAN coupled with NIST-REFPROP	Thermodynamic s	PR (pressure ratio); SR (split ratio)	1628 kg/s	550	32	19,828	7,69	Recompressio n s-CO2 Brayton cycle	Turbine: 92% Compress or: 85%	Hot side LTR: 0,011 Mpa;Hot side HTR: 0,031 Mpa; Cold side HTR: 0,087 Mpa; Cold side LTR: 0,11 Mpa;	5	/	>95	>95	142,05	radial turbine and radial compres ors	Zig Zag type Printed Circuit Heat Exchangers	2,6	46,38	0,58	/	/
Joo Hyun Park, Hyun Sun Park, Jin Gyu Kwon, Tae Ho Kim, Moo Hwan Kim	2018	Energy and Science Direct	Single obj	Cycle efficiency	A thermodynamic analysis model RCAM (Recompression Cycle Analysis Model) was developed in FORTRAN coupled with NIST-REFPROP	Thermodynamic s	PR (pressure ratio); SR (split ratio)	1544 kg/s	650	32	18,828	7,69	Recompressio n s-CO2 Brayton cycle	Turbine: 92% Compress or: 85%	Hot side LTR: 0,011 Mpa;Hot side HTR: 0,031 Mpa; Cold side HTR: 0,087 Mpa; Cold side LTR: 0,11 Mpa;	5,4	/	>95	>95	153,22	radial turbine and radial compres ors	Zig Zag type Printed Circuit Heat Exchangers	2,47	50,04	0,58	/	/

General data			Study typology					Layout and main parameters of the cycle						Assumptions							Components characteristics		Results				
Author	Year	Journal	Optimization V(single obj)/V(multi obj)	Objective function	Optimization algorithm	Thermodinamics/economic/…	Optimization variables	Mass flow rate [kg/s]	Max temperature [°C]	Min temperature [°C]	Max pressure [Mpa]	Min pressure [Mpa]	Cycle layout	Turbomachinery efficiencies	Pressure drops [kPa]	Pinch point of recuperators [°C]	Heat transfer coefficients	HTR effectiveness [%]	LTR effectiveness [%]	Net power [MW]	Axial or radial turbomachinery	Heat exchangers typology	Pressure ratio	Cycle efficiency [%]	Split Ratio	Costs	Exergy efficiency [%]
Ming-Jia Li, Yan-Jun Jie, Han-Hui Zhu, Guo-jia Qi, Meng-Jie Li	2018	Progress in Nuclear Energy and ScienceDirect	Single obj	Cycle efficiency	Genetic algorithm	Thermodynamics	SR (split ratio); PR (pressure ratio); RPR (ratio of pressure ratios)	/	465	32	25	7,86	Recompression s-CO2 Brayton cycle with single reheating	Turbine: 93% Compressor: 89%	Neglected	/	/	95	88	10	not specified	Shell and Tube heat exchangers	3,18	all system 41,	0,63	LCOE/EPC= 0,0536 $/kWh	/
Pan Wu, Chuntian Gao, Yanping Huang, Dan Zhang and Jianqiang	2020	Science and technology of Nuclear Installations	Single obj	Cycle efficiency	In-house steady thermodynamic analysis solver named SASCOB	Thermodynamics	CIP; TIP; recuperator UA	426,3 kg/s	460	32	20	7,4	Simple s-CO2 recuperative Brayton cycle	Turbine: 93% Compressor: 89%	Not neglected but the value is not specified (linearly distributed)	10,1	UA : 3 MW/K	/	/	35,9	not specified	Printed Circuit Heat Exchangers	2,7	35,9	/	/	/
Pan Wu, Chuntian Gao, Yanping Huang, Dan Zhang and Jianqiang	2020	Science and technology of Nuclear Installations	Single obj	Cycle efficiency	In-house steady thermodynamic analysis solver named SASCOB	Thermodynamics	CIP; TIP; recuperator UA	515 kg/s	460	55	20	7,4	Simple s-CO2 recuperative Brayton cycle	Turbine: 93% Compressor: 89%	Not neglected but the value is not specified (linearly distributed)	10	UA :4,2 MW/K	/	/	32,6	not specified	Printed Circuit Heat Exchangers	2,7	32,6	/	/	/
Pan Wu, Chuntian Gao, Yanping Huang, Dan Zhang and Jianqiang	2020	Science and technology of Nuclear Installations	Single obj	Cycle efficiency	In-house steady thermodynamic analysis solver named SASCOB	Thermodynamics	CIP; TIP; recuperator UA; SP;	563,92 kg/s	460	32	20	7,4	Recompression s-CO2 Brayton cycle	Turbine: 93% Compressor: 89%	Not neglected but the value is not specified (linearly distributed)	HTR: 15,7 °C; LTR: 10,1°C	UA HTR: 3,36 MW/K; UA LTR: 4,64 MW/K	/	/	40,38	not specified	Printed Circuit Heat Exchangers	2,7	40,38	0,7	/	/
Pan Wu, Chuntian Gao, Yanping Huang, Dan Zhang and Jianqiang	2020	Science and technology of Nuclear Installations	Single obj	Cycle efficiency	In-house steady thermodynamic analysis solver named SASCOB	Thermodynamics	CIP; TIP; recuperator UA; SP;	616,22 kg/s	460	55	20	7,4	Recompression s-CO2 Brayton cycle	Turbine: 93% Compressor: 89%	Not neglected but the value is not specified (linearly distributed)	HTR: 12 °C; LTR: 11,9°C	UA HTR: 3,24 MW/K; UA LTR: 5,76 MW/K	/	/	34,36	not specified	Printed Circuit Heat Exchangers	2,7	34,36	0,8	/	/
H.S. Pham, N.Alpy, J.H. Ferrasse, O.Boutin et al	2015	Energy and Science Direct	Multi obj	Cycle efficiency and recuperation power	CYCLOP (CYCLe Optimization) the CEA tool for power conversion cycle modeling allowing all cycle parameters to be modified and optimized using the deterministic Nelder-Mead algorithm, coupled with NIST-REFPROP	Thermodynamics	SR; CIP	/	275	35	20	8,53	Recompression s-CO2 Brayton cycle with single reheating	Turbine: 93% Compressor: 88%	Neglected	higher than 10°C	/	lower than 92,5	lower than 92,5	158,22	not specified	not specified	2,34	29,3	0,609	/	59,3
H.S. Pham, N.Alpy, J.H. Ferrasse, O.Boutin et al	2015	Energy and Science Direct	Multi obj	Cycle efficiency and recuperation power	CYCLOP (CYCLe Optimization) the CEA tool for power conversion cycle modeling allowing all cycle parameters to be modified and optimized using the deterministic Nelder-Mead algorithm, coupled with NIST-REFPROP	Thermodynamics	SR; CIP	/	508,2	35	25,3	8,1	Recompression s-CO2 Brayton cycle with intercooling	Turbine: 93% Compressor: 88%	Total pressure drop: 0,55 Mpa	10	/	lower than 92,5	lower than 92,5	329,25	not specified	not specified	3,12	43,9	0,662	/	69,1

General data			Study typology			Layout and main parameters of the cycle					Assumptions					Components characteristics		Results			
Author	Year	Journal	Optimizatio n Y(single obj)/Y(multi obj)	Objective function	Optimization algorithm	Thermodi namic/e conomic/...	Optimization variables	Mass flow rate [kg/s]	Max temperatu re [°C]	Min temperatu re [°C]	Max pressure [Mpa]	Min pressure [Mpa]	Cycle layout	Turbomac hinery efficiencies	Pressure drops [kPa]	Pinch point of recuperator s [°C]	Heat transfer coefficient s	HTR effectivn ess [%]	LTR effectivn ess [%]	Net power [MW]	Axial or radial turbomac hinery	Heat exchanger s typology	Pressure ratio	Cycle efficiency [%]	Split Ratio	Costs	Exergy efficiency [%]
Ziwei Bai, Guoqiang Zhang, Yongyi Li, Gang Xu, Yongping Yang	2017	Energy and Science Direct	Single obj	Cycle efficiency	Plant simulated by Aspen Plus with LK-PROCK	Thermody namics	TIT; TIP	76239,6 kg/s	630 ref /700	32	29,6 ref/32,8	7,4	Recompressi on s-CO2 Brayton cycle with intercooling	Turbine: 93% Compress or: 90%	In all the heat exchangers the pressure drop are in the Hot side: 0,1 Mpa; Cold side: 0,15 Mpa	6	/	not specified	not specified	1090	not specified	not specified	4 ref/ 4,43	52,33 ref/ 54,47- net:49,5% /51,46%	0,657	/	/
Xuwei Zhang, Kaixuan Yang, Ming Liu, Junjie Yan, Yingeng Ma	2019	Energy Conversio n and Managem ent and Science Direct	Single obj	Cycle efficiency	genetic algorithm	Thermody namics	TIT; TIP; CIT; CIP	7722,7 kg/s	600	32	30	7,7	Recompressi on s-CO2 Brayton cycle	Turbine: 93% Compress or: 90%	in all heat exchangers the pressure drops are in the Hot side: 0,1 Mpa; Cold side: 0,15 Mpa	6	/	/	/	1008,5	not specified	not specified	3,9	// net: 45,43	0,668	/	/
Xuwei Zhang, Kaixuan Yang, Ming Liu, Junjie Yan, Yingeng Ma	2019	Energy Conversio n and Managem ent and Science Direct	Single obj	Cycle efficiency	genetic algorithm	Thermody namics	TIT; TIP; CIT; CIP	7722,7 kg/s	600	32	30	7,7	Recompressi on s-CO2 Brayton cycle with single reheating	Turbine: 93% Compress or: 90%	in all heat exchangers the pressure drops are in the Hot side: 0,1 Mpa; Cold side: 0,15 Mpa	6	/	/	/	1077,04	not specified	not specified	3,9	49 // net:48,52	0,668	/	/
Hangzhi Li, Yifan Zhang, Yu Yang, Wenguang Han, Yaohua Yao, Wenqang Bai, Lei Zhang	2019	Applied Thermal Engineeri ng	Single obj	Cycle efficiency	computational code in FORTRAN coupled with NIST-REFPROP	Thermody namics	LPT inlet pressure; inlet temperature of RC; split ratio to MC and split ratio to SECO	2039 kg/s	600	32	32	7,6	Recompressi on s-CO2 Brayton cycle with single reheating	Turbine: 94% Compress or: 89%	Hot side recuperators: 0,1 Mpa; Cold side recuperators: 0,05 Mpa; PC: 0,1 Mpa; boiler reheater: 0,3 Mpa; boiler superheater: 0,8 Mpa	5	/	/	/	300	axial turbine and centrifugal compress or	Printed Circuit Heat Exchange rs	4,3 29	net: 50,21	0,6828 split to MC/ 0,11 secondary split to SECO	/	/
Mounir Mecheri, Yaseen Le Moullec	2016	Energy and Science Direct	Single obj	Cycle efficiency	The process simulations have been per-formed with Aspen Plus V8.0 software coupled with NIST-REFPROP	Thermody namics	pressure ratio; CIP	/	620	32	30	7,9	Recompressi on s-CO2 Brayton cycle with double reheating	Turbine: 93% Compress or: 89%	In all the heat exchangers the pressure drop are in: 0,1 Mpa for every component and stream	6	/	/	/	1009	not specified	not specified	3,8	52,4 % // net: 47,8%	/	/	/
Sebastian Michalski, David P Hanak and Vasilije Manovic	2020	Applied Energy and Science Direct	Two obj	maximizing cycle efficiency and minimizing the break-even price of electricity	The process simulations have been performad with Aspen Plus software coupled with NIST-REFPROP	Theono-economic	TIT; COP; pinch point temperature difference in recuperators	/	665	31,4	30	7,4	Recompressi on s-CO2 Brayton cycle with single reheating	Turbine: 93% Compress or: 85%	In the recuperators the pressure drop are in Hot side: 1%; Cold side: 0,5 %; cooler: 1% boiler FGC: 0,2% ; boiler carbonator: 0,8%; boiler CGC: 0,3%	5	1700 W/m2 for recuperat ors and 2900 W/m2 for cooler	/	/	565,64	not specified	not specified	4,05	net: 38,94%	/	BECel: 71,15 $/MWh ; SC: 2558,3 $/kW	/
Ming Liu, Kaixuan Yang, Xuwei Zhang, Junjie Yan	2020	Journal of Cleaner Producto n and Science Direct	Single obj	Plant efficiency	genetic algorithm	Thermody namics	SR; CIP of main compressor and recompressor; 1st reheat pressure; 2nd reheat pressure; pinch point temperature difference in HTR;	7473,7 kg/s	600	32	30	7,59	Recompressi on s-CO2 Brayton cycle with double reheating and intercooling	Turbine: 93% Compress or: 90%	Boiler: 0,19 Mpa; PC: 0,08 Mpa; Hot side HTR: 0,13 MPa; Hot side MTR: 0,15 Mpa; Hot side LTR: 0,13 Mpa; Cold side HTR:0,13 MPa ;Cold side MTR: 0,15 MPa ;Cold side LTR: 0,13 Mpa;	6	/	/	/	1081,67	not specified	not specified	3,95	52,38 % // net: 49,78%	0,6811	/	82,78
Yifan Zhang, Hangzhi Li, Wanlong Han, Wenqang Bai et al	2018	Energy and Science Direct	Single obj	Plant efficiency	computational code in FORTRAN coupled with NIST-REFPROP	Thermody namics	SR; (Boiler efficiency and Boiler discharge temperature)	6657,27 kg/s	600	32	31	7,6	Recompressi on s-CO2 Brayton cycle with single reheating	Turbine: 92% Compress or: 90%	neglected	5	/	/	/	1000	not specified	not specified	4,08	net: 50,71%	0,674	/	/

General data			Study typology			Layout and main parameters of the cycle							Assumptions						Components characteristics		Results				
Author	Year	Journal	Optimization (Single obj)/(multi obj)	Objective function	Optimization algorithm	Thermodinamic/economic/...	Optimization variables	Mass flow rate [kg/s]	Max temperature [°C]	Min temperature [°C]	Max pressure [Mpa]	Min pressure [Mpa]	Cycle layout	Turbomachinery efficiencies	Pressure drops [kPa]	Pinch point of recuperators [°C]	Heat transfer coefficients	HTR effectiveness [%]	LTR effectiveness [%]	Net power [MW]	Axial or radial turbomachinery	Heat exchangers typology	Pressure ratio	Cycle efficiency [%]	Split Ratio	Ratio of pressure ratios	Costs	Exergy efficiency [%]
Craig S. Turchi; Zhiwen Ma; Ty W. Neises; Michael J. Wagner	2013	Journal of Solar energy Engineering	Single obj	Cycle efficiency	EES (engineering equation solver)/NREL model	Thermodynamics	pressure ratio	/	700	32	25	7,35	simple s-CO2 recuperative Brayton cycle	Turbine: 93% Compressor: 89%	Neglected	10	/	95	/	100	axial turbine	not specified	3,4	40,4	/	/	/	/
Craig S. Turchi; Zhiwen Ma; Ty W. Neises; Michael J. Wagner	2013	Journal of Solar energy Engineering	Single obj	Cycle efficiency	EES (engineering equation solver)/NREL model	Thermodynamics	pressure ratio; split ratio	/	700	45	25	9,26	Recompression s-CO2 Brayton cycle	Turbine: 93% Compressor: 89%	Neglected	5	/	97	88	100	axial turbine	not specified	2,7	52,3	0,7	/	/	/
Craig S. Turchi; Zhiwen Ma; Ty W. Neises; Michael J. Wagner	2013	Journal of Solar energy Engineering	Single obj	Cycle efficiency	EES (engineering equation solver)/NREL model	Thermodynamics	pressure ratio; RPR; split ratio	/	700	45	25	5	Recompression with precooling s-CO2 Brayton cycle	Turbine: 93% Compressor: 89%	Neglected	5	/	97	88	100	axial turbine	not specified	5	52,2	0,58	0,37	/	/
Craig S. Turchi; Zhiwen Ma; Ty W. Neises; Michael J. Wagner	2013	Journal of Solar energy Engineering	Single obj	Cycle efficiency	EES (engineering equation solver)/NREL model	Thermodynamics	pressure ratio; RPR; split ratio	/	700	45	25	6,94	Recompression with main-compression intercooling s-CO2 Brayton cycle	Turbine: 93% Compressor: 89%	Neglected	5	/	97	90	100	axial turbine	not specified	3,6	52,6	0,65	0,6	/	/
Matteo Marchionni, Giuseppe Bianchi, Savvas A.Tassou	2018	Energy Procedia and ScienceDirect	Single obj	Net electrical power output	CycleTempo coupled with NIST thermophysical properties , the two software were further linked with a MATLAB script for the sensitivity analysis	Thermodynamics and Economics	TIT;	/	550	35	20	7,4	Simple s-CO2 recuperative Brayton cycle	Turbine: 85% Compressor: 70%	Neglected	15	/	not specified	not specified	0,115	not specified	plate heat exchanger	2,7	31	/	/	SC=1500 $/kW LCOE=0, 014 $/kWh	27
Matteo Marchionni, Giuseppe Bianchi, Savvas A.Tassou	2018	Energy Procedia and ScienceDirect	Single obj	Net electrical power output	CycleTempo coupled with NIST thermophysical properties , the two software were further linked with a MATLAB script for the sensitivity analysis	Thermodynamics and Economics	TIT;	/	400	35	20	7,4	Reheating s-CO2 Brayton cycle	Turbine: 85% Compressor: 70%	Neglected	15	/	not specified	not specified	0,095	not specified	plate heat exchanger	2,7	25	/	/	SC=1500 $/kW LCOE=0, 014 $/kWh	22,5
Matteo Marchionni, Giuseppe Bianchi, Savvas A.Tassou	2018	Energy Procedia and ScienceDirect	Single obj	Net electrical power output	CycleTempo coupled with NIST thermophysical properties , the two software were further linked with a MATLAB script for the sensitivity analysis	Thermodynamics and Economics	TIT; split ratio	/	500	35	20	7,4	Recompression s-CO2 Brayton cycle	Turbine: 85% Compressor: 70%	Neglected	15	/	not specified	not specified	0,113	not specified	plate heat exchanger	2,7	30	not specified	not specified	SC=2250 $/kW LCOE=0, 017 $/kWh	27
Matteo Marchionni, Giuseppe Bianchi, Savvas A.Tassou	2018	Energy Procedia and ScienceDirect	Single obj	Net electrical power output	CycleTempo coupled with NIST thermophysical properties , the two software were further linked with a MATLAB script for the sensitivity analysis	Thermodynamics and Economics	TIT; split ratio	/	400	35	20	7,4	Recompression s-CO2 Brayton cycle with reheating	Turbine: 85% Compressor: 70%	Neglected	15	/	not specified	not specified	0,098	not specified	plate heat exchanger	2,7	26	not specified	not specified	SC=2400 $/kW LCOE=0, 019 $/kWh	22,5

General data			Study typology					Layout and main parameters of the cycle						Assumptions							Components characteristics		Results					
Author	Year	Journal	Optimization Y(single obj)/Y(multi obj)	Objective function	Optimization algorithm	Thermodinamics/ economic/…	Optimization variables	Mass flow rate [kg/s]	Max temperature [°C]	Min temperature [°C]	Max pressure [Mpa]	Min pressure [Mpa]	Cycle layout	Turbomachinery efficencies	Pressure drops [kPa]	Pinch point of recuperators [°C]	Heat transfer coefficients	IITR effertivness [%]	LTR effectivmess [%]	Net power [MW]	Axial or radial turbomachinery	Heat exchangers typology	Pressure ratio	Cycle efficiency [%]	Split Ratio	Ratio of pressure ratios	Costs	Exergy efficiency [%]
T. Neises, C. Turchi	2013	Energy Procedia and ScienceDirect	Single obj	Cycle efficiency	all the optimizations were completed using the "Variable Metric" method build into EES (engineering equation solver)	Thermodynamics	pressure ratio;	/	650	50	25	7,35	Simple s-CO2 recuperative Brayton cycle	Turbine: 93% Compressor: 89%	Neglected	5	UA=3,04 MW/K	97	97	35	axial turbine and radial compressors	not specified	3,4	44,6	/	/	/	/
T. Neises, C. Turchi	2013	Energy Procedia and ScienceDirect	Single obj	Cycle efficiency	all the optimizations were completed using the "Variable Metric" method build into EES (engineering equation solver)	Thermodynamics	pressure ratio; split ratio	/	650	50	25	10	Recompression s-CO2 Brayton cycle	Turbine: 93% Compressor: 89%	Neglected	5	UA LTR=3,21 MW/K; UA HTR: 5,33 MW/K;	97	97	35	axial turbine and radial compressors	not specified	2,5	49,66	0,71	/	/	/
T. Neises, C. Turchi	2013	Energy Procedia and ScienceDirect	Single obj	Cycle efficiency	all the optimizations were completed using the "Variable Metric" method build into EES (engineering equation solver)	Thermodynamics	pressure ratio; ratio of pressure ratios; split ratio	/	650	50	25	5,5	Partial cooling s-CO2 Brayton cycle	Turbine: 93% Compressor: 89%	Neglected	5	UA LTR=1,73 MW/K; UA HTR: 2,60 MW/K	97	97	35	axial turbine and radial compressors	not specified	4,55	49,53	0,59	0,369	/	/
T. Neises, C. Turchi	2013	Energy Procedia and ScienceDirect	Single obj	Cycle efficiency	all the optimizations were completed using the "Variable Metric" method build into EES (engineering equation solver)	Thermodynamics	pressure ratio; fHTR (fraction of total conductance allocated to the high temperature recuperator); split ratio	/	650	50	25	8,56/ 10/ 10,05	Recompression s-CO2 Brayton cycle	Turbine: 93% Compressor: 89%	Neglected	/	UA recuperators: 5/ 10/ 15 MW/K	/	/	35	axial turbine and radial compressors	not specified	2,92/ 2,5/ 2,49	47,17/ 50,39/ 51,59	0,87/ 0,73/ 0,7	/	/	/
T. Neises, C. Turchi	2013	Energy Procedia and ScienceDirect	Single obj	Cycle efficiency	all the optimizations were completed using the "Variable Metric" method build into EES (engineering equation solver)	Thermodynamics	pressure ratio; fHTR (fraction of total conductance allocated to the high temperature recuperator); split ratio	/	650	50	25	5,58/ 5,96/ 6,06	Partial cooling s-CO2 Brayton cycle	Turbine: 93% Compressor: 89%	Neglected	/	UA recuperators: 5/ 10/ 15 MW/K	/	/	35	axial turbine and radial compressors	not specified	4,48/ 4,19/ 4,13	49,99/ 51,21/ 51,49	0,6/ 0,59/ 0,6	/	/	/
Yuqeng Ma, Xuwei Zhang, Ming Liu, Junjie Yan, Jiping Liu	2018	Energy and Science Direct	Single obj	Exergy efficiency	Mathematical models are established for each component of the system in MATLAB 2015A. Thermal properties of carbone dioxide are evaluated using REFPROP 9.0 while optimization is performed with genetic algorithm	Thermodynamics and Economics	pressure ratio; recuperators effectiveness; concentration of the solution LiBr-water; temerature approach in the generator (that is part of the absorption chiller)	104,21 kg/s	565	37,12	25	8,2	Recompression s-CO2 Brayton cycle	Turbine: 90% Compressor: 89%	Neglected	6 °C in the LTR and 10 °C in the HTR	/	95	95	10	not specified	Printed Circuit Heat Exchangers for recuperators (the others not specified)	3,05	45,84	not specified	/	COE= 13,72 $/kWh	cycle: 76,67
R. Vasquez Padilla, R.G. Benito and W. Stein	2014	Energy Procedia and ScienceDirect	Single obj	Exergy efficiency	Python 3.2 for mass, energy and exergy balances coupled with REFPROP for the thermodynamic properties of the CO2, SLSQP (Sequential Least Squares Programming) for the optimization	Thermodynamics	TIT; pressure ratio;	/	600	32	25	10	Recompression s-CO2 Brayton cycle with reheating	Turbine: 90% Compressor: 89%	Neglected	5	/	95	95	/	not specified	not specified	2,5	45,5	not specified	/	/	net: 35,1
M.A. Reyes-Belmonte, A. Sebastian, M.Romero, J. Gonzalez-Aguilar	2016	Energy and Science Direct	Single obj	Cycle efficiency	Governing equations and thermodynamic relations used for power cycle modelling have been encoded in MATLAB coupled with NIST-REFPROP	Thermodynamics	recuperator effectiveness; split ratio; TIT	95,3 kg/s	680	40	24,85	7,8	Recompression s-CO2 Brayton cycle	Turbine: 92% Compressor: 88%	relative pressure loss in all components: 0,01	not specified	/	95	95	/	not specified	not specified	3,18	47,18	0,75	/	/	/
José I.Linares, Maria J. Montes, Alexis Cantizano Consuelo Sanchez	2020	Applied Energy	Single obj	Cycle efficiency	Power cycles modeled with EES environment	Thermodynamics and Economics	SR (split ratio); TIP ; Pressure of reheating; TIT	/	638,4	35	30	8,5	Recompression s-CO2 Brayton cycle with single reheating	Turbine: 92% Compressor: 88%	40 kPa in every heat exchanger (recuperators, precooler, heater, reheater..) for every CO2 stream	5	/	/	/	50	not specified	Shell and Tube heat exchangers for precooler and recuperators and Printed Circuit Heat Exchangers for primary HX and Reheater	3,53	54,64	/	/	SC=8662 $/kW	/

General data			Study typology					Layout and main parameters of the cycle						Assumptions							Components characteristics		Results					
Author	Year	Journal	Optimization Y(single obj)/Y(multi obj)	Objective function	Optimization algorithm	Thermodinamics/ economic/…	Optimization variables	Mass flow rate [kg/s]	Max temperature [°C]	Min temperature [°C]	Max pressure [Mpa]	Min pressure [Mpa]	Cycle layout	Turbomachinery efficencies	Pressure drops [kPa]	Pinch point of recuperators [°C]	Heat transfer coefficients	HTR effectiveness [%]	LTR effectiveness [%]	Net power [MW]	Axial or radial turbomachinery	Heat exchangers typology	Pressure ratio	Cycle efficiency [%]	Split Ratio	Ratio of pressure ratios	Costs	Exergy efficiency [%]
José I.Linares, Maria j.Montes, Alexis Cantizano , Consuelo Sanchez	2020	Applied Energy	Single obj	Cycle efficiency	Power cycles modeled with EES environment	Thermodynamics and Economics	SR (split ratio); TIP ; Pressure of reheating; Pressure of intercooling; TIT	/	645,6	50	30	8,5	Recompression s-CO2 Brayton cycle with single reheating and intercooling	Turbine: 92% Compressor: 88%	40 kPa in every heat exchanger (recuperators, precooler, heater, reheater..) for every CO2 stream	5	/	/	/	50	not specified	Shell and Tube heat exchangers for precooler, intercooler and recuperators and Printed Circuit Heat Exchangers for primary HX and Reheater	3,53	52,56	/	/	SC=8742 $/kW	/
Dia Milani, Minh Tri Luu, Robbie McNaughton, Ali Abbas	2017	Energy Conversion and Management and Science Direct	Single obj	Cycle efficiency	Aspen PLUS coupled with NIST-REFPROP	Thermodynamics	Splitting fraction, Compression ratio of the main compressor; Expansion ratio of the first turbine	/	600	32	25	7,55	Recompression s-CO2 Brayton cycle with single reheating and intercooling	Turbine: 93% Compressor: 89%	Recuperator pressure drop: 25 kPa (for every stream); Heater and cooler: 80 kPa	5	U recuperators: 765 W/m2*K	/	/	10	not specified	Printed Circuit Heat Exchangers	3,31	52,7	0,622	/	/	/
Yuegeng Ma	2020	Bachelor Degree Thesis	Single obj	Cycle efficiency	Genetic Algorithm developed in MATLAB coupled with NIST-REFPROP	Thermodynamics	PR; SR;RPR Main Compressor; RPR Recompressor	952,95 kg/s	500	45	25	9,26	Recompression s-CO2 Brayton cycle with main compressor intercooling	Turbine: 93% Compressor: 89%	Hot side LTR: 0,020 Mpa;Hot side HTR: 0,060 Mpa; Cold side HTR: 0,030 Mpa; Cold side LTR: 0,040 Mpa; HX: 0,05 Mpa; Cooler:0,02 Mpa	5	/	95	95	100	axial turbine and radial compressors	not specified	2,7	46,56	0,68	RPR mc:0,16; RPR rc:0	/	/
Lei Sun, YH Xie, Di Zhang	2019	Materials Science and Engineering	Single obj	Exergy efficiency	genetic algorithm	Thermodynamics	TIP; CIP; CIT	/	600	32,37	24,95	7,64	simple s-CO2 Brayton cycle	Turbine: 85% Compressor: 80%	Neglected	10	/	/	/	/	not specified	Printed Circuit Heat Exchangers	3,27	/	/	/	/	41,31
Lei Sun, YH Xie, Di Zhang	2019	Materials Science and Engineering	Single obj	Exergy efficiency	genetic algorithm	Thermodynamics	TIP; CIP; CIT	/	600	32,21	24,91	7,87	Recompression s-CO2 Brayton cycle	Turbine: 85% Compressor: 80%	Neglected	10	/	/	/	/	not specified	Printed Circuit Heat Exchangers	3,17	/	/	/	/	47,78
Lei Sun, YH Xie, Di Zhang	2019	Materials Science and Engineering	Single obj	Exergy efficiency	genetic algorithm	Thermodynamics	TIP; CIP; CIT	/	600	32,07	24,82	9,42	simple s-CO2 Brayton cycle with main compression intercooling	Turbine: 85% Compressor: 80%	Neglected	10	/	/	/	/	not specified	Printed Circuit Heat Exchangers	2,63	/	/	/	/	52,27
Lei Sun, YH Xie, Di Zhang	2019	Materials Science and Engineering	Single obj	Exergy efficiency	genetic algorithm	Thermodynamics	TIP; CIP; CIT	/	600	32,42	24,96	7,61	simple s-CO2 Brayton cycle with single reheating	Turbine: 85% Compressor: 80%	Neglected	10	/	/	/	/	not specified	Printed Circuit Heat Exchangers	3,28	/	/	/	/	42,55
Yuegeng Ma; Tatiana Morozyuk; Ming Liu; Junjie Yan; Jiping Liu	2019	Applied Energy	Single obj	Plant efficiency	genetic algorithm	Exergoeconomic	pressure ratio of MC; RPR of MC-1; RPR of T-1; SR; effectiveness of HTR; effectiveness of LTR	/	550	45	25	7,72	Recompression s-CO2 Brayton cycle with main compressor intercooling and reheating	Turbine: 90% Compressor: 89%	PHX: 50 kPa; Hot side HTR:60 kPa; Cold side HTR: 30 kPa; Hot side LTR: 20 kPa; Cold side LTR: 40 kPa; Cooler: 20 kPa	5	/	96	97	62,57	not specified	not specified	3,24	net: 28,44	0,67	RPR MC-1: 0,22;RPR T-1:0,48	12,41 $/kWh	/
Yuegeng Ma; Tatiana Morozyuk; Ming Liu; Junjie Yan; Jiping Liu	2019	Applied Energy	Single obj	LCOE	genetic algorithm	Exergoeconomic	pressure ratio of MC; RPR of MC-1; RPR of T-1; SR; effectiveness of HTR; effectiveness of LTR	/	550	45	25	8,09	Recompression s-CO2 Brayton cycle with main compressor intercooling	Turbine: 90% Compressor: 89%	PHX: 50 kPa; Hot side HTR:60 kPa; Cold side HTR: 30 kPa; Hot side LTR: 20 kPa; Cold side LTR: 40 kPa; Cooler: 20 kPa	5	/	92	96	58,23	not specified	not specified	3,09	net: 26,47	0,73	RPR MC-1: 0,23	11,30 $/kWh	/

General data			Study typology				Layout and main parameters of the cycle						Assumptions						Components characteristics		Results		
Author	Year	Journal	Optimization S(single obj)/Y(multi obj)	Objective function	Optimization algorithm	Thermodynamics/economic…	Optimization variables	Mass flow rate [kg/s]	Max temperature [°C]	Min temperature [°C]	Max pressure [Mpa]	Min pressure [Mpa]	Cycle layout	Turbomachinery efficiencies	Pressure drops [kPa]	Pinch point of recuperators [°C]	Heat transfer coefficients	HTR effectiveness [%]	LTR effectiveness [%]	Net power [MW]	Axial or radial turbomachinery	Heat exchangers Typology	Pressure ratio	Cycle efficiency [%]	Split Ratio	Costs	Exergy efficiency [%]
Matteo Marchionni, Giuseppe Bianchi, Savvas A.Tassou	2018	Energy Procedia and ScienceDirect	Single obj	Net electrical power output	CycleTempo coupled with NIST thermophysical properties	Thermodynamics and Economics	TIT; split ratio	/	450	35	20	7,4	Pre-heating s-CO2 Brayton cycle	Turbine: 85% Compressor: 70%	Neglected	15	/	not specified	not specified	0,171	not specified	plate heat exchanger	2,7	28	not specified	SC=4000 $/kW LCOE=0,031 $/kWh	40
Matteo Marchionni, Giuseppe Bianchi, Savvas A.Tassou	2018	Energy Procedia and ScienceDirect	Single obj	Net electrical power output	CycleTempo coupled with NIST thermophysical properties	Thermodynamics and Economics	TIT; split ratio	/	500	35	20	7,4	Pre-heating s-CO2 Brayton cycle with split expansion	Turbine: 85% Compressor: 70%	Neglected	15	/	not specified	not specified	0,165	not specified	plate heat exchanger	2,7	27	not specified	SC=1500 $/kW LCOE=0,01 $/kWh	38
Matteo Marchionni, Giuseppe Bianchi, Savvas A.Tassou	2018	Energy Procedia and ScienceDirect	Single obj	Net electrical power output	CycleTempo coupled with NIST thermophysical properties	Thermodynamics and Economics	TIT; split ratio	/	550	35	20	7,4	Split-heating s-CO2 Brayton cycle with split expansion	Turbine: 85% Compressor: 70%	Neglected	15	/	not specified	not specified	0,124	not specified	plate heat exchanger	2,7	19	not specified	SC=1225 0 $/kW LCOE=0,012 $/kWh	29
Matteo Marchionni, Giuseppe Bianchi, Savvas A.Tassou	2018	Energy Procedia and ScienceDirect	Single obj	Net electrical power output	CycleTempo coupled with NIST thermophysical properties	Thermodynamics and Economics	TIT; split ratio	/	475	35	20	pre compressor inlet pressure: 6 MPa; MC inlet pressure: 7,4 MPa	Pre-heating s-CO2 Brayton cycle with pre-compression	Turbine: 85% Compressor: 70%	Neglected	15	/	not specified	not specified	0,174	not specified	plate heat exchanger	2,7	29	not specified	SC=2000 $/kW LCOE=0,016 $/kWh	42
Giovanni Manente and Mario Costa	2019	Energies	Single obj	Total heat recovery efficiency (cycle efficiency x heat recovery efficiency)	Power cycles modeled with EES environment	Thermodynamics	TIT; SR (split ratio);	/	550	32	20	7,63	Single flow split with dual expansion s-CO2 Brayton cycle	Turbine: 85% Compressor: 80%	Neglected	/	/	95	95	1	not specified	Printed Circuit Heat Exchangers	2,62	26,62	0,35	/	49,75
Giovanni Manente and Mario Costa	2019	Energies	Single obj	Total heat recovery efficiency (cycle efficiency x heat recovery efficiency)	Power cycles modeled with EES environment	Thermodynamics	TIT; SR (split ratio);	/	390	32	20	7,63	Partial Heating s-CO2 Brayton cycle	Turbine: 85% Compressor: 80%	Neglected	/	/	95	95	1	not specified	Printed Circuit Heat Exchangers	2,62	25,82	0,3	/	48,24
Giovanni Manente and Mario Costa	2019	Energies	Single obj	Total heat recovery efficiency (cycle efficiency x heat recovery efficiency)	Power cycles modeled with EES environment	Thermodynamics	TIT; SR (split ratio);	/	520	32	20	7,63	Dual Recuperated s-CO2 Brayton cycle	Turbine: 85% Compressor: 80%	Neglected	/	/	95	95	1	not specified	Printed Circuit Heat Exchangers	2,62	28,4	0,56	/	43,24
Min Seok Kim, Yoonhan Ahn, Boompoo Kim, Joong Ik Lee	2016	Energy and Science Direct	Single obj	Net power output	In-house code, KAIST-CCD developed by KAIST research team	Thermodynamics	mass flow rate; flow splits ratios, turbine outlet pressure; first compressor outlet pressure	36 kg/s	503,17	36,85	27,6	7,67	Dual heated and flow split cycle	Turbine: 90% Compressor: 85%	HTR and LTR hot side:42 kPa and 43 kPa ;HTR and LTR cold side: 140 kPa; Precooler: 42 kPa; HX: 140 kPa	HTR: 8 °C; LTR: 6°C	/	95	95	3,23	not specified	not specified	3,6	31,72	Flow split1: 0,5; Flow split2: 0,34	/	/
Alperen Tozlu, Aysegul Abusoglu, Emrah Ozahi	2018	Energy and Science Direct	Multi obj	Total cost rate [$/h] and exergy efficiency	In-house code, KAIST-CCD developed by KAIST research team	Thermodynamics and thermoeconomic	TIP; PR; LMTD; Tzero	11,09 kg/s	546,7	40	20,77	7,89	Simple s-CO2 recuperative Brayton cycle with intercooling	Turbine: 85% Compressor: 85%	Neglected	/	UA recuperator: 0,7 W/m2*K; UA cooler and intercooler: 2 W/m2*K; UA main HX: 1,1 W/m2*K	92	92	1,144	not specified	Shell and Tube heat exchangers	2,633	35,22	/	Total cost rate: 44,08 $/h	57,64

General data			Study typology				Layout and main parameters of the cycle						Assumptions					Components characteristics		Results				
Author	Year	Journal	Optimization Y(single obj)Y(multi obj)	Objective function	Optimization algorithm	Thermodi namics/ec onomic…	Optimization variables	Mass flow rate [kg/s]	Max temperature [°C]	Min temperatur e [°C]	Max pressure [Mpa]	Min pressure [Mpa]	Cycle layout	Turbomac hinery efficiencie s	Pressure drops [kPa]	Pinch point of recuperat ors [°C]	Heat transfer coefficients	HTR effectiven ess [%]	LTR effectiven ess [%]	Net power [MW]	Axial or radial turbomachine ry	Heat exchangers typology	Pressure ratio	Cycle efficiency [%]	Split Ratio	Costs	Exergy efficiency [%]
Giovanni Manente and Francesca Maria Fortuna	2019	Energy Conversio n and Managem ent and Science Direct	Multi obj	Max of total heat recovery efficiency and min of specific investment cost	Power cycles modeled with EES environment	Thermoec onomic	TIT; SR;	/	550	32	20	7,63	Single flow split with dual expansion s-CO2 Brayton cycle	Turbine: 85% Compress or: 80%	recuperators hot side:1,5% recu perators cold side:0,5%; Precooler: 0,5%; Heater: 1%	/	/	95	95	1	radial turbine	Printed Circuit Heat Exchangers	2,62	Total heat recovery efficiency: 20,62	0,35	SIC: 2430 $/kW	45,98
Giovanni Manente and Francesca Maria Fortuna	2019	Energy Conversio n and Managem ent and Science Direct	Multi obj	Max of total heat recovery efficiency and min of specific investment cost	Power cycles modeled with EES environment	Thermoec onomic	TIT; SR;	/	745	32	20	7,63	Single flow split with dual expansion s-CO2 Brayton cycle	Turbine: 85% Compress or: 80%	recuperators hot side:1,5% recu perators cold side:0,5%; Precooler: 0,5%; Heater: 1%	/	/	95	95	1	radial turbine	Printed Circuit Heat Exchangers	2,62	Total heat recovery efficiency: 25,27	0,28	SIC: 2025 $/kW	49,32
Giovanni Manente and Francesca Maria Fortuna	2019	Energy Conversio n and Managem ent and Science Direct	Multi obj	Max of total heat recovery efficiency and min of specific investment cost	Power cycles modeled with EES environment	Thermoec onomic	TIT; SR;	/	550	32	20	7,63	Dual flow split with dual expansion s-CO2 Brayton cycle	Turbine: 85% Compress or: 80%	recuperators hot side:1,5% recu perators cold side:0,5%; Precooler: 0,5%; Heater: 1%	/	/	95	95	1	radial turbine	Printed Circuit Heat Exchangers	2,62	Total heat recovery efficiency: 20,97	0,38/0,56	SIC: 2400 $/kW	46,76
Giovanni Manente and Francesca Maria Fortuna	2019	Energy Conversio n and Managem ent and Science Direct	Multi obj	Max of total heat recovery efficiency and min of specific investment cost	Power cycles modeled with EES environment	Thermoec onomic	TIT; SR;	/	750	32	20	7,63	Dual flow split with dual expansion s-CO2 Brayton cycle	Turbine: 85% Compress or: 80%	recuperators hot side:1,5% recu perators cold side:0,5%; Precooler: 0,5%; Heater: 1%	/	/	95	95	1	radial turbine	Printed Circuit Heat Exchangers	2,62	Total heat recovery efficiency: 26,45	0,3/0,4	SIC: 2150 $/kW	51,63
Abubakr Ayub	2018	Master of Science Thesis	Single obj	Exergy efficiency	Genetic algorithm	Thermody namics	PR; SR; MFRR (mass flow rate of CO2/mass flow rate of air of GT the topping cycle)	168 kg/s	465,95	31,1	18,5	7,4	Recompressi on s-CO2 Brayton cycle	Turbine: 90% Compress or: 80%	Neglected	/	/	85	70	10,7	radial turbine and compressors	not specified	2,5	39,4	0,55	/	61,9
Abubakr Ayub	2018	Master of Science Thesis	Single obj	Exergy efficiency	Genetic algorithm	Thermody namics	PR; SR; MFRR (mass flow rate of CO2/mass flow rate of air of GT the topping cycle)	115,5 kg/s	457,25	31,1	25,752	7,4	Pre-heating cycle	Turbine: 90% Compress or: 80%	Neglected	/	/	85	70	10,18	radial turbine and compressors	not specified	3,48	23,8	0,45	/	57
Pengcheng Fan, Chenqiang Yuan, Yuwei Sun, Xinping Yan, Mingjun Lu, Richard Bucknall	2020	Energy Conversio n and Managem ent and Science Direct	Multi obj	Max of net power output, energy and exergy efficiency and min of LCOE and HX area per unit power	Imperialist Competitive Algorithm in MATLAB	Thermo-economic	CIT; CIP; COP; SR; TIT; Turbine required mass flow rate	10,36	411,57	34	14,61	8,8	Recompressi on s-CO2 Brayton cycle	Turbine: 70% Compress or: 65%	Hot side LTR: 0,05 Mpa; Hot side HTR: 0,05 Mpa; Cold side HTR: 0,15 Mpa; Cold side LTR: 0,15 Mpa. HX: 0,05 Mpa; Precooler:0,05 Mpa	/	/	/	0,332	not specified	Printed Circuit Heat Exchangers	1,66	20,44	0,68	LCOE= 0,0018 $/kWh	34,07
Pengcheng Fan, Chenqiang Yuan, Yuwei Sun, Xinping Yan, Mingjun Lu, Richard Bucknall	2020	Energy Conversio n and Managem ent and Science Direct	Multi obj	Max of net power output, energy and exergy efficiency and min of LCOE and HX area per unit power	Imperialist Competitive Algorithm in MATLAB	Thermo-economic	CIT; CIP; COP; SR; TIT; Turbine required mass flow rate; SR between turbines	14,13	417,8	35	16,33	8,9	Dual turbine-aftermatter-compressor recompressi on s-CO2 Brayton cycle	Turbine: 70% Compress or: 65%	Hot side LTR: 0,05 Mpa;Hot side HTR: 0,05 Mpa, Cold side HTR: 0,15 Mpa; Cold side LTR: 0,15 Mpa. HX: 0,05 Mpa; Precooler:0,05 Mpa	/	/	/	0,4522	not specified	Printed Circuit Heat Exchangers	1,83	24,53	0,64	LCOE= 0,0069 $/kWh	41,47

General data			Study typology				Layout and main parameters of the cycle					Assumptions				Components characteristics	Results			
Author	Year	Journal	Optimization (single obj)/(multi obj)	Objective function	Optimization algorithm	Thermodinamics/economic/...	Optimization variables	Mass flow rate [kg/s]	Max temperature [°C]	Min temperature [°C]	Max pressure [Mpa]	Min pressure [Mpa]	Cycle layout	Turbomachinery efficiencies	Pressure drops [kPa]	Pinch point of recuperators [°C]	Heat transfer coefficients	HTR effectiveness [%]	LTR effectiveness [%]	Net power [MW]	Axial or radial turbomachinery	Pressure ratio	Cycle efficiency [%]	Split Ratio	Costs	Exergy efficiency [%]
Hua Tian, Liwen Chang, Gequn Shu, Lingfeng Shi	2017	Energy Conversion and Management	Multi-obj	Net power output, Exergy efficiency, EPC (electricity production cost	Genetic Algorithm	Thermo-economic	TIT; TIP	/	351,25	25	14,68	6,4	Regenerative and preheating cycle	Turbine: 70% Pump: 80%	neglected	Preheater and condenser: 5°C; regenerator: 15°C; gas-heater: 30 °C	/	/	/	0,2424	not specified	2,29	/	/	EPC: 0,583 $/kWh	36,88
Shubham Bamik, Satyaki Ray, Sudipta De	2016	Applied Thermal Engineering	Single-obj	Cycle first law efficiency	Genetic Algorithm	Thermodynamic	Pressure ratio, mass recompression ratio	/	170	14,28	12	5	Regenerative and recompression cycle	Turbine: 90% Pump and compressor: 85%	neglected	/	/	85	85	about 0,23	not specified	2,4	13,6	0,26	/	25
Chuang Wu, Xiao-Jiang Yan, Shun-sen Wang et al	2016	Energy	Single-obj	Net power output	Genetic Algorithm	Thermodynamic	TIT; TIP	/	230-480	25	17,8-30,22	6,4	Single pressure regenerative with dual expansion	Turbine: 75% Pump: 75%	neglected	regenerator: 10°C; gas-heater: 20 °C	/	/	/	0,2752-0,11968	axial turbines	2,78-4,72	12,18-23,22	/	/	/
Chuang Wu, Xiao-Jiang Yan, Shun-sen Wang et al	2016	Energy	Single-obj	Net power output	Genetic Algorithm	Thermodynamic	TIT; TIP	/	230-480	25	15,118-24,99	6,4	Single pressure regenerative with triple expansion	Turbine: 75% Pump: 75%	neglected	regenerator: 10°C; gas-heater: 20 °C	/	/	/	0,2666-0,1222	axial turbines	2,36-3,9	12,84-23,71	/	/	/
Ali Amini, Nima Mirkiani, Pedram Pakjesm Pourfard et	2015	Energy	Two-obj	Net power output and total bare module cost	Genetic Algorithm	Thermo-economic	TIT; TIP	about 200 kg/s	126	25,6	13,7	6,5	Simple cycle without regeneration	Turbine: 70% Pump: 80%	condenser: 5%; HX: 5%	/	/	/	/	4,04 (20 kW/kg)	centrifugal pump	2,1	5,03	/	26,25 $/kW	/
Nima Mirkiani, Ali Amini, Mehdi Ashjaee	2017	Energy	Two-obj	Net power output and total bare module cost	Genetic Algorithm	Thermo-economic	TIT; TIP	433,3-615,7	112-248	25,6	12,5-14,3	6,5	Simple cycle without regeneration	Turbine: 90% Pump: 80%	(Tube side: 0,02; Shell side: 0,05)	(condenser: 5°C; heater: 10 °C)	/	/	/	2-6,3 (about 10 kW/kg)	centrifugal pump	1,92-2,2	6,71-10,15	/	675-1150 $/kW	/
Shun-sen Wang, Chuang Wu, Jun Li	2018	Energy	Single-obj	Net power output	Genetic Algorithm	Thermodynamic	TIT; TIP; PP condenser; PP HTR, LTR, HX	5,71	450	25	29,233	6,4	Single pressure regenerative with dual expansion	Turbine: 80% Pump: 80%	neglected	condenser: 3°C; heater LTR and HTR: 5 °C	for all Heat exchangers: 1 600 W/(m2*K); condenser: 20 00 W/(m2*K)	/	/	0,51727 (90,67 kW/kg)	not specified	4,56	30,01	x1=0,4075	28,3 $/GJ	63,99
Shun-sen Wang, Chuang Wu, Jun Li	2018	Energy	Single-obj	total unit cost Cp,tot [$/ GJ]	Genetic Algorithm	Exergoeconomic	TIT; TIP; PP condenser; PP HTR, LTR, HEX	3,69	450	25	34,445	6,4	Single pressure single stage regenerative	Turbine: 80% Pump: 80%	neglected	condenser: 3°C; heater LTR and HTR: 5 °C	for all Heat exchangers: 3 000 W/(m2*K); condenser: 20 00 W/(m2*K)	/	/	0,41522 (112,52,5 2 kW/kg)	not specified	5,38	33,87	/	27,5 $/GJ	64,89

Acronyms

s-CO2	Supercritical Carbon Dioxide
NIST	National Institute of Standards and Technology
REFPROP	Reference Fluid PROPerties
ECS	Extended Corresponding States
DLL	Dynamic Link Library
PHX	Primary Heat Exchanger
HTR	High Temperature Recuperator
LTR	Low Temperature Recuperator
HX	Heat Exchanger
PC	Precooler
IC	Intercooler
RC	Recompression Compressor
MC	Main Compressor
SR	Split Ratio
ORC	Organic Rankine Cycle
SNL	Sandia National Laboratory
TAC	Alternator-Turbo-Compressor
BMPC	Bechtel Marine Propulsion Corporation
IST	Integrated System Test
SCIEL	Supercritical CO_2 Brayton Cycle Integral Experimental Loop
KAERI	Korea Atomic Energy Research Institute
KAIST	Korea Advanced Institute of Science&Technology
POSTECH	Pohang University of Science and Technology
SFR	Sodium-cooled Fast Reactor
LPT	Low Pressure Turbine
RPR	Ratio of Pressure Ratios
LPC	Low Pressure Compressor
HPT	High Pressure Turbine
HPC	High Pressure Compressor
PCHE	Printed Circuit Heat Exchanger
SwRI	Southwest Research Institute
GE	General Electric
KAPL	Knolls Atomic Power Laboratory
EPRI	Electric Power Research Institute
TRL	Technology Readiness Level
CSP	Concentrated Solar Power
SETO	Solar Energy Technologies Office
PV	Photovoltaic
GTI	Gas technology Institute
STEP	Supercritical Transformation Electric Power

US DOE	United States Department of Energy
RCBC	Recompression Closed Brayton Cycle
HRSG	Heat Recovery Steam Generator
P&IDs	Piping and Instrumentation Diagrams
NO_X	Nitrogen Oxides
SMR	Small and Medium Sized Reactors
IAEA	International Atomic Energy Agency
LFR	Lead-cooled Fast Reactor
GFR	Gas-cooled Fast Reactor
SCWR	Supercritical Water-cooled Reactor
VHTR	Very High Temperature Reactor
MSR	Molten Salt Reactor
PWR	Pressurized Water Reactor
TRISO	TRI-structural ISOtropic particle fuel
CIT	Compressor Inlet Termperature
CIP	Compressor Inlet Pressure
PR	Pressure Ratio
TIT	Turbine Inlet Temperature
TIP	Turbine Inlet Pressure
NGSA	Non-dominated Sorting Genetic Algorithm
CYCLOP	CYCLe Optimization
CEA	Atomic Energy Commission
CCS	Carbon Capture and Storage
CaL	Carbonate Looping
A-USC	Advanced Ultra-Supercritical
LHV	Lower Heating Value
PFBC	Pulverized Fluidized Bed Combustion
GSH	Gas-cooling wall and Superheater
FRH	First-stage Reheater
SRH	Second-stage Reheater
ECO	Economizer
MTE	Medium Temperature Economizer
APH	Air Preheater
MPT	Medium Pressure Turbine
TES	Thermal Energy Storage
HTF	Heat Transfer Fluid
PTC	Parabolic Trough Collector
SPT	Solar Power Tower
LFR	Linear Fresnel Reflector
PDS	Parabolic Dish System
EES	Engineering Equation Solver
SLSQP	Sequential Least Squares Programming
WHR	Waste Heat Recovery
IHX	Intermediate Heat Exchanger
RBC	Recompression Brayton Cycle
EPC	Electricity Production Cost
PFHE	Plate Fin Heat Exchanger
CiADS	Chinese Initiative Accelerator Driven System

GA	Genetic Algorithm
SMART	System Integrated Modular Advanced Reactor
RCAM	Recompression Cycle Analysis Model
HSH	High Temperature Superheater
LSH	Low Temperature Superheater
LECO	Low Temperature Economizer
NREL	National Renewable Energy Laboratory
KPIs	Key Performance Indicators
MCIC	Main Compression Intercooling
TIP	Turbine Inlet Pressure
HTT	High Temperature Turbine
LTT	Low Temperature Turbine
PHPC	Pre-Heating with Pre-compression
CDTPC	Carbon Dioxide Transcritical Power Cycle
GW	Gas Wall

Nomenclature

T	[°C] or [K]	Temperature
c_p	[J/kg/K]	Specific Heat
A	[m^2]	Surface
LCOE	[$/kWh] or [$/MWh]	Levelized Cost of Energy
$\dot{m}$	[kg/s]	Mass Flow Rate
$\dot{Q}$	[kW] or [MW]	Thermal Power
$\dot{W}_e$	[kW] or [MW]	Net Electrical Power Output
η	[-]	Efficiency
ρ	[kg/m^3]	Density
Z	[-]	Compressibility Factor
s	[J/K/kg]	Specific Entropy
UA	[kW/K] or [MW/K]	Conductance
β	[-]	Pressure ratio
p	[MPa]	Pressure
μ	[Pa·s]	Dinamic Viscosity
$\dot{E}$	[kW]	Exergy rate
h	[kJ/kg]	Specific Enthalpy
e	[kJ/kg]	Specific Exergy
X	[-]	Mass Fraction
eff	[-]	Effectiveness

Subscripts

cyc	cycle
p	pump
t	turbine
e	electrical
th	thermal
in	inlet
out	outlet
ph	physical
ch	chemical
0	reference state
HT	high temperature
LT	low temperature
HX	heat exchanger
i	component
d	destruction
is	isentropic

Bibliography

[1] Sulzer, “Verfahren zur erzeugung von arbeit aus warme,” 1948.

[2] D. P. Gokhshtein and G. P. Verkhivker, “Use of carbon dioxide as a heat carrier and working substance in atomic power stations,” *Soviet Atomic Energy*. 1969, doi: 10.1007/BF01371881.

[3] V. G. P. Gokhstein D. P, “Future Design of Thermal Power Stations Operating on Carbon Dioxide,” no. Thermal Engineering, pp. 36–38, 1971.

[4] G. Angelino, “Carbon dioxide condensation cycles for power production,” *J. Eng. Gas Turbines Power*, 1968, doi: 10.1115/1.3609190.

[5] ANGELINO G, “REAL GAS EFFECTS IN CARBON DIOXIDE CYCLES,” 1969.

[6] E. G. Feher, “The supercritical thermodynamic power cycle,” *Energy Convers.*, 1968, doi: 10.1016/0013-7480(68)90105-8.

[7] F. A. J. Strub R. A., “High Pressure Indirect COB2B Closed-Cycle Design Gas Turbines,” *Nucl. Gas Turbines*, pp. 51–61, 1970.

[8] J. R. Hoffmann and E. G. Feher, “150 kwe supercritical closed cycle system,” *J. Eng. Gas Turbines Power*, 1971, doi: 10.1115/1.3445409.

[9] G. Angelino, “Perspectives for the liquid phase compression gas turbine,” *J. Eng. Gas Turbines Power*, 1967, doi: 10.1115/1.3616657.

[10] V. Dostal, M. J. Driscoll, and P. Hejzlar, “A Supercritical Carbon Dioxide Cycle for Next Generation Nuclear Reactors,” *Tech. Rep. MIT-ANP-TR-100*, pp. 1–317, 2004, doi: MIT-ANP-TR-100.

[11] Y. Ma, “Optimal design of supercritical carbon dioxide cycle based system for concentrated solar power application,” *Diss. Tech. Univ. Berlin*, 2020.

[12] E. W. Lemmon and I. H. Bell, “REFPROP Documentation,” 2018.

[13] G. Liao *et al.*, “Effects of technical progress on performance and application of supercritical carbon dioxide power cycle: A review,” *Energy Convers. Manag.*, vol. 199, no. June, 2019, doi: 10.1016/j.enconman.2019.111986.

[14] Q. Zhu, “Power generation from coal using supercritical CO 2 cycle Power generation from coal using supercritical CO 2 cycle,” no. December, 2017.

[15] Y. Ahn *et al.*, “Review of supercritical CO2 power cycle technology and current status of research and development,” *Nucl. Eng. Technol.*, vol. 47, no. 6, pp. 647–661, 2015, doi: 10.1016/j.net.2015.06.009.

[16] M. J. Li, H. H. Zhu, J. Q. Guo, K. Wang, and W. Q. Tao, “The development technology and applications of supercritical CO2 power cycle in nuclear energy, solar energy and other energy industries,” *Appl. Therm. Eng.*, vol. 126, pp. 255–275, 2017, doi: 10.1016/j.applthermaleng.2017.07.173.

[17] J. Sarkar, “Review and future trends of supercritical CO2 Rankine cycle for low-grade heat conversion,” *Renew. Sustain. Energy Rev.*, vol. 48, pp. 434–451, 2015, doi:

10.1016/j.rser.2015.04.039.

[18] J. Pasch, T. Conboy, D. Fleming, and G. Rochau, “Brayton Cycle : Completed Assembly Description,” *Sandia Natl. Lab.*, no. October, pp. 1–40, 2012, [Online]. Available: http://www.ntis.gov/help/ordermethods.asp?loc=7-4-0#online.

[19] E. M. Clementoni and T. L. Cox, “Steady-state power operation of a supercritical carbon dioxide brayton cycle with thermal-hydraulic control,” in *The 4th International Symposium-Supercritical CO2 power cycles*, 2014, vol. 9, pp. 1–8, doi: 10.1115/GT2016-56038.

[20] K. J. Kimball, K. D. Rahner, J. P. Nehrbauer, and E. M. Clementoni, “Supercritical carbon dioxide brayton cycle development overview,” *Proc. ASME Turbo Expo*, vol. 8, pp. 1–27, 2013, doi: 10.1115/GT2013-94268.

[21] M. Utamura, H. Hasuike, and T. Yamamoto, “Demonstration test plant of closed cycle gas turbine with supercritical CO2 as working fluid,” *Strojarstvo*, vol. 52, no. 4, pp. 459–465, 2010.

[22] Y. Ahn, J. Lee, J. I. Lee, and J. E. Cha, “Design study of supercritical CO$_2$ integral experiment loop (SCIEL),” *Trans. Korean Nucl. Soc. Spring Meet.*, pp. 29–31, 2014.

[23] Y. Ahn, J. Lee, S. G. Kim, J. I. Lee, J. E. Cha, and S. W. Lee, “Design consideration of supercritical CO2 power cycle integral experiment loop,” *Energy*, vol. 86, pp. 115–127, 2015, doi: 10.1016/j.energy.2015.03.066.

[24] J. E. Cha, Y. Ahn, J. K. Lee, J. I. Lee, and H. L. Choi, “Installation of the Supercritical CO 2 Compressor Performance Test Loop as a First Phase of the SCIEL facility,” *Supercrit. CO2 Power Cycle Symp.*, 2014, [Online]. Available: https://sci-hub.st/https://koasas.kaist.ac.kr/bitstream/10203/211367/1/Draft ver 2.2 (2).pdf.

[25] J. J. Moore, S. Cich, M. Towler, T. Allison, J. Wade, and D. Hofer, “Commissioning of a 1 MWe Supercritical CO 2 Test Loop,” *6th Int. Symp. - Supercrit. CO2 Power Cycles*, pp. 1–36, 2018.

[26] Energy.Gov, “SunShot 2030.” .

[27] S. Macadam, W. W. Follett, M. Kutin, and G. Subbaraman, “Supercritical Co2 Power Cycle Projects At Gti,” *3rd Eur. Supercrit. CO2 Conf.*, no. September, 2019.

[28] C. Bing, “Title: 10 MW Supercritical CO 2 Turbine Test Mark Lausten,” pp. 1–34, 2014, [Online]. Available: https://www.osti.gov/servlets/purl/1117025.

[29] J. Marion, “10 MWe Supercritical Carbon Dioxide (sCO2) Pilot Power Plant,” pp. 1–8, 2018.

[30] S. Macadam, W. W. Follett, M. Kutin, and G. Subbaraman, “Supercritical Co2 Power Cycle Projects At Gti,” *3rd Eur. Supercrit. CO2 Conf.*, pp. 1–10, 2019, doi: 10.17185/duepublico/48911.

[31] D. Flin, “FIRST FIRE FOR LA PORTE CARBON CAPTURE DEMO.” .

[32] “NET POWER.” .

[33] A. Kacludis, S. Lyons, D. Nadav, and E. Zdankiewicz, “Waste Heat to Power (WH2P) Applications Using a Supercritical CO 2 -Based Power Cycle,” *Power-Gen Int.*, vol. 2, no. December, pp. 1–10, 2012.

[34] Q. Zhu, “Innovative power generation systems using supercritical CO2 cycles,” *Clean Energy*, vol. 1, no. 1, pp. 68–79, 2017, doi: 10.1093/ce/zkx003.

[35] “GIF Portal - Home - Generation IV Systems.” https://www.gen-4.org/gif/jcms/c_59461/generation-iv-systems (accessed Nov. 30, 2020).

[36] G. Locatelli, M. Mancini, and N. Todeschini, “Generation IV nuclear reactors: Current status and future prospects,” *Energy Policy*, vol. 61, pp. 1503–1520, 2013, doi: 10.1016/j.enpol.2013.06.101.

[37] “Generation IV nuclear reactors - Energy Education.” https://energyeducation.ca/encyclopedia/Generation_IV_nuclear_reactors (accessed Nov. 30, 2020).

[38] “Generation IV Nuclear Reactors: WNA - World Nuclear Association.” https://www.world-nuclear.org/information-library/nuclear-fuel-cycle/nuclear-power-reactors/generation-iv-nuclear-reactors.aspx (accessed Nov. 30, 2020).

[39] F. Crespi, G. Gavagnin, D. Sánchez, and G. S. Martínez, “Supercritical carbon dioxide cycles for power generation: A review,” *Appl. Energy*, vol. 195, pp. 152–183, 2017, doi: 10.1016/j.apenergy.2017.02.048.

[40] M. Marchionni, G. Bianchi, and S. A. Tassou, “Techno-economic assessment of Joule-Brayton cycle architectures for heat to power conversion from high-grade heat sources using CO2 in the supercritical state,” *Energy*, vol. 148, pp. 1140–1152, 2018, doi: 10.1016/j.energy.2018.02.005.

[41] Y. He, A. Dong, M. Xie, and Y. Liu, “A Design of Parameters with Supercritical Carbon Dioxide Brayton Cycle for CiADS,” *Sci. Technol. Nucl. Install.*, vol. 2018, 2018, doi: 10.1155/2018/3245604.

[42] M. J. Li, Y. J. Jie, H. H. Zhu, G. J. Qi, and M. J. Li, “The thermodynamic and cost-benefit-analysis of miniaturized lead-cooled fast reactor with supercritical CO2 power cycle in the commercial market,” *Prog. Nucl. Energy*, vol. 103, no. November, pp. 135–150, 2018, doi: 10.1016/j.pnucene.2017.11.015.

[43] H. S. Pham *et al.*, “Mapping of the thermodynamic performance of the supercritical CO2cycle and optimisation for a small modular reactor and a sodium-cooled fast reactor,” *Energy*, vol. 87, pp. 412–424, 2015, doi: 10.1016/j.energy.2015.05.022.

[44] E. A. Harvego and M. G. McKellar, “Icone19-43824 Evaluation and Optimization of a Supercritical Carbon Dioxide Power Conversion Cycle for Nuclear Applications,” *Proc. Int. Conf. Nucl. Eng.*, vol. 2011.19, no. 0, p. _ICONE1943-_ICONE1943, 2011, doi: 10.1299/jsmeicone.2011.19._icone1943_318.

[45] “GIF Portal - Sodium-Cooled Fast Reactor (SFR).” https://www.gen-4.org/gif/jcms/c_42152/sodium-cooled-fast-reactor-sfr (accessed Nov. 30, 2020).

[46] “Sodium-Cooled Fast Reactors as a Generation IV Nuclear Reactor.” http://large.stanford.edu/courses/2018/ph241/rojas1/ (accessed Nov. 30, 2020).

[47] “Lead-cooled Fast Reactor (LFR) — it.” https://www.enea.it/it/centro-ricerche-brasimone/attivita-di-ricerca/divisione-di-ingegneria-sperimentale/lead-cooled-fast-reactor-lfr (accessed Nov. 30, 2020).

[48] “GIF Portal - Lead-Cooled Fast Reactor (LFR).” https://www.gen-4.org/gif/jcms/c_42149/lead-cooled-fast-reactor-lfr (accessed Nov. 30, 2020).

[49] “GIF Portal - Very-High-Temperature Reactor (VHTR).” https://www.gen-4.org/gif/jcms/c_42153/very-high-temperature-reactor-vhtr (accessed Nov. 30, 2020).

[50] H. J. Yoon, Y. Ahn, J. I. Lee, and Y. Addad, "Potential advantages of coupling supercritical CO 2 Brayton cycle to water cooled small and medium size reactor," *Nucl. Eng. Des.*, vol. 245, pp. 223–232, 2012, doi: 10.1016/j.nucengdes.2012.01.014.

[51] J. H. Park, H. S. Park, J. G. Kwon, T. H. Kim, and M. H. Kim, "Optimization and thermodynamic analysis of supercritical CO2 Brayton recompression cycle for various small modular reactors," *Energy*, vol. 160, pp. 520–535, 2018, doi: 10.1016/j.energy.2018.06.155.

[52] P. Wu, C. Gao, Y. Huang, D. Zhang, and J. Shan, "Supercritical CO2 Brayton Cycle Design for Small Modular Reactor with a Thermodynamic Analysis Solver," *Sci. Technol. Nucl. Install.*, vol. 2020, 2020, doi: 10.1155/2020/5945718.

[53] Q. H. Deng, D. Wang, H. Zhao, W. T. Huang, S. Shao, and Z. P. Feng, "Study on performances of supercritical CO2 recompression Brayton cycles with multi-objective optimization," *Appl. Therm. Eng.*, vol. 114, pp. 1335–1342, 2017, doi: 10.1016/j.applthermaleng.2016.11.055.

[54] M. J. Li, Y. J. Jie, H. H. Zhu, G. J. Qi, and M. J. Li, "The thermodynamic and cost-benefit-analysis of miniaturized lead-cooled fast reactor with supercritical CO2 power cycle in the commercial market," *Prog. Nucl. Energy*, vol. 103, no. August, pp. 135–150, 2018, doi: 10.1016/j.pnucene.2017.11.015.

[55] "A self-sustaining heat removal system for safer nuclear power | Result In Brief | CORDIS | European Commission." https://cordis.europa.eu/article/id/258413-a-selfsustaining-heat-removal-system-for-safer-nuclear-power (accessed Nov. 25, 2020).

[56] "sCO2-HeRo." http://www.sco2-hero.eu/ (accessed Nov. 30, 2020).

[57] M. Mecheri and Y. Le, "Supercritical CO 2 Brayton cycles for coal- fi red power plants," vol. 103, pp. 758–771, 2016.

[58] S. Michalski, D. P. Hanak, and V. Manovic, "Advanced power cycles for coal-fired power plants based on calcium looping combustion: A techno-economic feasibility assessment," *Appl. Energy*, vol. 269, no. April, 2020, doi: 10.1016/j.apenergy.2020.114954.

[59] M. Liu, X. Zhang, K. Yang, Y. Ma, and J. Yan, "Optimization and comparison on supercritical CO2 power cycles integrated within coal-fired power plants considering the hot and cold end characteristics," *Energy Convers. Manag.*, vol. 195, no. May, pp. 854–865, 2019, doi: 10.1016/j.enconman.2019.05.077.

[60] J. Q. Guo, M. J. Li, J. L. Xu, J. J. Yan, and T. Ma, "Energy, exergy and economic (3E) evaluation and conceptual design of the 1000 MW coal-fired power plants integrated with S-CO2 Brayton cycles," *Energy Convers. Manag.*, vol. 211, no. February, 2020, doi: 10.1016/j.enconman.2020.112713.

[61] Z. Bai, G. Zhang, Y. Li, G. Xu, and Y. Yang, "A supercritical CO2 Brayton cycle with a bleeding anabranch used in coal-fired power plants," *Energy*, vol. 142, pp. 731–738, 2018, doi: 10.1016/j.energy.2017.09.121.

[62] H. Li *et al.*, "Preliminary design assessment of supercritical CO2 cycle for commercial scale coal-fired power plants," *Appl. Therm. Eng.*, vol. 158, no. May, 2019, doi: 10.1016/j.applthermaleng.2019.113785.

[63] Y. Zhang *et al.*, "Improved design of supercritical CO2 Brayton cycle for coal-fired

power plant," *Energy*, vol. 155, pp. 1–14, 2018, doi: 10.1016/j.energy.2018.05.003.

[64] "sCO2-Flex." sco2-flex.eu.

[65] "SUPERCRITICAL CO2 CYCLE FOR FLEXIBLE AND SUSTAINABLE SUPPORT TO THE ELECTRICITY SYSTEM | sCO2-Flex Project | H2020 | CORDIS | European Commission." https://cordis.europa.eu/project/id/764690 (accessed Nov. 25, 2020).

[66] D. Alfani *et al.*, "MULTI OBJECTIVE OPTIMIZATION OF FLEXIBLE SUPERCRITICAL CO2 COAL-FIRED POWER PLANTS," 2019, pp. 1–11.

[67] C. S. Turchi, Z. Ma, T. W. Neises, and M. J. Wagner, "Thermodynamic study of advanced supercritical carbon dioxide power cycles for concentrating solar power systems," *J. Sol. Energy Eng. Trans. ASME*, vol. 135, no. 4, pp. 1–7, 2013, doi: 10.1115/1.4024030.

[68] C. S. Turchi, Z. Ma, T. W. Neises, and M. J. Wagner, "Thermodynamic Study of Advanced Supercritical Carbon Dioxide Power Cycles for Concentrating Solar Power Systems," *J. Sol. Energy Eng.*, vol. 135, no. 4, Nov. 2013, doi: 10.1115/1.4024030.

[69] Y. Ma, T. Morozyuk, M. Liu, J. Yan, and J. Liu, "Optimal integration of recompression supercritical CO2 Brayton cycle with main compression intercooling in solar power tower system based on exergoeconomic approach," *Appl. Energy*, vol. 242, no. September 2018, pp. 1134–1154, 2019, doi: 10.1016/j.apenergy.2019.03.155.

[70] D. Milani, M. T. Luu, R. McNaughton, and A. Abbas, "Optimizing an advanced hybrid of solar-assisted supercritical CO2 Brayton cycle: A vital transition for low-carbon power generation industry," *Energy Convers. Manag.*, vol. 148, pp. 1317–1331, 2017, doi: 10.1016/j.enconman.2017.06.017.

[71] T. Neises and C. Turchi, "A comparison of supercritical carbon dioxide power cycle configurations with an emphasis on CSP applications," *Energy Procedia*, vol. 49, pp. 1187–1196, 2014, doi: 10.1016/j.egypro.2014.03.128.

[72] M. A. Reyes-Belmonte, A. Sebastián, M. Romero, and J. González-Aguilar, "Optimization of a recompression supercritical carbon dioxide cycle for an innovative central receiver solar power plant," *Energy*, vol. 112, pp. 17–27, 2016, doi: 10.1016/j.energy.2016.06.013.

[73] M. Binotti, M. Astolfi, S. Campanari, G. Manzolini, and P. Silva, "Preliminary Assessment of sCO2 Power Cycles for Application to CSP Solar Tower Plants," *Energy Procedia*, vol. 105, pp. 1116–1122, 2017, doi: 10.1016/j.egypro.2017.03.475.

[74] R. V. Padilla, R. G. Benito, and W. Stein, "An Exergy Analysis of Recompression Supercritical CO2 Cycles with and without Reheating," *Energy Procedia*, vol. 69, pp. 1181–1191, 2015, doi: 10.1016/j.egypro.2015.03.201.

[75] J. I. Linares, M. J. Montes, A. Cantizano, and C. Sánchez, "A novel supercritical CO2 recompression Brayton power cycle for power tower concentrating solar plants," *Appl. Energy*, vol. 263, no. February, 2020, doi: 10.1016/j.apenergy.2020.114644.

[76] Y. Ma, X. Zhang, M. Liu, J. Yan, and J. Liu, "Proposal and assessment of a novel supercritical CO2 Brayton cycle integrated with LiBr absorption chiller for concentrated solar power applications," *Energy*, vol. 148, pp. 839–854, 2018, doi: 10.1016/j.energy.2018.01.155.

[77] K. Wang, M. J. Li, J. Q. Guo, P. Li, and Z. Bin Liu, "A systematic comparison of different S-CO2 Brayton cycle layouts based on multi-objective optimization for applications in solar power tower plants," *Appl. Energy*, vol. 212, no. November 2017, pp. 109–121, 2018, doi: 10.1016/j.apenergy.2017.12.031.

[78] "SOLARSCO2OL - RINA.org." https://www.rina.org/en/media/CaseStudies/solarsco2ol (accessed Nov. 25, 2020).

[79] "Gen 3 Particle Pilot Plant (G3P3) : Sandia Energy." https://energy.sandia.gov/programs/renewable-energy/csp/current-research-projects/gen-3-particle-pilot-plant-g3p3/ (accessed Nov. 25, 2020).

[80] C. Forman, I. K. Muritala, R. Pardemann, and B. Meyer, "Estimating the global waste heat potential," *Renew. Sustain. Energy Rev.*, vol. 57, pp. 1568–1579, 2016, doi: 10.1016/j.rser.2015.12.192.

[81] G. Manente and M. Costa, "On the conceptual design of novel supercritical CO2 power cycles for waste heat recovery," *ECOS 2019 - Proc. 32nd Int. Conf. Effic. Cost, Optim. Simul. Environ. Impact Energy Syst.*, pp. 2219–2231, 2019.

[82] G. Manente and F. M. Fortuna, "Supercritical CO2 power cycles for waste heat recovery: A systematic comparison between traditional and novel layouts with dual expansion," *Energy Convers. Manag.*, vol. 197, no. June, 2019, doi: 10.1016/j.enconman.2019.111777.

[83] M. S. Kim, Y. Ahn, B. Kim, and J. I. Lee, "Study on the supercritical CO2 power cycles for landfill gas firing gas turbine bottoming cycle," *Energy*, vol. 111, pp. 893–909, 2016, doi: 10.1016/j.energy.2016.06.014.

[84] P. Pan, C. Yuan, Y. Sun, X. Yan, M. Lu, and R. Bucknall, "Thermo-economic analysis and multi-objective optimization of S-CO2 Brayton cycle waste heat recovery system for an ocean-going 9000 TEU container ship," *Energy Convers. Manag.*, vol. 221, no. June, p. 113077, 2020, doi: 10.1016/j.enconman.2020.113077.

[85] A. Tozlu, A. Abuşoğlu, and E. Özahi, "Thermoeconomic analysis and optimization of a Re-compression supercritical CO2 cycle using waste heat of Gaziantep Municipal Solid Waste Power Plant," *Energy*, vol. 143, pp. 168–180, 2018, doi: 10.1016/j.energy.2017.10.120.

[86] S. Sarco, "Project profile Consortium EE-18-2015 : New technologies for utilization of heat recovery in large industrial systems , considering production to transformation , H2020-EE-2015-1-PPP Grant aggreement no Email I-ThERM is a SPIRE PPP granted project The nee," no. 680599, 2020.

[87] I. Thermal and E. Recovery, "I - ThERM," 2020.

[88] "I-ThERM – Industrial Thermal Energy Recovery Conversion and Management." http://www.itherm-project.eu/ (accessed Nov. 30, 2020).

[89] A. Ayub, "Supercritical Carbon Dioxide Power Cycles for Waste Heat Recovery of Gas Turbine," p. 143, 2018.

[90] H. Tian, L. Chang, G. Shu, and L. Shi, "Multi-objective optimization of the carbon dioxide transcritical power cycle with various configurations for engine waste heat recovery," *Energy Convers. Manag.*, vol. 148, pp. 477–488, 2017, doi: 10.1016/j.enconman.2017.05.038.

[91] C. Wu *et al.*, "System optimisation and performance analysis of CO2 transcritical

power cycle for waste heat recovery," *Energy*, vol. 100, pp. 391–400, 2016, doi: 10.1016/j.energy.2015.12.001.

[92] S. sen Wang, C. Wu, and J. Li, "Exergoeconomic analysis and optimization of single-pressure single-stage and multi-stage CO2 transcritical power cycles for engine waste heat recovery: A comparative study," *Energy*, vol. 142, pp. 559–577, 2018, doi: 10.1016/j.energy.2017.10.055.

[93] S. Banik, S. Ray, and S. De, "Thermodynamic modelling of a recompression CO2 power cycle for low temperature waste heat recovery," *Appl. Therm. Eng.*, vol. 107, pp. 441–452, 2016, doi: 10.1016/j.applthermaleng.2016.06.179.

[94] N. Mirkhani, A. Amini, and M. Ashjaee, "Thermo-economic analysis of transcritical CO2 cycles with bounded and unbounded reheats in low-temperature heat recovery applications," *Energy*, vol. 133, pp. 676–690, 2017, doi: 10.1016/j.energy.2017.05.162.

[95] A. Amini, N. Mirkhani, P. Pakjesm Pourfard, M. Ashjaee, and M. A. Khodkar, "Thermo-economic optimization of low-grade waste heat recovery in Yazd combined-cycle power plant (Iran) by a CO2 transcritical Rankine cycle," *Energy*, vol. 86, pp. 74–84, 2015, doi: 10.1016/j.energy.2015.03.113.

[96] Z. Rao, T. Xue, K. Huang, and S. Liao, "Multi-objective optimization of supercritical carbon dioxide recompression Brayton cycle considering printed circuit recuperator design," *Energy Convers. Manag.*, vol. 201, no. September, 2019, doi: 10.1016/j.enconman.2019.112094.

[97] S. A. Wright, C. S. Davidson, and W. O. Scammell, "Thermo-Economic Analysis of Four sCO2 Waste Heat Recovery Power Systems," *5th Int. Symp. - Supercrit. CO2 Power Cycles*, pp. 1–16, 2016, [Online]. Available: http://www.sco2symposium.com/www2/sco2/papers2016/SystemModeling/059paper.pdf.

[98] Y. Liu, Y. Wang, and D. Huang, "Supercritical CO 2 Brayton cycle : A state-of-the-art review," vol. 189, 2019.

[99] J. M. and D. J. B. timothy J. Held, "A comparative study of heat rejection systems for sCO2 power cycles," in *The 5th International Symposium - Supercritical CO2 Power Cycles March 28-31, 2016, San Antonio, Texas A*, 2018, vol. 51, no. 1.

[100] X. Wang and Y. Dai, "Exergoeconomic analysis of utilizing the transcritical CO2 cycle and the ORC for a recompression supercritical CO2 cycle waste heat recovery: A comparative study," *Appl. Energy*, vol. 170, pp. 193–207, 2016, doi: 10.1016/j.apenergy.2016.02.112.

[101] Z. Gua-Yan, W. En, and T. Shan-Tung, "Techno-economic study on compact heat exchangers," 2008, doi: 10.1002/er.1449.